UDC 636.2.09: 591.11: 636.083 "322" https://doi.org/10.31548/ujvs2021.04.001

BLOOD FATTY ACID COMPOSITION IN COWS DEPENDING ON THE TYPE OF AUTONOMIC REGULATION IN SUMMER PERIOD

I. A. HRYSHCHUK[1],
Graduate Student, Department of Animal Biochemistry and Physiology named after Academician M. F. Gulyi
https://orcid.org/0000-0003-2571-6876
E-mail: hitmane2012@gmail.com
V. I. KARPOVSKYI[1],
Doctor of Veterinary Sciences, Professor, Department of Animal Biochemistry and Physiology named after Academician M. F. Gulyi
https://orcid.org/0000-0003-3858-0111
E-mail: karpovskiy@meta.ua
V. V. DANCHUK[1],
Doctor of Agricultural Sciences, Professor, Ukrainian Laboratory of Quality and Safety of Agricultural Products
https://orcid.org/0000-0003-2156-1758
E-mail: dan-vv1@ukr.net
B. V. GUTYJ[2],
Doctor of Veterinary Sciences, Professor, Department of Pharmacology and Toxicology
https://orcid.org/0000-0002-5971-8776
E-mail: bvh@ukr.net
K. KUBIAK[3],
Doctor Habilitatus, Professor, Department of Internal Medicine and Clinic of Diseases of Horses, Dogs and Cats
https://orcid.org/0000-0001-9640-2597
S. V. MIDYK[1],
Candidate of Veterinary Sciences, Research Department for Monitoring the Safety of Agricultural Products, Ukrainian Laboratory of Quality and Safety of Agricultural Products
http://orcid.org/0000-0002-2682-2884
E-mail: svit.mid@gmail.com
R. V. POSTOI[1],
Doctor of Veterinary Sciences
https://orcid.org/0000-0001-5278-2102
E-mail: ruslana-postoy@meta.ua

***V. O. TROKOZ*[1],**
Doctor of Agricultural Sciences, Professor, Department of Biochemistry and Physiology of Animals named after Academician M. F. Gulyi
https://orcid.org/0000-0001-8619-195X
E-mail: trokoz@nubip.edu.ua
[1]National University of Life and Environmental Sciences of Ukraine, 15 Heroyiv Oborony st., Kyiv 03041, Ukraine
[2]Stepan Gzhytskyi National University of Veterinary Medicine and Biotechnologies Lviv, 50 Pekarska st., Lviv 79010, Ukraine
[3]Wrocław University of Environmental and Life Sciences, 25 Norwida st., Wrocław 50-375, Poland

Abstract. *Abstract. Coordination of physiological activity and intensity of metabolism in various organs and tissues of a productive animal depending on environmental conditions and own needs is provided by the regulatory activity of the corresponding nerve centers. However, the features of the autonomic regulation of the nervous system in this matter can have a significant impact not only on the physiological activity of animals but also on their productivity. Therefore, the question of studying the influence of autonomic regulation on the animal body in general and the interaction of the autonomic system and lipid metabolism is quite relevant.*

Groups of animals were formed by determining the state of the cardiovascular system according to the Baevskyi method. Blood plasma was used for the study, lipid extraction was performed by the Folch method. Fatty acid analysis was performed on a Trace GC Ultra gas chromatograph (USA) with a flame ionization detector.

Studies have shown that the relative content of saturated fatty acids in blood of normotonics was the highest compared with other groups: sympathotonics – by 1.9%; vagotonics – 0.48%. Regarding the concentration of saturated fatty acids in sympathotonics, it should be noted that the content of stearic acid was the highest (18.07 ± 0.01; P < 0.001), and saturated fatty acids from C6 to C16 were characterized by the lowest values (P < 0.01–0.05) in comparison with other groups.

The total content of unsaturated fatty acids in blood plasma of sympathotonics and vagotonics was 1.19% and 0.49% higher, respectively, compared with normotonics. Quite interesting is the fact that sympathotonics were characterized by the highest content of polyunsaturated fatty acids, the content of which decreased in the range C18:2n6 > C20:4n6 > C18:3n3 > C22:6n3 > C22:5n3, a similar sequence we observed in other groups, although the relative concentration of acids could fluctuate. Normotonics were characterized by the highest levels of some polyunsaturated fatty acids (C18:3n3, C22:5n3, and C22:6n3; P < 0.05–0.01), while levels of some unsaturated fatty acids (C18:1n9 and C20:3n6) were the lowest.

Thus, the type of nervous activity has a significant effect on the ratio of fatty acids in blood plasma and autonomic regulation affects the metabolic processes in the body of cows.

Keywords: *cows, autonomic regulation, lipids, fatty acid composition*

Introduction

Currently, it is a very important issue to study the effect of autonomic regulation on lipid metabolism in animal (Martin et al., 2021). This is because the type of peripheral nervous system of the animal depends on the type of nervous activity and has a significant impact on the course of metabolic processes in its body (Chang et al., 2020). This question has a significant contribution to the understanding of what will depend on the productivity of the animal and its reproductive capacity (Carrell et al., 2021). Depending on the influence of autonomic regulation on the body, each environmental and external factor has a lever of influence on the course of internal processes (Bouffiou et al., 2020).

On the example of an animal with a predominance in the body of sympathetic nervous activity, each effect on it will be reflected in a significant reaction, which further negatively affects the normal course of metabolic processes in its body (Fernandez-Novo et al., 2020). It should also be noted that an animal that is more sensitive to changes in the environment will have increased production of cortisol, which will further increase the cost of energy reserves of nutrients and the use of nutrient-derived nutrients (Colditz, 2021). Lipids play an important role in the animal's body, they are carriers of high energy value, are used by the body as a structural element, are a part of the regulatory element in the system playing a role in influencing the life of individual cells and the body as a whole (Bionaz et al., 2020).

Analysis of recent researches and publications

In the modern world, the study and understanding of the factors that affect the condition of the animal and its productivity play a significant role in creating highly productive livestock (Chen et al., 2021). Minor changes in the environment and the progression of stressors are strongly associated with the general condition of the animal (Estévez-Moreno, 2021). Many people face the fact that each animal responds differently to different circumstances and has different productivity (Hemphill et al., 2020). It is known that milk quality is affected by such indicators as genetic characteristics, the general physiological condition of the animal, it's feeding, exercise, type of keeping, and external conditions, etc. (Shanks, 2021). We understand these concepts and use them to improve them and get better results in our economy (Ujita et al., 2021). Quite a few issues have been studied and analyzed by scientists to obtain data that will help others to improve their work (Abdel-Hamid et al., 2017).

One such study is the study of the effect of autonomic regulation on lipid metabolism. Each animal has systems that control and maintain the mechanisms that regulate the body's constant homeostasis. Considering the nervous system, we understand that it has two – higher nervous and autonomic nervous systems. They play a role in controlling and regulating the stability of the body depending on the influence of both environmental and internal factors. These systems are strongly related to each other even though scientists describe them as higher nervous activity characterizing it as type of animal temperament, and the autonomic nervous system as a reflection of sympathetic or parasympathetic nervous systems that work in harmony or dominate each other. In this regard, we can conclude that everything is interconnected and if one part of the system has characteristic features, they will affect other systems, which will be reflected in the general condition of the animal's body, including lipid metab-

olism. Each animal has its own type of autonomous system, which plays the role of a mechanism that responds and acts depending on different stimuli (Lees et al., 2020). The whole organism has a whole system of nerve endings and analyzing organs that control the living organism and make changes in it (Danchuk et al., 2020).

The nervous system can affect almost all aspects of the development in cattle, including growth, reproduction, and immunity. For example, a sympathotonic animal gains weight more slowly than a normotonic animal (Parham et al., 2021). This is since animals with a predominance in the body of the sympathetic nervous system are more aggressive and react sharply to changes in the environment, they expend a lot of energy in this regard, deteriorating the development of this animal (Chang et al., 2020). It was also investigated that animals, in which excitation processes predominate, have worse insemination rates in contrast to animals with moderate nervous processes. Low carcass and fat content are observed in meat products, and bruises and injuries are noticeable on the carcass, which reduces the quality and cost of meat (Libis-Márta et al., 2021). Also, the fattening of animals for slaughter, depending on the autonomic regulation, will have a different result in the weight gain of the animal (Sant'Anna et al., 2019).

Types of nervous activity have a significant impact on animals. Considering the conditions of detention, studies have been conducted, determining that the strongest manifestation of milk production affects the nervous system in the first lactation, this is since the animal has significant life changes, in this regard, it is influenced by stress factors (Mincu et al., 2021). Over time, the animal gets used to this effect, and in the next lactation, there are no such active reactions of the body (Antanaitis et al., 2021).

Stress conditions have a very negative effect on animal health. A very influential stress factor for the animal is its transportation to another farm, slaughterhouse, etc. (Marçal-Pedroza et al., 2021). During this load, the animal will not have a positive result of any type of autonomic regulation. But here the role is that depending on what type of nervous process predominates, the animal will react differently to the influencing factor, and in the future, it will affect the acclimatization and quality of animal raw materials (Melendez et al., 2021).

Immunity also depends on the type of nervous activity, as calves with weak nervous processes have a low immune response to vaccines (Smith et al., 2021). In the study of the immune system comparing the signs of autonomic processes, it was found that bulls with aggressive temperament had a lower proliferation of lymphocytes *in vivo* and lower concentrations of IgG specific for vaccines *in vivo*, compared with calmer bulls (Altman, 2019).

Many studies have been conducted to investigate the metabolism in the body. The path of lipid conversion from food and their circulation in the body has been well studied (Antanaitis et al., 2021). With feed, cattle receive relatively few lipids, but many polyunsaturated fatty acids, especially linolenic acid. In the rumen, lipids are hydrolyzed and released fatty acids are bio-hydrogenated by a microbial population, with 90% of linolenic acid being lost and increasing the amount of stearic acid. Free fatty acids are adsorbed in the rumen and turn into the abomasum, their absorption is almost absent in the rumen (Alexandre et al., 2020).

Microorganisms in the rumen are also involved in the synthesis of lipids and when moving them with food into the abomasum, they are broken down by

digestive enzymes, releasing fatty acids (Zeineldin et al., 2018). All fatty acids enter the duodenum, where they mix with the secretions of pancreatic acid (lipase and phosphatase) and bile containing lipid (phosphatidylcholine) and bile acids (taurine conjugates) (Vinyard et al., 2021). Lipases and phospholipases partially hydrolyze microbial lipids and any food lipids that do not hydrolyze in the rumen. The contents of the duodenum move to the distal part of the small intestine, where absorption occurs (Fortin et al., 2017). Most fatty acids are absorbed in the form of free fatty acids (Bernard et al., 2017). Free fatty acids are esterified, using the glycerol-3-phosphate pathway and partially by the monoacylglycerol pathway (Brake & Swanson, 2018). Before esterification, there is some desaturation of stearic acid to oleic, this process is characteristic only for ruminants (Xin et al., 2020). Then triacylglycerols, phospholipids, and cholesterol esters are created, which are used for the synthesis of chylomicrons, which are then secreted into the lymph (Kairenius et al., 2018). Triacylglycerols are the major lipids of lymph, accounting for 70–80% of the total weight of lipids in ruminants and playing the role of a major source of fatty acids for tissues (Danchuk, 2006). Once triacylglycerols enter the bloodstream, they are hydrolyzed by lipoprotein lipase, which is synthesized by body tissues such as muscle, fat, and the mammary gland, which subsequently releases fatty acids for tissue use (Li et al., 2018), for the synthesis of structural components such as cell membranes, biologically active substances such as prostaglandins, as a source of energy and to create a reserve for the future, or for the synthesis of milk (Toral et al., 2018).

The purpose of the study is to investigate the effect of autonomic regulation on blood fatty acid composition in cows.

Materials and methods of research

The research was carried out on cows of the Ukrainian, black-spotted breed of the 3rd–4th lactation. Types of the autonomic regulation were determined by the state of the cardiovascular system according to the Baevskyi method, the essence of which is that an electrocardiogram is recorded in the animal and the mode in the range of cardio intervals is determined. Then we formed 3 groups of animals: sympathotonic – a type of the nervous activity where the sympathetic nervous system predominates over the parasympathetic; vagotonic – a type of the nervous activity where parasympathetic nervous activity predominates over the sympathetic; normotonic – a type of the nervous activity with balanced parasympathetic and sympathetic nervous activity. The material for the study was blood samples obtained from the jugular vein in the morning before feeding. Blood was stabilized with heparin, plasma was obtained by centrifugation. In addition, information was taken on the daily productivity of the animals that they had on the day of blood sampling.

Extraction of lipids from blood plasma was performed by the Folch method (Folch et al., 1957). The next step in sample preparation was the hydrolysis and methylation of fatty acids in lipids derived from blood plasma. To do this, 4 cm^3 of methyl sodium hydroxide solution was added to 100 mg of the obtained fat, the reflux condenser was connected to the flask containing it and boiled until the fat droplets disappeared, stirring the contents of the flask at intervals of 30–60 seconds. To the contents of the flask, 5 cm^3 of boron methyl fluoride solution was added, continuing to boil for up to 1 hour. Three cm^3 of hexane was added

to the boiling mixture through the top of the reflux condenser and removed from the heating element. To a still hot solution, 20 cm^3 of saturated sodium chloride solution was added and stirred for 15 seconds. The upper (hexane) layer was selected for study (Sinyak et al., 1976). Analysis of methyl esters of volatile fatty acids was performed on a Trace GC Ultra gas chromatograph (USA) with a flame ionization detector. Chromatography conditions: column temperature 140–240 ºC, detector temperature 260 ºC. The sample was introduced into the chromatograph using a TriPlus autosampler at a dose of 1 µl. The duration of the analysis was 65 minutes.

Identification of fatty acids was performed using a standard sample Supelco 37 Component FAME Mix. Quantitative evaluation of the fatty acid spectrum of lipids was performed by the method of internal normalization, determining their content in percent. The study was performed in 3 parallels.

The following fatty acids were detected by gas chromatography: caproic (C6:0), caprylic (C8:0), capric (C10:0), lauric (C12:0), myristic (C14:0), myristoleic (C14:1), pentadecanoic (C15:0), palmitic (C16:0), palmitoleic (C16:1n9), stearic (C18:0), oleic (C18:1n9), linoleic (C18: 2n6), arachidic (C20:0), linolenic (C18:3n3), cis-11-eicosenoic (C20:1n9), cis-8,11,14-eicosatrienoic (C20:3n6), arachidonic (C20:4n6), docosapentaenoic (C22:5n3), and cis-4,7,10,13,16,19-docosahexaenoic (C22:6n3).

Statistical processing of experimental data was performed by conventional methods of variation statistics. The probability of the difference in indicators was assessed by Student's t-test. Differences between the compared indicators were considered significant at the level of significance $P < 0.05$, $P < 0.01$, $P < 0.001$.

Results of the research and their discussion

It is known that the fatty acid composition of blood in animals depends on many factors, among which the main ones are the type of productive animal, age, the composition of the diet, the intensity of rumen digestion, and its physiological state.

According to the results of research, the absence of clinical signs of pathology is not a guarantee of similarity of the main characteristics of the fatty acid composition of blood plasma in dairy cows (Fig. 1) under the same conditions of feeding and keeping. One of the physiological factors that should be considered in the chromatography of fatty acids in blood plasma of lactating cows is the types of autonomic regulation (normotonic; sympathotonic; and vagotonic).

According to Fig. 1, the type of nervous activity of a productive animal has a significant impact on their daily milk productivity. At this stage of our study, it is difficult to fully judge how close the relationship is between blood fatty acid composition in cows (Table 1), the type of their nervous activity, and the level of productivity. However, a superficial analysis of the results shows that normotonics were characterized by the highest level of daily milk yield, and the total content of saturated fatty acids (SFA) in this experimental group was also the highest. It is difficult to say how much this is related to the level of motor activity and stress resistance, but we can safely say that the increase in motor activity is provided by increasing the intensity of ATP synthesis and β-oxidation of fatty acids. However, this issue needs further study.

Animals-normotonics have a type of nervous activity, where the sympathetic and parasympathetic nervous systems

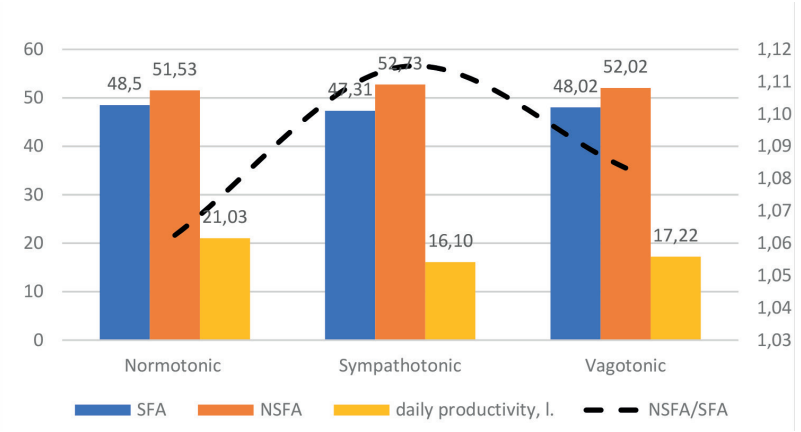

Fig. 1. The ratio of blood fatty acids and daily milk productivity in cows with different types of autonomic regulation

have a balanced effect on the animal's body, so we chose it as a guide to compare the features of lipid metabolism in other types. Thus, as can be seen from Fig. 1, the content of SFA was the highest in blood of normotonics in comparison with other groups – sympathotonics (by 1.9%) and vagotonics (by 0.48%).

According to the results, the relatively high content of SFA was provided by C6:0, C10:0, C15:0, C16:0, and C20:0.

Regarding the concentration of SFA in sympathotonics, it should be noted that the content of stearic acid in comparison with others was the highest (18.07 ± 0.01) and 0.89% higher than that observed in normotonics ($P < 0.001$). SFA from C6:0 to C16:0 in sympathotonics were characterized by the lowest relative content compared with other experimental groups (C6:0, $P < 0.05$; C10:0, $P < 0.01$; C16:0, $P < 0.05$).

It is known that the content of fatty acids with an odd number of carbon atoms in blood may depend on grazing time and the botanical composition of the pasture. However, even under the same feeding conditions of lactating cows, as shown by chromatographic studies presented in Table 1, it may depend on the type of autonomic regulation of nervous activity. We are talking about pentadecanoic acid (C15:0), the relative content of which in blood of animals decreased in the range: normotonics > sympathotonics > vagotonics, with significant differences in vagotonics both in comparison with normotonics ($P < 0.01$) and sympathotonics ($P < 0.05$).

Dairy cows, the intensity of nervous activity of which is characterized as vagotonic, in terms of the relative content of SFA in blood, occupied mainly an intermediate position between the values observed in sympathotonics and normotonics.

The total plasma content of unsaturated fatty acids (UFA) in animals classified as sympathotonics and vagotonics was 1.19% and 0.49% higher, respectively, compared with normotonics. Quite interesting is the fact that sympathotonics were characterized by the highest content of polyunsaturated fatty acids (PUFA), the content of which decreased in the range of C18:2n6 > C20:4n6 > C18:3n3 > C22:6n3 > C22:5n3, a similar sequence was observed in other groups, although the relative concentration of acids could fluctuate.

1. Fatty acid content (%) in blood plasma of cows according to autonomic regulation (M ± m; n = 5)

Fatty acid	Groups of cows		
	Normotonics	Sympathotonics	Vagotonics
Caproic, C6:0	1.11 ± 0.06	0.82 ± 0.04*	0.98 ± 0.02
Caprylic, C8:0	0.61 ± 0.04	0.69 ± 0.01	0.61 ± 0.01
Capric, C10:0	1.00 ± 0.05	0.76 ± 0.02**	0.81 ± 0.01**
Lauric, C12:0	0.42 ± 0.03	0.43 ± 0.01	0.54 ± 0.02*
Myristic, C14:0	3.10 ± 0.04	2.67 ± 0.06	2.86 ± 0.03
Myristoleic, C14:1	0.64 ± 0.04	0.56 ± 0.01	0.67 ± 0.01
Pentadecanoic, C15:0	0.45 ± 0.02	0.42 ± 0.01	0.37 ± 0.01**
Palmitic, C16:0	24.48 ± 0.44	23.30 ± 0.21*	23.82 ± 0.04
Palmitoleic, C16:1n9	2.14 ± 0.14	2.19 ± 0.01	2.46 ± 0.03
Stearic, C18:0	17.18 ± 0.23	18.07 ± 0.01**	17.91 ± 0.02*
Oleic, C18:1n9	23.15 ± 0.16	23.39 ± 0.18	24.51 ± 0.28**
Linolenic, C18:2n6	15.33 ± 0.37	16.21 ± 0.14	15.45 ± 0.27
Arachidic, C20:0	0.15 ± 0.01	0.15 ± 0.01	0.12 ± 0.01
α-Linolenic acid, C18:3n3	1.33 ± 0.01	1.04 ± 0.01***	0.89 ± 0.01***
Cis-11-eicosenoic, C20:1n9	0.42 ± 0.02	0.45 ± 0.01	0.40 ± 0.01
Cis-8,11,14-eicosatrienoic, C20:3n6	0.10 ± 0.01	0.14 ± 0.01*	0.12 ± 0.01
Arachidonic, 20:4n6	7.24 ± 0.18	7.74 ± 0.13	6.43 ± 0.15***
Docosapentaenoic, C22:5n3	0.31 ± 0.01	0.30 ± 0.01	0.27 ± 0.01*
Cis-4,7,10,13,16,19-docosahexaenoic, C22:6n3	0.88 ± 0.01	0.71 ± 0.01***	0.82 ± 0.03

Note: * $P < 0.05$, ** $P < 0.01$, *** $P < 0.001$ – compared with normotonics; data are presented as the mass fraction of fatty acid in % of the sum of fatty acids.

Normotonics, even though they had the lowest content of UFA, compared to other experimental groups, still for some PUFAs (C18:3n3, C22:5n3, and C22:6n3) were characterized by the highest values ($P < 0.05$–0.01) compared with other groups, while the SFA (C18:1n9 and C20:3n6) were the lowest compared with other experimental groups.

As shown in Fig. 2, normotonics were characterized by the highest concentration of omega-3 fatty acids in blood. Sympathotonics have a higher concentration of omega-6 fatty acids by 1.42% and 2.1% compared with vagotonics and normotonics, respectively.

Vagotonics were characterized by the lowest concentration of linolenic acid ($P < 0.001$), eicosenoic acid ($P < 0.05$), arachidonic acid ($P < 0.001$), and docosapentaenoic acid ($P < 0.05$) compared with animals with other types of the nervous system.

It is known that both the types of the nervous system and the intensity of motor activity can affect the performance of dairy animals, regardless of their level of nutrition. Obviously, increasing physical activity can only to some extent ensure stable productivity, on the other hand, overuse of energy due to β-oxidation of

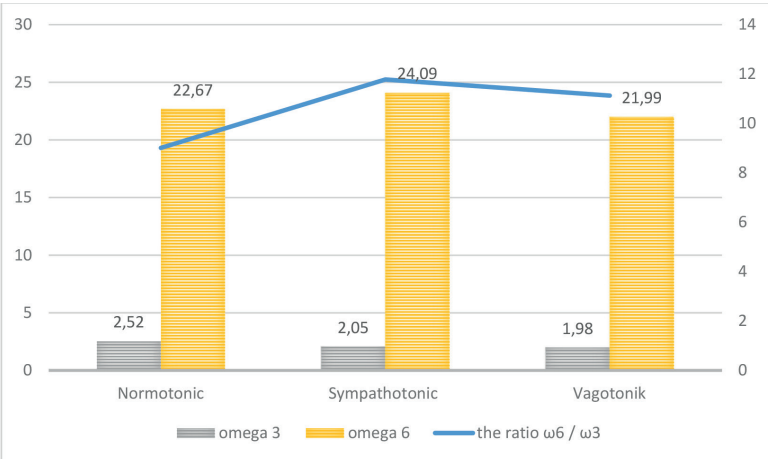

Fig. 2. The ratio of ω6/ω3 fatty acids in blood of cows with different types of autonomic regulation

saturated fatty acids can significantly affect not only their concentration in blood but also obviously their content in milk. This is what we associate with a decrease in the relative content of SFA in sympathotonics, which may be one of the hallmarks of this type of nervous activity.

Conclusion

The ratio of fatty acids in blood plasma of lactating cows depends to some extent on the type of autonomic nervous regulation and may be related to the level of their daily milk productivity. Normotonics are characterized by the highest level of daily milk productivity, relatively high content of saturated fatty acids and slightly lower level of unsaturated fatty acids. Sympathotonics and vagotonics were characterized by a lower level of daily milk productivity and a higher percentage of unsaturated fatty acids in blood. The content of fatty acids in blood with an odd number of carbon atoms may depend on the type of autonomic nervous regulation: the relative content of pentadecanoic acid (C15:0) in blood of animals decreased in a number: normotonics > sympathotonics > vagotonics, differences in vagotonics were observed both in comparison with normotonics ($P < 0.01$) and sympathotonics ($P < 0.05$).

References

Abdel-Hamid, S. E., Fattah, D. M. A., Ghanem, H. M., & Manaa, E. A. (2017). Temperament during milking process and its effect on behavioral, productive traits and biochemical parameters in friesian dairy cows. Advances in Animal and Veterinary Sciences, 5(12), 508-513. doi: 10.17582/journal.aavs/2017/5.12.508.513

Alexandre, P. A., Reverter, A., Berezin, R. B., Porto-Neto, L. R., Ribeiro, G., Santana, M. H., ... & Fukumasu, H. (2020). Exploring the Regulatory Potential of Long Non-Coding RNA in Feed Efficiency of Indicine Cattle. Genes, 11(9), 997. doi: 10.3390/genes11090997

Altman, A. W. (2019). Relationships between animal temperament and systemic immune responses in beef cattle exposed to conditions associated with conventional management. Animal and Food Sciences, 98. doi: 10.13023/etd.2019.033

Antanaitis, R., Juozaitienė, V., Jonike, V., Čukauskas, V., Urbšienė, D., Urbšys, A., ... & Paulauskas, A. (2021). Relationship between temperament and stage of lactation, productivity and milk composition of dairy cows. Animals, 11(7), 1840. doi: 10.3390/ani11071840

Bernard, L., Toral, P. G., & Chilliard, Y. (2017). Comparison of mammary lipid metabolism in dairy cows and goats fed diets supplemented with starch, Plant oil, or fish oil. Journal of dairy science, 100(11), 9338-9351. doi: 10.3168/jds.2017-12789

Bionaz, M., Vargas-Bello-Pérez, E., & Busato, S. (2020). Advances in fatty acids nutrition in dairy cows: from gut to cells and effects on performance. Journal of Animal Science and Biotechnology, 11(1), 1-36. doi: 10.1186/s40104-020-00512-8

Bouffiou, J., Boles, J. A., & Thomson, J. M. (2020). Investigating the relationship between temperament and performance traits in feedlot cattle. Journal of Animal Science, 98, 383-383. doi: 10.1093/jas/skaa278.674

Carrell, R. C., Smith, W. B., Kinman, L. A., Mercadante, V. R., Dias, N. W., & Roper, D. A. (2021). Cattle stress and Pregnancy responses when imposing different restraint methods for conducting fixed time artificial insemination. Animal Reproduction Science, 225, 106672. doi: 10.1016/j.anireprosci.2020.106672

Chang, Y., Brito, L. F., Alvarenga, A. B., & Wang, Y. (2020). Incorporating temperament traits in dairy cattle breeding programs: challenges and opportunities in the Phenomics era. Animal Frontiers, 10(2), 29-36. doi: 10.1093/af/vfaa006

Chen, X., Ogdahl, W., Hanna, L. L. H., Dahlen, C. R., Riley, D. G., Wagner, S. A., ... & Sun, X. (2021). Evaluation of beef cattle temperament by eye temperature using infrared thermography technology. Computers and Electronics in Agriculture, 188, 106321. doi: 10.1016/j.compag.2021.106321

Colditz, I. G. (2021). Adrenergic tone as an intermediary in the temperament syndrome associated with flight speed in beef cattle. Frontiers in Animal Science, 2, 6. doi: 10.3389/fanim.2021.652306

Danchuk, O. V., Karposvkyi, V. I., Tomchuk, V. A., Zhurenko, O. V., Bobryts'ka, O. M., & Trokoz, V. O. (2020). Temperament in cattle: a method of evaluation and main characteristics. Neurophysiology, 52(1), 73-79. doi: 10.1007/s11062-020-09853-6

Estévez-Moreno, L. X., Miranda-de la Lama, G. C., Villarroel, M., García, L., Abecia, J. A., Santolaria, P., & María, G. A. (2021). Revisiting cattle temperament in beef cow-calf systems: Insights from farmers' perceptions about an autochthonous breed. Animals, 11(1), 82. doi: 10.3390/ani11010082

Fernandez-Novo, A., Pérez-Garnelo, S. S., Villagrá, A., Pérez-Villalobos, N., & Astiz, S. (2020). The effect of stress on reproduction and reproductive technologies in beef cattle – A review. Animals, 10(11), 2096. doi: 10.3390/ani10112096

Folch, J., Leez, M., & Stanley, G. A. (1957). Simple method for the isolation and purification of total lipides from animal tissues. Journal of Biological Chemistry, 226(2), 497-501.

Fortin, É., Blouin, R., Lapointe, J., Petit, H. V., & Palin, M. F. (2017). Linoleic acid, α-linolenic acid and enterolactone affect lipid oxidation and expression of lipid metabolism and antioxidant-related genes in hepatic tissue of dairy cows. British Journal of Nutrition, 117(9), 1199-1211. doi: 10.1017/S0007114517000976

Hemphill, C. H., Reuter, R. R., Neel, J. P., & Goodman, L. (2020). Effects of acclimation on cattle response to humans while being handled. Journal of Animal Science, 98, 61-62. doi: 10.1093/jas/skz397.140

Kairenius, P., Leskinen, H., Toivonen, V., Muetzel, S., Ahvenjärvi, S., Vanhatalo, A., ... & Shingfield, K. J. (2018). Effect of dietary fish oil supplements alone or in combination with sunflower and linseed oil on ruminal lipid metabolism and bacterial populations in lactating cows. Journal of dairy science, 101(4), 3021-3035. doi: 10.3168/jds.2017-13776

Lees, A. M., Salvin, H. E., Colditz, I., & Lee, C. (2020). The influence of temperament on body temperature response to handling in Angus cattle. Animals, 10(1), 172. doi: 10.3390/ani10010172

Li, X., Li, Y., Ding, H., Dong, J., Zhang, R., Huang, D., ... & Li, X. (2018). Insulin suppresses the AMPK signaling Pathway to regulate lipid metabolism in Primary cultured hepatocytes of dairy cows. Journal of Dairy Research, 85(2), 157-162. doi: 10.1017/S002202991800016X

Libis-Márta, K., Póti, P., Egerszegi, I., Bodnár, Á., & Pajor, F. (2021). Effect of selected factors (body weight, age, parity, litter size and temperament) on the entrance order into the milking parlour of Lacaune ewes, and its relationship with milk production. Journal of Animal and Feed Sciences, 30(2), 111-118. doi: 10.22358/jafs/135727/2021

Marçal-Pedroza, M. G., Campos, M. M., Sacramento, J. P., Pereira, L. G. R., Machado, F. S., Tomich, T. R., ... & Sant'Anna, A. C. (2021). Are dairy cows with a more reactive temperament less efficient in energetic metabolism and do they Produce more enteric methane? Animal, 15(6), 100224. doi: 10.1016/j.animal.2021.100224

Martin, D. M., Moraes, R. F., Cintra, M. C. R., Lang, C. R., Monteiro, A. L. G., Oliveira, L. B. D., ... & Weiblen, R. (2021). Beef cattle behavior in integrated crop-livestock systems. Ciência Rural, 52. doi: 10.1590/0103-8478cr20210143

Meléndez, D. M., Marti, S., Haley, D. B., Schwinghamer, T. D., & Schwartzkopf-Genswein, K. S. (2021). Effects of conditioning, source, and rest on indicators of stress in beef cattle transported by road. Plos one, 16(1), e0244854. doi: 10.1371/journal.pone.0244854

Mincu, M., Gavojdian, D., Nicolae, I., Olteanu, A. C., & Vlagioiu, C. (2021). Effects of milking temperament of dairy cows on Production and reproduction efficiency under tied stall housing. Journal of Veterinary Behavior. Journal of Veterinary Behavior, 44, 12-17. doi: 10.1016/j.jveb.2021.05.010

Parham, J. T., Blevins, S. R., Tanner, A. E., Wahlberg, M. L., Swecker Jr, W. S., & Lewis, R. M. (2021). Subjective methods of quantifying temperament in heifers are indicative of Physiological stress. Applied Animal Behaviour Science, 234, 105197. doi: 10.1016/j.applanim.2020.105197

Sant'Anna, A. C., Valente, T. D. S., Magalhães, A. F. B., Espigolan, R., Ceballos, M. C., de Albuquerque, L. G., & Paranhos da Costa, M. J. R. (2019). Relationships between temperament, meat quality, and carcass traits in Nellore cattle. Journal of animal science, 97(12), 4721-4731. doi: 10.1093/jas/skz324

Shanks, P. (2021). Influence of dietary manipulation on the relationship between temperament measures and growth in beef cattle: endophyte exposure, phytogenic supplementation, and controlled feeding. Theses and Dissertations – Animal and Food Sciences, 131. doi: 10.13023/etd.2021.293

Smith, P., Carstens, G., Runyan, C., Ridpath, J., Sawyer, J., & Herring, A. (2021). Effects of multivalent brd vaccine treatment and temperament on performance and feeding behavior responses to a BVDV1b Challenge in Beef Steers. Animals, 11(7), 2133. doi: 10.3390/ani11072133

Ujita, A., Seekford, Z., Kott, M., Goncherenko, G., Dias, N. W., Feuerbacher, E., ... & Mercadante, V. R. (2021). Habituation protocols improve behavioral and physiological responses of beef cattle exposed to students in an animal handling class. animals, 11(8), 2159. doi: 10.3390/ani11082159

Danchuk, V. V. (2006). Peroksydne okysnennia u silskohospodarskykh tvaryn i ptytsi. Kamianets–Podilskyi: Abetka.

Vinyard, J. R., Sarmikasoglou, E., Bennett, S. L., Arce-Cordero, J. A., Aines, G., Estes, K., & Faciola, A. P. (2021). Adaptation of in vitro methodologies to estimate the intestinal digestion of lipids in ruminants. Translational Animal Science, 5(3), txab135. doi: 10.1093/tas/txab135

Xin, X. B., Yang, S. P., Li, X., Liu, X. F., Zhang, L. L., Ding, X. B., ... & Guo, H. (2020). Proteomics insights into the effects of MSTN on muscle glucose and lipid metabolism in genetically edited cattle. General and comparative endocrinology, 291, 113237. doi: 10.1016/j.ygcen.2019.113237

Zeineldin, M., Barakat, R., Elolimy, A., Salem, A. Z., Elghandour, M. M., & Monroy, J. C. (2018). Synergetic action between the rumen microbiota and bovine health. Microbial Pathogenesis, 124, 106-115. doi: 10.1016/j.micpath.2018.08.038

Sinyak, K. M., Orgel, M. Ya., & Kruk, V. I. (1976). Method for the preparation of blood lipids for gas chromatographic research. Labaratorna sprava, 1, 37-41.

Грищук І. А., Карповський В. І. , Данчук В. В., Гутий Б. В. , Куб'як К. , Мідик С. В., Постой Р. В., Трокоз В. О. (2021). ЖИРНОКИСЛОТНИЙ СКЛАД КРОВІ КОРІВ ЗАЛЕЖНО ВІД ТИПУ АВТОНОМНОЇ РЕГУЛЯЦІЇ В ЛІТНІЙ ПЕРІОД.

Ukrainian Journal of Veterinary Sciences, 12(4): 5–16, https://doi.org/10.31548/ujvs2021.04.001

Анотація. *Координація фізіологічної діяльності та інтенсивності обміну речовин у різних органах і тканинах продуктивної тварини залежно від умов середовища та власних потреб забезпечується регуляторною діяльністю відповідних нервових центрів. Проте особливості автономної регуляції нервової системи в цьому питанні можуть суттєво впливати не тільки на фізіологічну діяльність тварин, а й на їхню продуктивність. Тому досить актуальним є питання вивчення впливу автономної регуляції на організм тварин загалом та взаємодії автономної системи та ліпідного обміну.*

Групи тварин формували за допомогою визначення стану серцево-судинної системи за Баєвським. Для дослідження використовували плазму крові, екстракцію ліпідів проводили за методом Фолча. Аналіз жирних кислот проводили на газовому хроматографі Trace GC Ultra (США) з полум'яно-іонізаційним детектором. Дослідженнями встановлено, що відносний вміст насичених жирних кислот був найвищим у крові нормотоніків: на 1,9%, ніж у симпатотоніків і на 0,48%, ніж у ваготоніків. Що стосується концентрації насичених жирних кислот у симпатотоніків, то треба зазначити, що вміст стеаринової кислоти в крові був найвищим (18,07 ± 0,01; P < 0,001) порівнюючи з іншими групами, а насичені жирні кислоти від С6 до С16 характеризувалися найнижчими значеннями в порівнянні до інших дослідних груп (С6:0, P < 0,05; С10:0, P < 0,01; С16:0, P < 0,05).

Загальний вміст ненасичених жирних кислот у плазмі крові тварин, які належать до симпатотоніків і ваготоніків, був відповідно на 1,19% та 0,49% вищим порівнюючи з нормотоніками. Досить цікавим є факт, що симпатотоніки характеризувалися найвищім вмістом поліненасичених жирних кислот, вміст яких знижувався в ряді С18:2n6 > С20:4n6 > С18:3n3 > С22:6n3 > С22:5n3; аналогічну послідовність ми спостерігали і в інших групах, хоча відносна концентрація кислот могла коливатися. Нормотоніки, не дивлячись на те, що мали найнижчий вміст ненасичених жирних кислот, порівнюючи з іншими дослідними групами, однаково за деякими поліненасиченими жирними кислотами (С18:3n3, С22;5n3, С22:6n3) характеризувалися найвищими рівнем (P < 0,05–0,01) порівнюючи з іншими групами, тоді як вміст ненасичених жирних кислот (С18:1n9, С20:3n6) був найнижчим.

Отже, тип нервової діяльності має значний вплив на співвідношення жирних кислот у плазмі крові й автономна регуляція впливає на обмінні процеси в організмі корів.

Ключові слова: *корови, автономна регуляція, ліпіди, жирнокислотний склад*

UDC: 636.09.5:519.245:611.718:591.3 https://doi.org/10.31548/ujvs2021.04.002

APPROXIMATION OF GROWTH INDICATORS AND ANALYSIS OF INDIVIDUAL GROWTH CURVES BY LINEAR DIMENSIONS OF TUBULAR BONES IN CHICKENS OF MEAT PRODUCTION DIRECTION DURING POSTNATAL PERIOD OF ONTOGENESIS

***S. A. TKACHUK*[1],**
Doctor of Veterinary Sciences, Professor, Department of Veterinary Hygiene named after Professor A. K. Skorokhodko
https://orcid.org/0000-0002-6923-1793
E-mail: ohdin@ukr.net
***O. S. PASNICHENKO*[2],**
Candidate of Veterinary Sciences, Assistant, Department of Normal and Pathological Morphology and Forensic Veterinary Medicine
https://orcid.org/0000-0003-0378-8641
E-mail: missKolbeshkina@gmail.com
***L. B. SAVCHUK*[3],**
Candidate of Agricultural Sciences, Associate Professor, Department of Normal and Pathological Physiology and Morphology
https://orcid.org/0000-0002-5720-3533
E-mail: savchuk.2015@ukr.net
[1]National University of Life and Environmental Sciences of Ukraine, 15 Heroyiv Oborony st., Kyiv 03041, Ukraine
[2]Odesa State Agrarian University, 13 Panteleimonovskaya st., Odesa 65012, Odesa, Ukraine
[3]State Agrarian and Engineering University in Podilia, 13 Shevchenko st., Kamianets-Podilskyi 32316, Khmelnytsky region, Ukraine

Abstract. *Medical and biological sciences, including morphology, now require the introduction of the latest information technologies and mathematical methods to process the obtained and accumulated research results. To study the growth dynamics of body weight in domestic birds, classical growth models, Gompertz, were used for the purpose of quantitative description of the growth processes in biological objects, in particular for the growth and development of birds – Von Bertalanffy, Richards, and hyperbolastic models.*

The research material was tubular bones of the thoracic (humerus, ulna, and radius) and pelvic (femur, tibia, and tarsometatarsus) limbs in birds of meat production (broiler chickens and laying hens from the parent broiler flock of Cobb 500 strain) of different age groups during the postnatal period of ontogenesis.

An appropriate regression analysis of experimental data based on known growth models was performed to solve the goal of obtaining growth curves and identifying special points (extremes, inflections, etc.), to build a picture of the overall development of the body as a whole and individual bones of the extremities. The most biologically suitable growth models for describing the growth dynamics of the body as a whole and individual studied bones were determined.

The absence of a unified growth model of linear parameters of different tubular bones in meat-type chickens during the postnatal period of ontogenesis was established. This implies the need for a clear selection of growth models taking into account age, species, breed, keeping and feeding conditions of domestic birds.

The growth model that best describes the body weight dynamics of broiler chickens is the hyperbolastic growth model of the H3 type, and in laying hens from the parent broiler flock – the Brody growth model.

Keywords: *growth models, tubular bones, body weight, meat-type chickens*

Introduction

The size and shape of living organisms are crucial for their survival and reproduction. Morphological adaptations of animals in terms of motor activity or feeding are classic examples in evolutionary biology (Cooney et al., 2016; Pigot et al., 2020). Instead, the dynamics of morphological transformations are mainly the result of the development during ontogenesis. Tubular bones, like most living tissues, are able to adapt their internal microstructure throughout life, and subsequently the associated mechanical properties to its specific mechanical and physiological environment in a process known as bone reconstruction (García-Aznar et al., 2005). Thus, morphological characteristics of tissues, in particular, tubular bones, affect the ability of animals to perform environmentally important tasks that are essential for their growth, survival, and suitability. At the same time, the thoracic and pelvic limbs of birds are specialized to perform various functions. Tubular bone growth and their relationship during ontogenesis are crucial to our understanding of morphological changes among species (Yan & Zhang, 2020).

Therefore, medical and biological sciences, including morphology, currently require the introduction of state-of-the-art information technology and mathematical methods to process the obtained and accumulated research results. Among the various methods in the assessment of morphological adaptations during ontogenesis is the methodology of selection of mathematical models and the formation of qualitative and quantitative patterns that describe the main features of the phenomenon under study. This is the stage where it is necessary to collect data on the structure and nature of this system's functioning, its properties, and manifestations. This stage ends with the creation of a qualitative model of the object (Tabatabai et al., 2007; Ahmadi & Golian, 2008; Dovhan et al., 2009).

Analysis of recent researches and publications

There are different types of housing conditions in poultry. Therefore, it is necessary to use methods with optimal reliability to assess and predict bird health. One such accurate method is nonlinear mathematical models to determine the

dynamics of growth processes, both individual organs and the body as a whole (Porter et al., 2010; Ramos et al., 2013).

At the same time, the relevance of individual selection of these models for different species of domestic animals is noted (Griebeler et al., 2013).

In particular, the linear dimensions of the tubular bones in broilers are more variable than body weight and bone structure. This is proved by the study of forced movement during the day, which affects the change in the length and width of the bones. At the same time, body weight and mineral density are maintained (Pinhasi et al., 2009).

Thus, the relative wing length and load on it affect the bird's ability to fly, and body weight is a contradictory sign of the ability to fly both within and among species (Foutz et al., 2007; Jones et al., 2019).

At the same time, comparing the length growth of the tubular bones of the wing and pelvic limb in birds, it was found that pelvic limb bones grow faster than the wings with a predominance of craniocaudal growth gradient. The study of the proportional bone growth by their length is more important in determining the degree of maturity than just the body mass index (Kaplan et al., 2016).

Classical Gompertz growth models (Cetin et al., 2007; Tjørve et al., 2017) were used to study the growth dynamics of bird body weight, in particular for bird growth and development (Tjørve et al., 2009), Bertalanfi (Tjørve et al., 2010; Zheng et al., 2020), Richards (E. Tjørve et al., 2010; Arando et al., 2021). However, hyperbolastic growth models designed to quantify the growth processes of biological objects are now widely used (Tabatabai et al., 2007).

At the same time, the criteria of compliance and flexibility of growth models were evaluated by comparing the root mean square error, the adjusted coefficient of determination, and the criteria of flexibility. All criteria were then reviewed in a pooled index to determine the most effective model for describing and predicting patterns of turkey body weight gain. The most suitable model for male growth was the logistic model, and for females – the Richards model (Arando et al., 2021).

Today, one of the problems in growing meat-type chickens is lameness, a phenotypic manifestation of different housing conditions. Meat-type chickens gain weight quickly and therefore develop limb disorders that lead to a high mortality rate in heavy birds. It should be noted that many abnormalities in bone development can be initiated at an early age, lameness appears only later due to conformational, environmental, or infectious problems. Some scientists have estimated the prediction of the development of this disease using mathematical models (Huff et al., 2006; Moraes et al., 2007).

The obtained growth rates should be adapted to the selective environmental factors of each bird species. However, the main forces of the growth and development are still unclear, especially when studying several features simultaneously. Therefore, the study of growth patterns can be best performed in poultry due to a sufficient number of indicators for calculation (Remeš et al., 2020).

Determining the parameters of the growth rate is important not only for the biological characteristics and productive qualities of different bird species but also to prevent possible violations of the integrity of the organism that occur at different stages of the postnatal ontogenesis.

The purpose of the study is to select methods for determining approximation growth models and individual growth

curves for body weight, length, sagittal and segmental diameters of the studied bones of the thoracic and pelvic limbs in broiler chickens and laying hens of the broiler parent flock.

Materials and methods of research

The object of the study were broiler chickens of the Cobb 500 strain at the age of 1, 8, 15, 22, 28, 43, and 50 days and laying hens of the broiler parent flock of the same strain at the age of 1, 10, 51, 114, 175, 228, 350, and 410 days. In both age groups, the selection deadlines coincided with the technological cycle of use.

Broiler chickens were raised in the production enterprise CJSC Complex Agromars, a village of Gavrylivka (Kyiv region), and laying hens of the parent flock of broilers in the conditions of the production enterprise LLC Ruby Roses Agricol Co., LTD, a village of Morozivka (Kyiv region).

The studied poultry was kept in "floor" conditions according to the generally accepted technology for meat-type chickens. The feeding diet was balanced in terms of nutrients according to age.

After slaughter, the chickens were weighed on Casio HL-4 electronic scales and the bones of the thorax (wings) and pelvis were removed by standard methods.

The research material was tubular bones of the thoracic (humerus, ulna, and radius) and pelvic (femur, tibia, and tarsometatarsus) limbs of poultry meat production (broiler chickens and laying hens of the parent flock of cross-bred Cobb 500 broilers of different age groups, postnatal period of ontogenesis.

First of all, the linear dimensions were determined according to the generally accepted scheme, which was tested on different mammal species and humans using a caliper U-10 (022504) with an accuracy of 0.05 mm. In total, 3150 measurements were performed according to the measurement scheme. Data on linear dimensions in millimeters were entered into osteological charts and subjected to statistical processing to obtain average values.

To solve this goal, to obtain growth curves and identify special points (extrema, inflections, etc.) to build a picture of the overall development of the body as a whole and individual limb bones, a corresponding regression analysis of experimental data based on known growth models was performed. We determined the most biologically suitable growth models for describing the growth dynamics of the body as a whole and individual studied bones. The approximation of each of these functions was evaluated by the values of biologically determined parameters, in particular, the indicator in chicken hatching, the indicator in the asymptotics (i.e. the indicator for the adult organism) for biological reasons and the value of standard deviation (SD).

The above calculations were carried out by means of the Wolfram Mathematica 6.0 mathematical package using the Levenberg-Markart algorithm in order to solve the corresponding optimization problems.

In this work, the abbreviated notation of the selected growth functions in the form: $w\ (t)$ – body weight, $l\ (t)$ – bone length, $a\ (t)$ – sagittal diameter, $e\ (t)$ – segmental diameter, with the symbol t affects a certain moment in the life (i.e. age) of the bird. The symbols w, l, a, and e are also used in the indices to denote other growth characteristics (growth rates, inflection points, etc.). The generalized parameter (w, l, a, and e) is denoted by the symbol p.

It was also found necessary to establish

the features of individual growth curves *w (t)* and for the tubular bones of the limbs in broiler chicken *a (t), e (t),* and *l (t)*, in particular, the age of maximum growth rate *(T)* and the maximum growth rate *(V)*, the current relative growth rate *(Q)*, the age position of the maximum relative growth rate *(C)* and the maximum relative growth rate *(N)*. If the parameters of the selected growth functions are available, the calculation of *T, V, N,* and *Q* becomes a trivial arithmetic problem.

Results of the research and their discussion

To solve this goal, the selection of methods and their generalization was carried out. Growth curves (functions) for body weight, length, sagittal and segmental diameters of the studied bones of the thoracic and pelvic limbs of broiler chickens and laying hens of the parent broiler flock were determined by the selected method.

The generalized values of the obtained biologically significant results of approximation of growth parameters of tubular bones for broiler chickens are given in Tables 1–3.

From the indicators shown in Table 1, it follows that they can be used to select the most successful models to describe *l (t)* for the corresponding bones in broiler chickens. The defined models in the specified Table are marked in bold.

By pointing to the indicators in Table 2, you can turn the most distant models for the description of *a (t)* for the type of bones in chicken broilers. The model values in the table are also indicated in bold.

Using the indicators presented in Table 3, models can be used to describe the growth of *e (t)* of tubular bones in broiler chickens. The models selected for the description in the table are also marked in bold.

In addition, according to the principle of analogy, an approximation of the growth indices for broilers was carried out, the results of that for hatched, the definitive mass of broilers, and the root mean square error are presented in Table 4.

The results of Table 5 are followed by the preference of the model H3 to describe *w (t)* in broilers.

However, an approximation of the corresponding experimental data of laying hens was performed. The same model functions were tested as in the case of broiler chickens (Tables 5–7).

From the indicators given in Table 5, it follows that they can be used to select the most successful models to describe *l (t)* for the corresponding tubular bones in the hens of the parent flock. The defined models in the specified the table are marked in bold.

From the indicators given in Table 6, you can choose the most successful models to describe *a (t)* of the corresponding bones in chickens of the parent flock. The defined models in the specified Table are also marked in bold.

From the indicators given in Table 7, you can choose the most successful models to describe *e (t)* of the corresponding bones in chickens of the parent flock. The defined models in the specified Table are also marked in bold.

The mentioned model functions were also tested to approximate the weight gain of laying hens. Biologically significant results of these tests are presented in Table 8.

For the convenience of further analyzes of all types, the selected model functions are summarized together with the corresponding parameters in a separate Table 9.

The information in Table 9 is the basic information for further studies of growth processes in tubular bones of experimental birds.

The analysis of the data given in

1. Biologically determined indicators of different approximation of growth models for l (t) of tubular bones in broiler chickens, mm

Selected growth models	The name of the bone					
	Humerus			Ulna		
	l_∞	l_0	*SD*	l_∞	l_0	*SD*
Von Bertalanffy	141.717	30.404	3.319	74.003	11.453	2.230
Brody	540.200	30.335	3.469	**80.234**	**8.503**	**1.659**
Gompertz	89.017	28.933	3.883	72.262	12.460	2.609
Logistic	99.442	30.448	3.110	70.702	13.427	3.126
Richards	82.730	27.927	5.705	71.663	10.258	2.502
Weibull	68.426	34.481	1.548	90.348	3.926	1.527
H1	92.677	30.503	3.016	79.549	5.532	1.375
H2	68.093	34.279	1.365	99.547	1.111	1.525
H3	**70.056**	**33.910**	**1.635**	94.255	3.150	1.504
	Radius			Femur		
	l_∞	l_0	*SD*	l_∞	l_0	*SD*
Von Bertalanffy	64.716	9.038	7.850	74.003	11.453	2.230
Brody	**67.864**	**5.288**	**7.446**	80.234	8.503	1.659
Gompertz	63.795	10.206	8.138	72.262	12.460	2.609
Logistic	62.978	11.270	8.514	70.702	13.427	3.126
Richards	69.692	2.575	7.402	**71.663**	**10.258**	**2.502**
Weibull	68.703	4.497	7.441	140.623	14.628	4.305
H1	65.874	4.806	7.090	91.167	14.549	4.022
H2	71.262	2.539	7.549	116.966	11.932	4.249
H3	68.727	4.474	7.441	118.318	14.984	4.285
	Tarsometatarsus			Tibia		
	l_∞	l_0	*SD*	l_∞	l_0	*SD*
Von Bertalanffy	94.781	20.528	1.747	117.503	10.927	16.258
Brody	113.119	19.463	2.165	132.080	4.537	14.775
Gompertz	90.265	20.971	1.588	**114.094**	**12.916**	**17.784**
Logistic	**85.788**	**21.563**	**1.405**	111.685	14.447	19.596
Richards	92.225	20.813	1.654	131.979	4.578	14.775
Weibull	83.206	23.838	1.469	131.060	4.888	14.774
H1	83.023	21.891	1.281	126.765	4.147	14.698
H2	82.247	22.552	1.301	145.129	0.644	14.896
H3	74.250	74.250	1.288	113.474	8.257	15.631

Note: The growth models highlighted in bold type are the most acceptable in terms of the biological change p_0, $p\infty$ and the accuracy of the description of the experimental data.

2. Biological values of the indicators of the approximate of growth models of a (t) of tubular bones in broiler chickens, mm

Selected growth models	The name of the bone					
	Humerus			Ulna		
	$a_\infty \times 10$	$a_0 \times 10^2$	$SD \times 10^4$	$a_\infty \times 10$	$a_0 \times 10^3$	$SD \times 10^3$
Von Bertalanffy	8.747	10.331	9.024	6.387	13.077	1.661
Brody	9.664	6.756	11.195	7.052	0	2.355
Gompertz	8.511	11.498	8.270	6.330	29.534	1.694
Logistic	8.334	12.574	7.641	6.299	39.148	1.726
Richards	8.534	11.380	8.346	6.431	3.001	1.654
Weibull	8.046	16.559	7.395	6.309	6.191	1.562
H1	8.158	13.123	6.911	6.350	13.605	1.616
H2	**8.082**	**15.192**	**7.013**	6.415	14.650	1.710
H3	8.242	15.333	7.664	8.560	≈ 0	2.445
	Radius			Femur		
	$a_\infty \times 10$	$a_0 \times 10^2$	$SD \times 10^4$	$a_\infty \times 10$	$a_0 \times 10^3$	$SD \times 10^4$
Von Bertalanffy	4.245	6.097	2.303	9.075	108.711	4.173
Brody	5.203	5.334	2.748	10.010	66.739	3.097
Gompertz	4.035	6.401	2.129	**8.838**	**122.809**	**5.172**
Logistic	3.875	6.739	1.963	8.649	134.699	6.519
Richards	4.036	6.399	2.130	10.302	55.026	3.070
Weibull	3.573	9.030	1.624	35.224	50.607	7.014
H1	3.726	7.132	1.786	21.631	36.929	3.134
H2	3.593	8.415	1.654	11.836	4.752	3.050
H3	**3.513**	**7.638**	**1.537**	10.742	71.479	3.011
	Tarsometatarsus			Tibia		
	$a_\infty \times 10$	$a_0 \times 10^2$	$SD \times 10^3$	$a_\infty \times 10$	$a_0 \times 10^2$	$SD \times 10^4$
Von Bertalanffy	6.832	8.890	1.303	8.488	12.654	11.519
Brody	7.634	6.480	1.411	9.324	8.899	8.618
Gompertz	6.631	9.740	1.269	8.265	13.922	12.936
Logistic	6.475	10.566	1.242	**8.065**	**15.067**	**14.607**
Richards	6.641	9.700	1.271	14.327	≈ 0	6.194
Weibull	6.283	12.941	1.234	18.160	≈ 0	6.052
H1	6.371	9.890	1.213	16.706	4.9068	6.054
H2	**6.345**	**11.547**	**1.229**	18.215	≈ 0	6.328
H3	9.279	6.880	1.418	18.162	≈ 0	6.052

Note: The growth models highlighted in bold type are the most acceptable in terms of the biological change p^0, p^∞ and the accuracy of the description of the experimental data.

3. Biological values of indicators of the approximate of growth models for *e (t)* of tubular bones in broiler chickens, mm

Selected growth models	The name of the bone					
	Humerus			Ulna		
	$e_\infty \times 10$	$e_0 \times 10^2$	$SD \times 10^4$	$e_\infty \times 10$	$e_0 \times 10^2$	$SD \times 10^4$
Von Bertalanffy	6.731	7.848	13.302	4.824	7.762	6.534
Brody	7.125	4.612	16.506	5.014	5.679	7.823
Gompertz	6.620	8.833	11.954	4.766	8.399	6.018
Logistic	6.537	9.808	10.660	4.715	9.169	5.432
Richards	6.612	8.824	11.981	4.767	8.386	6.219
Weibull	6.292	17.515	6.265	4.574	14.016	3.974
H1	6.449	10.819	8.794	4.636	9.837	4.835
H2	6.298	16.879	5.645	**4.570**	**13.596**	**3.893**
H3	**6.268**	**12.453**	**3.608**	5.975	6.23	8.336
	Radius			Femur		
	$e_\infty \times 10$	$e_0 \times 10^2$	$SD \times 10^4$	e_∞	$e_0 \times 10^2$	$SD \times 10^4$
Von Bertalanffy	3.178	6.317	9.398	0.967	11.097	4.637
Brody	3.506	5.970	10.157	1.046	6.300	6.055
Gompertz	3.143	6.457	9.047	0.946	12.636	4.536
Logistic	3.024	6.727	8.571	**0.930**	**13.983**	**4.771**
Richards	3.113	6.457	9.039	0.949	1.2347	4.530
Weibull	**2.835**	**10.517**	**5.364**	1.003	8.701	5.355
H1	2.983	6.824	8.085	0.939	8.718	4.395
H2	2.841	10.392	5.393	0.956	10.439	4.556
H3	4.253	6.251	10.139	1.147	6.772	6.230
	Tarsometatarsus			Tibia		
	e_∞	$e_0 \times 10^2$	$SD \times 10^4$	$e_\infty \times 10$	$e_0 \times 10^2$	$SD \times 10^4$
Von Bertalanffy	1.148	1.943	5.537	16.918	2.355	13.934
Brody	1.314	1.678	5.584	208.251	2.332	15.063
Gompertz	1.106	2.043	5.768	14.001	2.368	13.433
Logistic	1.068	2.148	6.262	12.140	2.386	12.867
Richards	1.203	1.838	5.466	16.496	2.340	13.955
Weibull	1.194	1.926	5.456	9.148	2.905	8.457
H1	1.113	1.417	5.943	10.904	2.414	12.243
H2	1.197	1.494	5.565	9.084	2.827	9.500
H3	**1.567**	**1.546**	**5.595**	**9.168**	**2.935**	**8.557**

Note: The growth models highlighted in bold type are the most acceptable in terms of the biological change p^0, p^∞ and the accuracy of the description of the experimental data.

4. Summary table of results of approximation of growth data of body weight in broiler chickens, g

Growth model	w_∞	w_0	*SD*
Von Bertalanffy	3656.92	0.43	2922.63
Brody	1.79×10^8	< 0	16500.90
Gompertz	3133.92	18.50	2125.19
Logistic	2983.12	28.10	1993.54
Richards	3124.92	18.33	2125.20
Weibull	263.95	51.39	2592.46
H1	2660.35	40.00*	2372.43
H2	2765.47	40.00	2138.05
H3	**2813.69**	40.00	**2304.35**

Note: * When approximated by hyperbolastic functions, it was taken into account that the average body weight of broiler chickens at the time of hatching is at the level of 40 g. The growth models highlighted in bold type are the most acceptable in terms of the biological change p^0, p^∞ and the accuracy of the description of the experimental data.

Table 9 shows the acceptability of the hyperbolastic model of type H3 for the formation of body weight because this model gives the most biologically probable indicators of p_0 and p under the lowest value of R_2.

Different parametric models are acceptable for the studied linear parameters of tubular bones, which indicates the need to select growth models for each case in the study of different species of animals (Zheng et al., 2020).

For the analysis of individual growth curves, information on the characteristics of individual growth curves, in particular, the values of $p\infty$, p_0, *T, V,* and *N*, may be of some practical interest. We have performed a comparative analysis of these characteristics for different *p* of a particular bone (Yan & Zhang, 2020).

In order to obtain the values of *T, V,* and *N* for *p* bones, the known technology of finding the inflection points of analytical functions was used. Therefore, the search for inflection points is actually reduced to finding the roots of the second derivatives of the growth function from Table 9.

For relatively simple growth functions (Weibull, Gompertz), which have a simple form of the second derivative, this problem was solved analytically (Tjørve et al, 2017). For other growth functions (hyperbolastic), the problem of finding these roots was solved by numerical methods of the Wolfram Mathematica® 6.0 package. The results of these calculations for *T, V,* and *N* are presented in Table 10.

Dashes indicate no inflection point. In this case, the absolute growth rate has the maximum value during hatching and gradually decreases with age.

From Table 10, it is seen that all tubular bones of laying hens are characterized by the absence of the inflection point on the growth curves *a (t)*, which causes the absence of a period of intensive growth in the growth of sagittal diameter at the beginning of the postnatal period of ontogenesis.

That is, the maximum growth rate of this diameter is at the beginning of the postnatal period and in subsequent age periods only decreases. This increase in

5. Biologically determined indicators of different approximation of growth models for l (t) of tubular bones in laying hens, mm

Selected growth models	The name of the bone					
	Humerus			Ulna		
	l_∞	l_0	$SD\times10^2$	l_∞	l_0	$SD\times10^3$
Von Bertalanffy	8.267	1.123	5.237	8.710	1.362	17.389
Brody	8.253	1.650	4.732	8.660	1.775	29.392
Gompertz	8.247	1.797	4.570	8.637	1.895	36.218
Logistic	8.238	1.947	4.428	8.607	2.000	46.305
Richards	8.249	1.757	4.615	8.769	$< 10^{-3}$	9.627
Weibull	8.227	2.258	4.341	8.897	< 0	4.541
H1	8.226	2.401	4.364	**8.895**	**0.248**	**4.536**
H2	**8.225**	**2.178**	**4.364**	8.980	0.078	4.178
H3	8.508	< 0	9.495	9.005	0.692	4.100
	Radius			Femur		
	l_∞	$l_0\times10$	$SD\times10^3$	l_∞	l_0	$SD\times10^4$
Von Bertalanffy	7.490	6.436	10.251	9.664	1.155	53.749
Brody	7.477	12.329	7.909	9.622	1.700	11.180
Gompertz	7.470	13.836	7.369	9.603	1.853	15.645
Logistic	7.463	15.203	7.150	9.579	1.993	42.677
Richards	7.471	13.620	7.434	9.618	1.737	10.814
Weibull	**7.462**	**15.650**	**6.980**	9.613	1.797	9.501
H1	7.463	10.071	7.160	9.618	0.785	10.717
H2	7.462	15.437	7.223	9.623	1.590	13.372
H3	8.282	2.573	101.612	**9.613**	**1.640**	**9.051**
	Tarsometatarsus			Tibia		
	l_∞	l_0	$SD\times10^3$	l_∞	l_0	$SD\times10^2$
Von Bertalanffy	8.703	0.755	5.262	13.080	1.818	7.135
Brody	8.679	1.389	3.033	13.042	2.526	4.548
Gompertz	8.668	1.552	2.987	13.002	2.939	2.789
Logistic	8.656	1.695	3.688	13.002	2.939	2.789
Richards	8.673	1.488	2.932	13.026	2.718	3.693
Weibull	7.171	1.500	2.803	**12.960**	**3.555**	**2.167**
H1	8.673	0.667	2.954	13.023	1.299	3.971
H2	8.674	1.425	3.094	12.962	3.326	2.230
H3	**8.671**	**1.487**	**2.802**	13.097	1.277	22.192

Note: The growth models highlighted in bold type are the most acceptable in terms of the biological change p^0, p^∞ and the accuracy of the description of the experimental data.

6. Biologically determined indicators of different approximation of growth models for a (t) of tubular bones in laying hens, mm

Selected growth models	The name of the bone					
	Humerus			Ulna		
	$a_\infty \times 10$	$a_0 \times 10^2$	$SD \times 10^3$	$a_\infty \times 10$	$a_0 \times 10$	$SD \times 10^5$
Von Bertalanffy	9.337	22.541	2.063	7.651	1.804	13.060
Brody	9.270	25.324	2.193	7.604	2.043	13.886
Gompertz	12.556	26.329	2.269	7.584	2.133	16.285
Logistic	9.199	27.529	2.414	7.554	2.250	22.757
Richards	9.504	0	1.933	7.633	1.900	12.690
Weibull	9.752	0	1.876	7.626	1.948	12.476
H1	10.978	4.242	1.870	7.630	1.013	11.959
H2	10.000	1.475	1.849	7.650	1.724	13.899
H3	**9.937**	**19.698**	**1.809**	**7.598**	**1.703**	**7.161**
	Radius			Femur		
	$a_\infty \times 10$	$a_0 \times 10^2$	$SD \times 10^5$	$a_\infty \times 10$	$a_0 \times 10^3$	$SD \times 10^4$
Von Bertalanffy	4.403	19.742	14.229	8.847	240.409	5.624
Brody	**3.679**	**12.836**	**14.870**	8.802	267.164	7.194
Gompertz	4.325	20.343	17.401	8.780	276.452	8.059
Logistic	4.280	20.765	20.272	8.740	286.197	9.743
Richards	4.465	19.367	12.435	8.953	3.208	3.646
Weibull	26.010	7.303	4.094	9.078	0	3.350
H1	7.813	10.784	2.988	9.770	39.013	3.720
H2	> 100	2.381	3.909	9.244	18.202	3.474
H3	16.318	≈ 0	3.369	**9.400**	**197.614**	**3.713**
	Tarsometatarsus			Tibia		
	$a_\infty \times 10$	$a_0 \times 10^4$	$SD \times 10^4$	$a_\infty \times 10$	$a_0 \times 10$	$SD \times 10^4$
Von Bertalanffy	6.859	1664.399	3.725	8.177	2.444	13.955
Brody	6.801	1878.231	5.165	8.163	2.648	12.260
Gompertz	6.776	1957.349	5.949	8.156	2.725	11.575
Logistic	6.737	2043.843	7.359	8.143	2.859	10.540
Richards	7.027	0	1.964	8.157	2.719	11.635
Weibull	7.241	0	1.546	8.210	1.096	19.261
H1	8.207	316.356	1.412	8.138	2.902	10.165
H2	**7.664**	**5.159**	**1.432**	8.113	3.201	9.538
H3	7.408	1432.926	1.861	**8.129**	**2.785**	**8.073**

Note: The growth models highlighted in bold type are the most acceptable in terms of the biological change *p0, p∞* and the accuracy of the description of the experimental data.

the sagittal diameter can be explained by the predominance of factors inhibiting the growth of sagittal diameter of tubular bones over the factors of its acceleration. Moreover, this prevalence is observed throughout the postnatal period of ontogenesis (experimental) laying hens of the parent broiler herd (Remeš et al., 2020).

In addition to the sagittal diameter, we can assume that this behavior is also

7. Biologically determined indicators of different approximation of growth models for e (t) of tubular bones in laying hens, mm

Selected growth models	The name of the bone					
	Humerus			Ulna		
	$e_\infty \times 10$	$e_0 \times 10^3$	$SD \times 10^3$	$e_\infty \times 10$	$e_0 \times 10$	$SD \times 10^4$
Von Bertalanffy	7.504	< 0	7.269	4.898	1.293	6.992
Brody	7.504	< 0	7.269	4.892	1.480	6.854
Gompertz	7.504	7.335	7.269	4.889	1.542	6.818
Logistic	7.504	19.154	7.269	4.883	1.628	6.807
Richards	7.504	≈ 0	7.269	4.889	1.542	6.819
Weibull	7.504	≈ 0	7.269	**4.885**	**1.684**	**6.760**
H1	**7.504**	**44.660**	**7.269**	4.885	1.278	6.801
H2	7.504	68.999	7.269	4.883	1.627	6.824
H3	8.037	≈ 0	8.834	4.851	1.471	6.947
	Radius			Femur		
	$e_\infty \times 10$	$e_0 \times 10^4$	$SD \times 10^4$	$e_\infty \times 10$	$e_0 \times 10^2$	$SD \times 10^4$
Von Bertalanffy	3.725	1211.982	12.068	9.385	22.152	7.051
Brody	3.679	1283.649	14.870	9.350	25.761	8.368
Gompertz	3.663	1313.890	16.311	9.333	26.881	9.065
Logistic	3.635	1361.934	19.325	9.304	28.003	1.025
Richards	4.271	3.126	6.334	9.443	0	5.642
Weibull	5.465	0	6.240	9.495	≈ 0	5.284
H1	**4.249**	**4205.523**	**6.155**	**9.508**	**4.343**	**5.145**
H2	5.678	19.083	6.291	9.576	2.891	5.515
H3	5.085	5082.130	51.317	9.495	≈ 0	5.284
	Tarsometatarsus			Tibia		
	e_∞	$e_0 \times 10^3$	$SD \times 10^4$	$e_\infty \times 10$	$e_0 \times 10^2$	$SD \times 10^3$
Von Bertalanffy	1.041	303.583	37.973	9.119	16.462	2.685
Brody	1.035	330.393	58.633	9.083	20.543	2.702
Gompertz	1.032	340.334	70.144	9.065	21.777	2.724
Logistic	1.026	352.342	93.784	9.040	23.046	2.770
Richards	1.061	3.573	10.822	9.115	17.063	2.685
Weibull	1.078	9.305	7.581	9.110	17.127	2.685
H1	**1.077**	**75.400**	**7.611**	9.115	7.365	2.686
H2	1.107	36.377	7.606	9.117	16.370	2.691
H3	1.115	269.22	9.726	**9.115**	**16.497**	**2.684**

Note: The growth models highlighted in bold type are the most acceptable in terms of the biological change p0, p∞ and the accuracy of the description of the experimental data.

8. Summary table of results of approximation of growth data of body weight in laying hens, g

Growth model	w_∞	w_0	*SD*
Von Bertalanffy	243.33	5245.90	57732.70
Brody	47.01	**6537.61**	**33784.10**
Gompertz	352.748	4913.25	86110.70
Logistic	0	7870.24	31754.24
Richards	315.98	5031.62	73448.55
Weibull	≈ 0	8560.02	31317.92
H1	50.00	63808.20	35682.28
H2	50.00	6899.78	38404.96
H3	50.00	7952.67	32249.47

Note: The growth models highlighted in bold type are the most acceptable in terms of the biological change p0, p∞ and the accuracy of the description of the experimental data.

9. The most acceptable approximations of the growth of tubular bones and body weight in broiler chickens and laying hens, mm

The name of the bone	*l* (*t*)	*a* (*t*)	*e* (*t*)
Broiler chickens *w* (*t*): H3: *M* = 2713.69, α = 2673.69, β = 0.000181414, γ = 2.41066, θ = 0.00166361			
Humerus	H3: M = 70.0562 α = 36.1457 β = 0.000633271 γ = 2.119 θ = 7.21822×10^{-6}	H2: M = 0.808165 α = 4.90089 β = 0.11606 γ = 1.0387	H3: M = 0.625752 α = 0.501221 β = 6.97168×10^{-6} γ = 3.72442 θ = 0.02516
Ulna	Brody: B = 0.894021 k = 0.0351153 M = 80.234	-	H2: M =0.458035 α =2.68738 β = 0.0487252 γ = 1.50633
Radius	Brody: B = 0.922084 K = 0.0461969 M = 67.8641	H3: M = 0.351316 α = 0.274938 β = 0.0000517819 γ = 2.86125 θ = 0.018792	Weibull: k = 0.0000316808 m = 0.105182 M = 0.179191 β = 3.26981
Femur	Ричардс: B = 0.570888 k = 0.0571839 M = 71.6627 μ = 2.29763	Gompertz: L = 1.97354 M = 0.883751 α = 0.0694911	Logistic: k = 0.0879022 M = 0.929591 μ = 2.73291
Tibia	Gompertz: L = 2.17857 M = 114.094 α = 0.0683775	Logistic: k = 0.068346 M = 0.806512 μ = 2.4203	H3: M = 0.914752 α = 0.624297 β = 0.00064504 γ = 2.13112 θ = 0

Tarsometatarsus	Logistic: k = 0.0551342 M = 85.7876 μ = 1.99219	H2: M = 0.634489 α = 5.09938 β = 0.194285 γ = 0.936812	H3: M = 1.56447 α = 1.41006 β = 0.0112256 γ = 0 θ = 0.0208725
Laying hens *w* (*t*): Brody: *M* = 6537.61, *B* = 0.992808, *k* = 0.00333459			
Humerus	H2: M = 8.22537 α = 3.15005 β = 0.00510514 γ = 1.02602	H3: M = 0.99373 α = 0.796746 $\beta = 7.30852\times10^{-7}$ γ = 2.14373 θ = 0.0173553	H1: M = 0.750404 α = 15.8027 β = 0.200098 θ = 0.180303
Ulna	H1: M = 8.89477 α = 36.3884 β = 0.00721397 θ = 0.800526	H3: M = 0.759775 α = 0.589478 $\beta = 9.01315\times10^{-9}$ γ = 3.58625 θ = 0.0164941	Weibull: M = 0.320103 k = 0.00709267 m = 0.168373 β = 1.27428
Radius	Weibull: M = 5.89785 k = 0.00656149 m = 1.56503 β = 1.34392	Von Bertalanffy: B = 0.296024 k = 0.00986984 M = 0.367936	H1: M = 0.42479 α = 9.10076 β = 0.00558144 θ = 0.467032
Femur	H3: M = 9.61272 α = 7.97292 β = 0.0233235 γ = 1.06994 θ = -0.0114563	H3: M = 0.94003 α = 0.742415 β = 0 γ = 0.669368 θ = 0.216069	H1: M = 0.950838 α = 20.8933 β = 0.00873147 θ = 0.832502
Tibia	Weibull: k = 0.00164194 m = 3.55469 M = 9.40693 β = 1.60955	H3: M = 0.812858 α = 0.534372 $\beta = 1.64534\times10^{-8}$ γ = 3.73593 θ = 0.0139368	H3: M = 0.911457 α = 0.74649 β = 0.0263728 γ = 0.998023 θ = -0.00499139
Tarsometatarsus	H3: M = 8.67074 α = 7.18375 β = 0.00864064 γ = 1.24041 θ = 0.00171335	H2: M = 0.766396 α = 1684.22 β = 6.68533 γ = 0.107594	H1: M = 1.07727 α = 13.2873 β = 0.00474761 θ = 0.669921

observed in the growth and development of the segmental diameter of the radial, femoral, tibial, and metatarsal bones, in which *T* is quite close to 0.

Only for the humerus and ulna, the growth curve of segmental diameter has a significant (quite distant from 0) inflection point, which may be due to the influence of torsional loads, which have a fairly high level of action in these bones.

However, a completely different picture is observed regarding the distribution of inflection points in the tubular bones of broiler chickens, where all inflections (except T_l of ulna and T_e of tarsometatarsus) are reliable. In addition, the T_e of the humerus and ulna in chickens is larger than the corresponding parameters of laying hens.

The presence of inflection *a (t)* of tubular bones in chickens, in contrast

10. Individual characteristics of the development of individual tubular bones in experimental birds birds

The name of the bone	$l(t)$	$a(t)$	$e(t)$
Broiler chickens$w(t)$: $T = 27.737$, $V = 72.654$, $N = 5.882\times10^{-2}$, C = 5.58461			
Humerus	$T = 23.904V = 9.977\times10^{-1}N = 2.047\times10^{-2}$ C = 19.2213	$T = 16.033V = 2.162\times10^{-2}N = 5.119\times10^{-2}$ C = 5.16865	$T = 19.556$ $V = 2.153\times10^{-2}$ $N = 5.046\times10^{-2}$ C = 0
Ulna	-	$T = 6.605V = 3.043\times10^{-2}N = 1.996\times10^{-1}$ C = 0.675032	$T = 16.396V = 1.458\times10^{-2}N = 5.060\times10^{-2}$ C = 11.6958
Radius	-	$T = 21.158$ $V = 8.23938\times10^{-3}N = 3.81449\times10^{-2}$ C = 0	$T = 21.257V = 9.55721\times10^{-3}N = 4.90442\times10^{-2}$ C = 17.9777
Femur	$T = 4.745V = 1.952N = 1.013\times10^{-1}$ C = 0	$T = 9.783V = 2.259\times10^{-2}N = 6.949\times10^{-2}$ C = 0	$T = 11.437V = 2.551\times10^{-2}N = 6.435\times10^{-2}$ C = 0
Tibia	$T = 11.388V = 2.870N = 6.838\times10^{-2}$ C = 0	$T = 12.933V = 1.689\times10^{-2}N = 4.836\times10^{-2}$ C = 0	$T = 23.333V = 1.780\times10^{-2}N = 3.251\times10^{-2}$ C = 16.3312
Tarsometatarsus	$T = 12.502V = 1.400N = 3.671\times10^{-2}$ C = 0	$T = 15.326V = 1.520\times10^{-2}N = 4.872\times10^{-2}$ C = 0	-
Laying hens $w(t)$: there is no inflection point			
Humerus	$T = 27.8238V = 0.0937657N = 0.0213174$ C = 7.76348	-	$T = 13.9236V = 0.0305553N = 0.084365$ C = 0
Ulna	$T = 1.31197V = 0.313971N = 0.514416$ C = 0	-	$T = 14.5581$ $V = 0.00486297$ $N = 0.0211101$ C = 0
Radius	$T = 15.2725$ $V = 0.102825$ $N = 0.0354976$ C = 5.61676	$T < 0$	$T = 0.388981V = 0.0190749N = 0.386832$ C = 0
Femur	$T = 7.02549V = 0.123033N = 0.0501829$ C = 1.64339	-	$T = 0.983014V = 0.047113N = 0.547511$ C = 0
Tibia	$T = 29.3819V = 0.133631N = 0.0204947$ C = 2.77722	-	-
Tarsometatarsus	$T = 10.6745V = 0.123758N = 0.0462142$ C = 15.8117	-	$T = 0.646768$V = $0.0559817N = 0.50977$ C = 0

Note: Units: T – day, V – g/day in the case of w (t) or mm/day in other cases, N – day-1, C – day.

to laying hens, may be explained by the conditions of keeping these birds that change the biological patterns of ontogenetic growth, which are manifested in chickens of the parent broiler flock.

Broilers are kept in conditions aimed at maintaining the maximum rate of weight gain. In this case, this rate of mass growth may occur due to the suboptimal functioning of other parts of the body. Therefore, the factors influencing the diametrical development of bones in the case of broiler chickens are more unpredictable, which may cause an abnormally

large acceleration of diametrical bone growth in broiler chickens during the 6th–23rd day of the postnatal period.

The pattern of growth of the bone length of the extremities is more stable. Both broiler chickens and laying hens have T_l (except for the radial bone). Given the proximity to 0 T_l of the ulna in laying hens, the patterns of distribution of acceleration and inhibition factors in increasing the length of the tubular bones of broiler chickens and laying hens can be considered qualitatively similar. The exclusion of the radial bone from the general picture may be explained by the increased growth rate of those tubular bones in the wing that perceive the force of torsional, bending loads in broiler chickens against the background of limited overall metabolism, which causes virtually no factors accelerating radial bone growth. This bone mainly performs the auxiliary function of the lever of movements, which holds the muscle groups and has no significant longitudinal loads (Blom & Clas, 2004).

Analysis of the V_l values of the respective bones in broiler and laying hens indicates an increased growth rate of tubular bone length in chickens compared to laying hens, due to housing conditions that contribute to a rapid weight gain of birds. However, a similar pattern is observed for the values of V_e of ulna and humerus.

Maximum relative velocities do not give a clear comparative picture between broiler chickens and laying hens, which may be due to the behavior of the growth curve of the bird's body weight. Thus, for broilers, it was found that $T_w \approx 28$ days, and in the general case indicates a later period of inhibition of development of the whole organism than individual tubular bones.

However, for laying hens, no inflection points were found at all in the body weight growth curve, which may also be caused by the conditions of the bird, aimed at the optimal physiological functioning of all parts of the body.

Conclusions and future perspectives

The main purpose of the selection of mathematical models is the formation of qualitative and quantitative patterns of age development of the studied objects. The growth models used in the studies may be of practical value for assessing the dynamics of changes in body weight and linear parameters of tubular bones. Therefore, the most acceptable growth models for these parameters should be recommended for widespread use in poultry farming to increase poultry meat productivity.

The performed approximation analysis makes it possible to analytically determine the age periods of the prevalence of one parameter over another and comparative analysis between different tubular bones allows to analyze their functional activity at different age periods.

In addition, a comparative analysis of similar parameters between broiler chickens and laying hens allows us to draw some conclusions about the influence of housing conditions and genetics on the development of similar tubular bones in chickens.

The lack of a unified growth model of the linear parameters of different tubular bones in meat-type chickens during the postnatal period of ontogenesis indicates the need for a clear selection of growth models taking into account age, species, breed, housing and feeding conditions. The growth model that best describes the body weight dynamics of broiler chickens is the hyperbolastic growth model of the H3 type, and the laying hens of the parent broiler flock are the Brody growth model.

In the future, we plan to compare the growth rate of body weight, as an integral characteristic of the development of the organism, with the growth rate of individual tubular bones.

References

Ahmadi, H., & Golian, A. (2008). Non-linear hyperbolastic growth models for describing growth curve in classical strain of broiler chicken. Research Journal of Biological Siences, 3(11), 1300-1304. doi: rjbsci.2008.1300.1304

Arando, A., González-Ariza, A., Lupi, T. M., Nogales, S., León, J. M., & Navas-González, F. J. (2021). Comparison of non-linear models to describe the growth in the Andalusian turkey breed. Italian Journal of Animal Science, 20(1), 1156-1167. doi: 10.1080/1828051X.2021.1950054

Blom, J., & Clas, L. (2004). A comparative study of growth, skeletal development and eggshell composition in some species of birds. Journal of Zoology, 262(4), 361-369. doi: 10.1017/S0952836903004746

Cetin, M., Sengul, T., Sogut, B., & Yurtseven, S. (2007). Comparison of growth models of male and female Partridges. Journal of Biological Science, 7(6), 964-968. doi: 10.3923/jbs.2007.964.968

Cooney, C. R., Seddon, N., & Tobias, J. A. (2016). Widespread correlations between climatic niche evolution and species diversification in birds. Journal Animal Ecology, 85(4), 869-878. doi: 10.1111/1365-2656.12530

Dovhan, Y. P., Hladkykh, V. Yu., & Shevchuk, Yu. H. (2009). Zastosuvannia metodu matematychnoho modeliuvannia z metoiu prohnozuvannia stanu miazovo-venoznoi pompy homilky [Application of the method of mathematical modeling in order to predict the state of the muscle-venous pump of the lower leg]. Visnyk morfolohii, 15, 184-188.

Foutz, T. L., Griffin, A. K., Halper, J. T., & Rowland G. N. (2007). Effects of increased physical activity on juvenile avian bone. Transactions of the ASABE, 50(1), 213-219. doi: 10.13031/2013.22402

García-Aznar, J. M., Rueberg, T. & Doblare, M. (2005). A bone remodelling model coupling microdamage growth and repair by 3D BMU-activity. Biomechanics and Modeling in Mechanobiology, 4(2-3), 67-147. doi: 10.1007/s10237-005-0067-x.

Griebeler, E. M., Klein, N., & Sander, P. M. (2013). Aging, maturation and growth of sauropodomorph dinosaurs as deduced from growth curves using long bone histological data: An assessment of methodological constraints and solutions. Plos One, 8(6), e67012. doi: 10.1371/journal.pone.0067012

Huff, G. R., Huff, W. E., Rath, N. C., Balog, J. M., Anthony, N., & Nestor, K. (2006). Stress-induced Colibacillosis and turkey osteomyelitis complex in turkeys selected for increased body weight. Poultry Science, 85(2), 266-272. doi: 10.1093/ps/85.2.266

Jones,T. M., Benson, T. J., & Ward, M. P. (2019). Does the size and developmental stage of traits at fledging reflect juvenile flight ability among songbirds? Functional Ecology, 34(4), 799-810. doi: 10.1111/1365-2435.13513

Kaplan, S., Narinc, D., & Gurcan, E. K. (2016). Genetic parameter estimates of weekly body weight and Richard's growth curve in Japanese quail. Europian Poultry Science, 80, 1-10. doi: 10.1399/eps.2016.165

Moraes, V. M. B., Malheiros, R. D., Furlan, R. L. Bruno, L. D. G., Malheiros, E. B., & Macari, M. (2007). Effect of environmental temperature during the first week of brooding on broiler chick body weight, viscera and bone development. Brazil Journal Poultry Science, 4(1), 1-8. doi: 10.1590/S1516-635X2002000100003

Pigot, A. L., Sheard, C., Miller, E. T., Bregman, T. P., Freeman, B. G., Roll, U., ... & Tobias, J. A. (2020). Macroevolutionary convergence connects morphological form to ecological function in birds. Nature Ecology & Evolution, 4, 230-239. doi: 10.1038/s41559-019-1070-4

Pinhasi, R., Shaw, P., White, B., & Ogden, A. R. (2009). Morbidity, rickets and long-bone growth in post-medieval Britain a cross-population analysis. Annals of Human Biology, 33(3), 372-389. doi: 10.1080/03014460600707503

Porter, T., Kebreab, E., Darmani, K. H., Lopez, S., Strathe A. B., & France, J. (2010). Flexible alternatives to the Gompertz equation for describing growth with age in turkey hens. Poultry Science, 89(2), 371-378. doi: 10.3382/ps.2009-00141

Ramos, S. B., Caetano, S. L., Savegnago, R. P., Nunes, B. N., Ramos, A. A., & Munari, D. P. (2013). Growth curves for ostriches (Struthio camelus) in a Brazilian population. Poultry Science, 92(1), 277-282. doi: 10.3382/ps.2012-02380

Remeš, V., Matysioková, B., & Vrána, J. (2020). Adaptation and constraint shape the evolution of growth patterns in passerine birds across the globe. Frontiers in Zoology, 17, 29. doi: 10.1186/s12983-020-00377-7

Tabatabai, M. A., Bursac, Z., Wiliams, D. K., & Singh, K. P. (2007). Hyperbolastic survival model. Theoretical Biology and Medical Modelling, 4(40), 325-335. doi: 10.1186/1742-4682-4-40

Tjørve, K. M. C., & Tjørve, E. (2017). The use of Gompertz models in growth analyses, and new Gompertz-model approach: An addition to the Unified-Richards family. Plos One, 12(6), e0178691. doi: 10.1371/journal.pone.0178691

Tjørve, K. M. C., García-Peña, G. E., & Székely, T. (2009). Chick growth rates in charadriiformes: Comparative analyses of breeding climate, development mode and parental care. Journal of Avian Biology, 40(5), 553-558. doi: 10.1111/j.1600-048X.2009.04661.x

Tjørve, K. M. C., & Tjørve, E. (2010). Shapes and functions of bird-growth models: How to characterize chick postnatal growth. Zoology, 113(6), 326-333. doi: 10.1016/j.zool.2010.05.003

Tjørve, E., & Tjørve, K. M. C. (2010). A unified approach to the richards-model family for use in growth analyses: Why we need only two model forms. Journal of Theoretical Biology, 267(3), 417-425. doi: 10.1016/j.jtbi.2010.09.008

Yan, J., & Zhang, Z. (2020). Post-hatching gr owth of the limbs in an altricial bird species. Veterinary Medicine and Science, 7(1), 210-218. doi: 10.1002/vms3.357

Zheng, N., Cadigan, N., & Morgan, M. J. (2020). A spatiotemporal Richards-Schnute growth model and its estimation when data are collected through length-stratified sampling. Environmental and Ecological Statistics, 27, 415-446. doi: 10.1007/s10651-020-00450-8

Ткачук С. А., Пасніченко О. С., Савчук Л. Б. (2021). АПРОКСИМАЦІЯ РОСТОВИХ ПОКАЗНИКІВ ТА АНАЛІЗ ІНДИВІДУАЛЬНИХ РОСТОВИХ КРИВИХ ЗА ЛІНІЙНИМИ ПРОМІРАМИ ТРУБЧАСТИХ КІСТОК КУРЕЙ М'ЯСНОГО НАПРЯМУ ПРОДУКТИВНОСТІ В ПОСТНАТАЛЬНОМУ ПЕРІОДІ ОНТОГЕНЕЗУ.

Ukrainian Journal of Veterinary Sciences, 12(4): 17–35, https://doi.org/10.31548/10.31548/ujvs2021.04.002

Анотація. *Медико-біологічні науки, у тому числі й морфологія, нині потребують впровадження найсучасніших інформаційних технологій та математичних методів для обробки отриманих і накопичених результатів дослідження. Для вивчення ростової динаміки маси тіла свійської птиці застосовували класичні ростові моделі – Гомпертца, зокрема для росту та розвитку птиці – Берталанфі, Річардса та гіперболастичні, для кількісного описання ростових процесів біологічних об'єктів.*

Матеріалом досліджень були трубчасті кістки грудної (плечова, ліктьова та променева) та тазової (стегнова, великогомілкова та заплесно-плеснова) кінцівок птиці м'ясного напряму продуктивності (курчат-бройлерів та курей-несучок батьківського стада бройлерів кросу Cobb-500) різних вікових груп постнатального періоду онтогенезу.

Для вирішення поставленої мети щодо отримання ростових кривих і виявлення особливих точок (екстремумів, перегинів тощо), для побудови картини сукупного розвитку тіла загалом та деяких кісток кінцівок, проведено відповідний регресійний аналіз експериментальних даних на базі відомих ростових моделей. Водночас визначалися найбільш придатні з біологічної точки зору ростові моделі для описання динаміки росту тіла загалом та деяких досліджуваних кісток.

Встановлено відсутність уніфікованої ростової моделі лінійних параметрів різних трубчастих кісток курей м'ясного напряму продуктивності в постнатальному періоді онтогенезу. З цього слідує необхідність чіткого підбору ростових моделей із врахуванням віку, виду, породи, умов утримання та годівлі свійської птиці.

Ростовою моделлю, що найкраще описує динаміку маси тіла курчат-бройлерів, є гіперболастична ростова модель типу Н3, а курей-несучок батьківського бройлерного стада – ростова модель Броді.

Ключові слова: *ростові моделі, трубчасті кістки, маса тіла, кури мясного напряму продуктивності*

UDC: 577.546.3:599.32 https://doi.org/10.31548/ujvs2021.04.004

INFLUENCE OF HEAVY METALS ON ANTIOXIDANT SYSTEM AND BIOCHEMICAL INDEXES IN RATS

I. V. KALININ,
Doctor of Biological Sciences, Professor, Department of Animal Biochemistry and Physiology named after Academician M. F. Gulyi
https://orcid.org/0000-0002-3740-7600
E-mail: kalininihor@gmail.com
V. A. TOMCHUK,
Doctor of Veterinary Sciences, Professor, Department of Animal Biochemistry and Physiology named after Academician M. F. Gulyi
https://orcid. org/0000-0003-0622-6345
E-mail: tomchuk_viktor@ukr.net
V. A. GRYSHCHENKO,
Doctor of Veterinary Sciences, Professor, Department of Animal Biochemistry and Physiology named after Academician M. F. Gulyi
https://orcid. org/0000-0001-6601-1392
E-mail: viktoriya_004@ukr.net
National University of Life and Environmental Sciences of Ukraine,
15 Heroyiv Oborony st., Kyiv 03041, Ukraine

Abstract. *The study was undertaken to examine the effect of heavy metals on the antioxidant system and biochemical indexes in the organism of rats. The influence of heavy metals on indexes The influence of heavy metals on the indicators of the antioxidant system (the antioxidant enzyme activities – glutathione peroxidase, glutathione reductase, catalase, and superoxide dismutase) and the processes of lipid peroxidation (the content of hydroperoxides and products of thiobarbituric acid) was determined. It is established, that the antioxidant system functions more intensively in blood and liver of rats under the action of heavy metals. The study of enzyme activity showed the activation of the latter under conditions of heavy metal intoxication 1.5–2.0 times (depending on the heavy metal) compared with the control. We found that blood levels of total and direct bilirubin, creatinine, and urea increased in intoxicated rats from all experimental groups compared with intact animals. However, a decrease in the content of albumin, total protein, cholesterol, and triglycerides was also found in all experimental groups, in comparison with intact rats. Under the action of heavy metals, the activity of total α-amylase, lactate dehydrogenase, and glucose concentration increases in blood of rats. According to the results of studies in intoxicated animals compared with the intact group, there was a change in the cation-anion pool, in particular, a tendency to decrease the content of sodium and inorganic phosphorus and increase chlorides, magnesium, calcium, and potassium.*

Keywords: *rats, blood, liver, copper, zinc, cadmium, lead, antioxidant system*

Introduction

Environmental contamination by heavy metals raises concerns about human health. It has become evident that increasing human activities have modified the global cycle of heavy metals, including the toxic non-essential elements. Heavy metals are among the most toxic and it is reported that their increased concentration in agricultural soils is known to come from the application of phosphate fertilizers, sewage sludge, wastewater, and pesticides. The accumulation of toxicants in the air, soil, plants, water, and sewage sludge has overwhelmed the natural capacity in many ecosystems, resulting in the potential for humans to be exposed to heavy metals (Djuric et al., 2015; Saghazadeh & Rezaei, 2017).

As necessary microelements for physiological activities, copper and zinc play a significant part in normal development and organisms' homeostasis maintenance. However, high-level exposure to these elements may also induce adverse health effects (Maret et al., 2006; Cdos & Fernandes, 2008). The toxic effect of heavy metals is due to their influence on metabolic enzyme systems and induced oxidative stress in the animal body. The toxic molecular mechanisms of different heavy metals vary, although they also have some similarities (El Yamani et al., 2017; Husak et al., 2018).

Oxidative stress is the imbalance that occurs when there is an increased production of free radicals that exceeds the body's ability to neutralize it. Alteration of chemical reactions at the cellular level leads to the appearance of free radicals and peroxides that affect the intracellular structures – proteins, lipids, and DNA, with the disruption of intrinsic mechanisms at this level. Free radicals are normally produced in the body due to the influence of external factors, such as pollution, cigarette smoke, or internal, due to intracellular metabolism when antioxidant mechanisms are exceeded (Fig. 1).

Oxidative stress under the action of heavy metals defined as a persistent imbalance between the production of highly reactive molecular species (chiefly oxygen and nitrogen) and antioxidant defense, is implicated in a broad variety of chronic and acute diseases, including such diseases as diabetes (Wang et al., 2014; Kumar & Sharma, 2019).

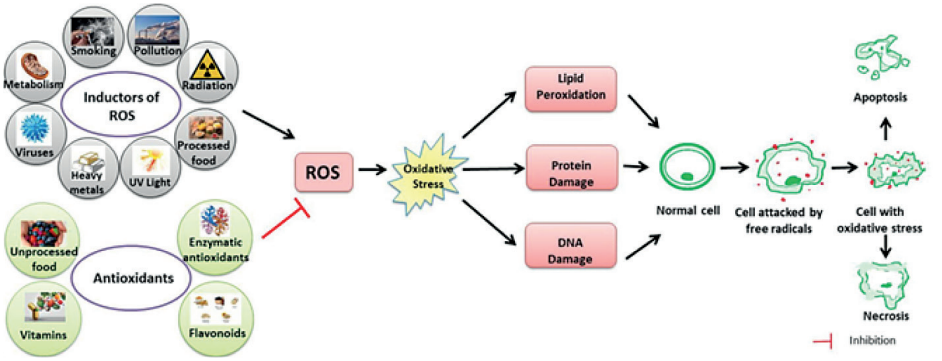

Fig. 1. Schematic figure of the link between reactive oxygen species (ROS), oxidative stress and their effects on the body

Source: Sharifi-Rad et al. (2020).

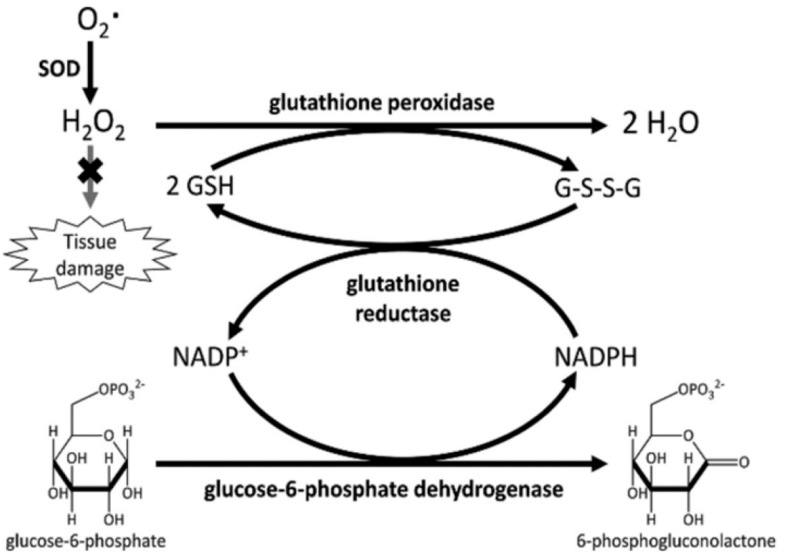

Fig. 2. Primary enzymes (SOD or peroxidases) act directly in scavenging ROS. Secondary enzymes, such as glutathione reductase and glucose-6-phosphate dehydrogenase, support the action of primary enzymes regenerating NAPDH and reduced glutathione.

Source: Sharifi-Rad et al. (2020).

Negative environmental factors, including heavy metals, lead to a breakdown of antioxidant protection due to any external influence and cause increased free radical oxidation. This is accompanied by a change in the conformation of lipids, which leads to a violation of the structural and functional properties of biomembranes, increasing their lability and permeability, imbalance of enzyme systems of membranes, disruption of electron transport chains in mitochondria. In addition, the products of free radical oxidation damage proteins, thiol compounds, and nucleotide phosphates, change the degree of glycolysis, damage nuclear DNA with the formation of its single-strand breaks (Lodovici & Bigagli, 2011).

The activity of the thiol-disulfide system may indicate the state of antioxidant reserves of the body, it responds to its effects and the external nature of the change of redox potential, which characterizes the ratio of the concentration of renewed sulfhydryl (SH) and oxidized disulfide (SS) groups (thiol-disulfide coefficient). It is known that the TDC can be an in-integrative indicator of adaptive capabilities of the organism (Fig. 2) (Sharifi-Rad et al., 2020).

The aim of this study is to assess the influence of copper, zinc, lead, and cadmium on the functioning of the antioxidant system and biochemical indexes in rat tissues.

Materials and methods of research

The study was conducted on white male rats of the same age, weighing 180–

200 g, kept under standard conditions of a vivarium, with free access to food and water. Five groups of animals were formed: the first – intact (control), the second – rats orally administered a solution of copper sulfate at a dose of 3 mg/kg, the third – rats orally administered a solution of zinc sulfate at a dose of 2 mg/kg, the fourth – rats orally administered a solution of cadmium sulfate at a dose of 1.5 mg/kg, the fifth – rats orally administered a solution of lead nitrate at a dose of 1.7 mg/kg. Intoxication was performed within 14 days, then the rats were decapitated under ether anesthesia for extraction of blood and liver for further research. The work was carried out in accordance with the European Convention for the Protection of Vertebrate Animals Used for Experimental and other Scientific Purposes (Strasbourg, France, 1986).

Blood was obtained by well-known methods and preparations of a homogeneous fraction of liver cells were conducted by differential centrifugation (Severyn & Soloveva, 1989). The content of thiobarbituric acid reactive substances (TBARS) was determined by Stalnaya & Haryshvyly (1977), diene conjugates – by Gavrilov et al. (1988). In the course of the research, we used the following methods to determine the activity of enzymes: superoxide dismutase (EC 1.15.1.1) by Orehovych (1977), catalases (EC 1.11.1.9) by Koroliuk (1988), glutathione peroxidase (GP) (EC 1.11.1.9) and glutathione transferase (GT) (EC 2.5.1.18) by Mannervik (1985), Vlasova et al. (1990). The content of reduced form of glutathione (GSH) was established by the Ellman method (1959).

The content of heavy metals in blood and liver was determined by spectrometric method (Havezov & Tsalev, 1983), using the absorption mode in acetylene-air flame on the atomic absorption spectrometer (SpectrAA-55B, VARIAN, USA). Standard solutions of these metals were used as controls.

Blood biochemical analysis (activity of alkaline phosphatase (EC 3.1.3.1), alanine aminotransferase (EC 2.6.1.2), aspartate aminotransferase (EC 2.6.1.1), gamma-glutamyl transpeptidase (EC 2.3.2.2), lactate dehydrogenase (EC 1.1.1.27), cholinesterase (EC 3.1.1.8), total α-amylase (EC 3.2.1.1), bilirubin (total and direct), creatinine, urea, glucose, albumin, total protein, cholesterol, triglycerides, chlorides, magnesium, inorganic phosphorus, calcium, sodium, and potassium) was performed using a semi-automatic biochemical analyzer (Micro Lab 300, Netherlands).

The probability of the results was determined using Student's t-test. Statistical calculations were performed using the Microsoft Excel 2007 program (Kucherenko et al., 2001).

Analysis of recent researches and publications

It was found that in rats intoxicated with copper, zinc, cadmium, and lead ions, activation of lipid peroxidation was revealed in blood and liver, which was assessed by the accumulation of TBARS (Table 1).

Copper sulfate intoxication leads to an increase in TBARS by 40% in blood and 31% in the liver, zinc sulfate – by 42% in blood and 31% in the liver, cadmium sulfate – by 66% in blood and 38% in the liver, lead nitrate – by 61% in blood and 36% in the liver, in comparison with the control group of animals.

The content of diene conjugates in rat tissues (Table 2) was determined as the ratio of optical density at 233 and 218 nm.

1. The content of TBARS in rat tissues under conditions of heavy metal intoxication (M ± m, n = 8)

Rats	TBARS	
	Blood, mmol/L	Liver, μmol/mg protein
Intact	1.34 ± 0.05	0.74 ± 0.03
Intoxicated with $CuSO_4$	1.87 ± 0.09*	0.97 ± 0.04*
Intoxicated with $ZnSO_4$	1.91 ± 0.04*	0.95 ± 0.05*
Intoxicated with $CdSO_4$	2.23 ± 0.08*	1.02 ± 0.07*
Intoxicated with $Pb(NO_3)_2$	2.16 ± 0.05*	1.01 ± 0.05*

Note: * P < 0.05 compared with intact rats.

After intoxication of rats with heavy metal ions, the content of diene conjugates in blood and liver tissues increases. Thus, the content of diene conjugates in blood increased by 16% after copper sulfate intoxication, 18% – zinc sulfate, 24% – cadmium sulfate, 26% – lead nitrate, compared with the control group.

The body's antioxidant defense system controls and inhibits all stages of free radical reactions, from their initiation to the formation of hydroperoxides and malondialdehyde.

Studies of the activity of superoxide dismutase and catalase are shown in Table 3.

Therefore, intoxication with heavy metal ions leads to a decrease in the activity of SOD and CAT in the studied tissues of rats, especially in the case of intoxication with cadmium and lead ions.

The study of the activity of glutathione-dependent enzymes in rat tissues is shown in Table 4.

In blood of rats under conditions of copper sulfate intoxication, the

2. The content of diene conjugates in rat tissues under conditions of heavy metal intoxication (M ± m, n = 8)

Rats	Diene conjugate content (E233/E218)	
	Blood	Liver
Intact	0.84 ± 0.04	0.97 ± 0.05
Intoxicated with $CuSO_4$	0.98 ± 0.07	1.02 ± 0.09
Intoxicated with $ZnSO_4$	0.99 ± 0.05	1.04 ± 0.07
Intoxicated with $CdSO_4$	1.04 ± 0.06*	1.10 ± 0.08*
Intoxicated with $Pb(NO_3)_2$	1.06 ± 0.09*	1.08 ± 0.04*

Note: * P < 0.05 compared with intact rats.

3. The activity of superoxide dismutase (SOD) and catalase (CAT) in rat tissues under conditions of heavy metal intoxication (M ± m, n = 8)

Rats	Blood		Liver	
	SOD (IU/mg of protein)	CAT (μmol/L min)	SOD (IU/mg of protein)	CAT (μmol/L min)
Intact	0.83 ± 0.05	11.2 ± 1.10	2.83 ± 0.32	0.18 ± 0.03
Intoxicated with $CuSO_4$	0.68 ± 0.02	10.1 ± 0.90	2.68 ± 0.17	0.12 ± 0.02*
Intoxicated with $ZnSO_4$	0.70 ± 0.04	10.7 ± 0.70	2.71 ± 0.15	0.14 ± 0.03*
Intoxicated with $CdSO_4$	0.60 ± 0.03*	8.5 ± 0.90*	1.37 ± 0.14*	0.09 ± 0.01*
Intoxicated with $Pb(NO_3)_2$	0.62 ± 0.05*	8.9 ± 0.80*	1.72 ± 0.19*	0.11 ± 0.01*

Note: * P < 0.05 compared with intact rats.

4. The activity of glutathione peroxidase (GP) and glutathione transferase (GT) and the content of reduced form of glutathione (GSH) in rat tissues under conditions of heavy metal intoxication (M ± m, n = 8)

Rats	Blood			Liver		
	GP (mmol/ min•L)	GT (mmol/ min•L)	GSH (mmol/L)	GP (μmol/ min•mg protein)	GT (μmol/ min • mg protein)	GSH (μmol/mg • protein)
Intact	0.273 ± 0.12	68.0 ± 4.71	0.379 ± 0.04	0.37 ± 0.02	0.48 ± 0.05	0.80 ± 0.04
Intoxicated with $CuSO_4$	0.214 ± 0.11*	35.7 ± 3.68*	0.294 ± 0.03*	0.34 ± 0.03	0.46 ± 0.07	0.67 ± 0.05
Intoxicated with $ZnSO_4$	0.211 ± 0.14*	34.1 ± 3.52*	0.276 ± 0.07*	0.36 ± 0.05	0.44 ± 0.03	0.62 ± 0.07
Intoxicated with $CdSO_4$	0.170 ± 0.09*	27.4 ± 2.90*	0.252 ± 0.02*	0.28 ± 0.04*	0.39 ± 0.02*	0.31 ± 0.03*
Intoxicated with $Pb(NO_3)_2$	0.181 ± 0.10*	29.7 ± 3.10*	0.263 ± 0.05*	0.30 ± 0.03*	0.41 ± 0.04*	0.39 ± 0.05*

Note: * P < 0.05 compared with intact rats.

following decreases: GP activity by 22%, GT activity by 47% and the content of reduced glutathione by 23%; zinc sulfate – GP activity by 23%, GT activity by 50% and the content of reduced glutathione by 27%; cadmium sulfate – GP activity by 38%, GT activity by 60% and the content of reduced glutathione by 34%; lead nitrate – GP activity by 34%, GT activity by 57% and the content of reduced glutathione by 31%, respectively, compared with the control group of animals.

Under conditions of intoxication with copper sulfate and zinc sulfate, the activity of GP and GT in the liver of rats changes slightly. The activity of GP and GT in the liver under exposure to cadmium ions is reduced by 25% and 19%, respectively, compared with the control. Under exposure to lead ions, the activity of GP and GT in the liver

5. Biochemical indexes of rat blood serum under conditions of heavy metal intoxication (M ± m, n = 8)

Indexes	Intact	Intoxicated rats			
		Cu	Zn	Cd	Pb
Alkaline phosphatase, U/L	291.2 ± 27.40	535.4 ± 85.21*	537.3 ± 86.11*	589.5 ± 87.16*	554.7 ± 86.94*
Alanine aminotransferase, U/L	78.4 ± 6.34	132.8 ± 10.73*	135.3 ± 11.12*	176.2 ± 12.31*	163.6 ± 12.11*
Aspartate aminotransferase, U/L	162.3 ± 14.87	253.6 ± 21.32*	254.9 ± 22.41*	338.7 ± 31.24*	285.4 ± 23.10*
γ-Glutamyl transpeptidase, U/L	24.7 ± 2.21	39.2 ± 3.91*	40.5 ± 4.17*	43.4 ± 4.85*	41.2 ± 4.38*
Lactate dehydrogenase, U/L	323.5 ± 32.12	650.3 ± 54.74*	653.4 ± 55.23*	724.6 ± 61.14*	692.1 ± 55.73*
Cholinesterase, U/L	34.3 ± 4.91	41.4 ± 5.13	40.1 ± 5.03	43.2 ± 5.94*	42.3 ± 5.18*
Total α-amylase, U/L	517.8 ± 89.84	746.3 ± 115.12*	749.2 ± 123.14*	809.3 ± 141.25*	792.1 ± 134.21*
Bilirubin:					
total, μmol/L	3.6 ± 0.21	3.8 ± 0.20	3.9 ± 0.23	4.9 ± 0.27*	4.7 ± 0.29*
direct, μmol/L	0.9 ± 0.01	1.0 ± 0.02	1.0 ± 0.03	1.2 ± 0.03*	1.2 ± 0.03*
Creatinine, μmol/L	0.9 ± 0.01	1.0 ± 0.02	1.0 ± 0.03	1.2 ± 0.03*	1.2 ± 0.03*
Urea, mmol/L	69.3 ± 6.12	102.4 ± 8.93*	104.1 ± 9.23*	118.5 ± 11.54*	112.6 ± 10.15*
Glucose, mmol/L	6.2 ± 0.90	11.4 ± 1.25*	11.1 ± 1.15*	12.9 ± 2.32*	12.3 ± 2.21*
Albumin, g/L	5.1 ± 0.70	6.7 ± 1.10*	7.1 ± 1.32*	8.3 ± 1.41*	8.1 ± 1.38*
Total protein, g/L	42.6 ± 3.31	33.8 ± 2.52	34.9 ± 2.73	31.4 ± 2.21*	32.1 ± 2.32*
Cholesterol mmol/L	74.7 ± 3.70	61.3 ± 2.43	62.1 ± 2.63	56.2 ± 2.12*	58.4 ± 2.21*
Triglycerides, mmol/L	1.2 ± 0.07	0.9 ± 0.02*	0.9 ± 0.03*	0.8 ± 0.01*	0.8 ± 0.02*
Chlorides, mmol/L	1.0 ± 0.02	0.5 ± 0.02*	0.5 ± 0.03*	0.4 ± 0.01*	0.4 ± 0.02*
Magnesium, mmol/L	86.3 ± 7.43	106.1 ± 9.72	105.7 ± 9.50	112.4 ± 10.92*	111.3 ± 10.23*
Inorganic phosphorus, mmol/L	1.7 ± 0.12	2.3 ± 0.21*	2.4 ± 0.24*	2.6 ± 0.28*	2.5 ± 0.25*
Calcium, mmol/L	2.5 ± 0.23	1.4 ± 0.10*	1.5 ± 0.12*	1.2 ± 0.09*	1.3 ± 0.10*
Sodium, mmol/L	1.9 ± 0.11	2.9 ± 0.20*	2.8 ± 0.25*	3.5 ± 0.37*	3.3 ± 0.45*
Potassium, mmol/L	144.2 ± 12.34	127.3 ± 11.81*	128.1 ± 11.90*	122.3 ± 11.15*	123.2 ± 11.75*
Alkaline phosphatase, U/L	5.3 ± 0.30	7.4 ± 0.60*	7.6 ± 0.71*	8.4 ± 0.90*	8.1 ± 0.84*

Note: * $P < 0.05$ compared with intact rats.

of rats decreased by 19% and 15%, respectively, compared with control animals.

It should be noted that the content of reduced form of glutathione in the liver of intoxicated rats decreased more intensively: $CuSO_4$ – by 17%, $ZnSO_4$ – by 23%, $CdSO_4$ – by 61%, $Pb(NO_3)_2$ – by 51%, compared with the control group of animals. This change, in our opinion, can be explained by the fact that glutathione is involved in the protective reactions of cellular organelles.

Studies have shown that the action of heavy metals reduces the activity of antioxidant system enzymes and the

concentration of reduced glutathione in blood of animals.

Biochemical analysis of rat blood under the influence of xenobiotics on metabolic processes in the body is shown in Table 5. The study of enzyme activity showed the activation of the latter under conditions of heavy metal intoxication in 1.5–2.0 times (depending on a xenobiotic), compared with control, which is an important sign of confirmation of pathological processes, taking into account the organ-specificity of enzymes.

A decrease in the de Ritis ratio was found in all groups of intoxicated rats, compared with the group of intact rats, which indicates inflammatory processes in the liver.

The increase in the activity of the studied enzymes is probably caused by the destruction of hepatocytes and the development of intrahepatic cholestasis, which causes their intensive entry into blood. In addition, the change in the activity of gamma-glutamyl transpeptidase in the serum is of important diagnostic value in the simultaneous defeat of the liver parenchyma and hepatobiliary tract and its activity is a sign of hepatotoxicity. The increase in the level of gamma-glutamyl transpeptidase also indicates the stimulation of the activity of microsomal enzymes.

Hypoproteinemia and a decrease in albumin content in the serum of rats under conditions of intoxication may indicate a decrease in the intensity of protein synthesis in hepatocytes.

Thus, the increase in serum activity of the studied enzymes may indicate damage to liver cells, and may also be a consequence of the mobilization of protective and compensatory mechanisms in the entry of xenobiotics into the body.

Any functional manifestation of a living organism is provided by the action of the corresponding enzyme systems, so the change in the activity of the corresponding enzymes correlates with other studied blood biochemical parameters. We found that in intoxicated rats of all experimental groups, levels of total and direct bilirubin, creatinine, urea, and glucose were increased compared with intact animals. However, a decrease in the content of albumin, total protein, cholesterol, and triglycerides was also found in all experimental groups, compared with intact rats.

According to the results of studies in intoxicated animals, compared with the intact group, there was a change in the cation-anion pool, in particular, a tendency to decrease in the content of sodium and inorganic phosphorus, and increase in chlorides, magnesium, calcium, and potassium. This change is probably due to a decrease in total protein and albumin levels, as well as an increase in organic acids.

The entry of heavy metals into a living organism leads to occurrence of oxidative stress, which triggers a set of interdependent pathological reactions that cause the activation of the pool and accumulation of TBARS, as shown in our previous works. Such data are consistent with the indicators of the thiol-disulfide balance system (Table 6) in the protein fraction of blood and liver in rats.

In blood of all experimental groups, the thiol-disulfide ratio decreased: in the second – by 1.5 times, in the third – by 1.7 times, in the fourth and fifth – almost by 3 times, compared with a group of intact rats. A decrease in thiol-disulfide ratio was also found in the liver of all experimental groups: in the second – by 1.8 times, in the third – by 2 times, in the fourth – almost by 3 times, and the fifth – by 2.3 times, compared

6. Thiol-disulfide balance of blood and liver of rats under conditions of heavy metal intoxication (M ± m, n = 8)

Indexes	Intact	Intoxicated rats			
		Cu	Zn	Cd	Pb
Blood, μmol/mL					
-SH-groups	14.36 ± 1.52	12.84 ± 1.42	12.61 ± 1.23	11.08 ± 1.0*	11.76 ± 1.21*
-SS-groups	4.53 ± 0.63	6.05 ± 0.82*	6.73 ± 0.87*	10.41 ± 0.7*	10.29 ± 0.67*
Thiol-disulfide ratio	3.17 ± 0.58	2.12 ± 0.32*	1.87 ± 0.28*	1.06 ± 0.17*	1.14 ± 0.19*
Liver, μmol/g					
-SH-groups	19.72 ± 1.94	15.24 ± 1.6*	14.76 ± 1.48*	12.87 ± 1.29*	13.73 ± 1.32*
-SS-groups	5.34 ± 0.78	7.45 ± 0.72*	7.94 ± 0.72*	9.68 ± 0.95*	8.79 ± 0.64*
Thiol-disulfide ratio	3.69 ± 0.62	2.04 ± 0.31*	1.86 ± 0.24*	1.33 ± 0.19*	1.56 ± 0.21*

Note: * $P < 0.05$ compared with intact rats.

with control. A decrease in the thiol-disulfide ratio indicates an increase in the concentration of free radicals and depletion of antioxidants' sedentary reserves of the body, which is a reflection of the dynamics of positive process under the negative action of xenobiotics.

Changes in the biochemical function of the liver are accompanied by signs of toxic hepatitis with hepatocellular insufficiency, as evidenced by increased activity of aminotransferases, lactate dehydrogenase, decreased cholesterol and triglycerides, increased glucose, and impaired excretory function of the liver – increase in the presence of gamma-glutamyl transpeptidase, alkaline phosphatase. Increased activity of cholinesterase, total α-amylase, and creatinine is a sign of renal failure, pathology of filtration in the glomeruli of the kidneys, and the occurrence of nephritis.

The content of total protein and albumin in the serum during intoxication with the studied heavy metals is reduced, which indicates damage to liver and kidney cells. An increase in urea content in the serum is a sign of increased protein catabolism, acute renal failure, as well as a shift in the relationship between the processes of urea formation and its excretion in the urine. It was found that in all groups of intoxicated animals, the content of inorganic sodium and phosphorus is reduced and chlorides, magnesium, calcium, and potassium is increased, which is a sign of nephritis and previously mentioned disorders of acid-base status (compensated acidosis).

Conclusions and future perspectives

This article summarizes the results obtained, indicating a violation of the prooxidant-antioxidant balance. It should be noted that the glutathione peroxidase system is universal in the decomposition of peroxides and prevents the initiation of secondary reactions of lipid oxidation and participates in the inactivation of products of oxidative metabolism of heavy metals in rats.

It was found that heavy metal intoxication of rats leads to the activation

of studied blood enzymes (alkaline phosphatase, alanine and aspartate aminotransferases, gamma-glutamyl transpeptidase, lactate dehydrogenase, cholinesterase, and total α-amylase) in comparison with the intact group.

In all experimental groups, the content of total and direct bilirubin, creatinine, urea, glucose, chloride, magnesium, calcium, and potassium was increased compared with intact animals.

A decrease in the content of albumin, total protein, cholesterol, triglycerides, sodium, and inorganic phosphorus was also found in all experimental groups, compared with intact rats.

Heavy metal intoxication in rats leads to a decrease in the content of -SH-groups and an increase in the content of -SS-groups in blood and liver of all experimental groups, as a consequence – a decrease in thiol-disulfide ratio indicating the strengthening of free radical processes oxidation, depletion of antioxidant reserves of the body, and confirmatory modifications of protein molecules.

In conclusion, oxidative stress is an important pathogenetic link for animals, and studies in this field may be important elements in the future to better understand and manage various diseases, including in humans.

References

Aggarwal, V., Tuli, H., Varol, A., Thakral, F., Yerer, M., Sak, K., … & Sethi, G. (2019). Role of reactive oxygen species in cancer progression: molecular mechanisms and recent advancements. Biomolecules, 9(11), 735. doi: 10.3390/biom9110735.

Antunes dos Santos, A., Ferrer, B., Marques Gonçalves, F., Tsatsakis, A. M., Renieri, E. A., Skalny, A. V., … & Aschner, M. (2018). Oxidative stress in methylmercury-induced cell toxicity. Toxics, 6(3), 47. doi: 10.3390/toxics6030047.

Engwa, G. A., Ferdinand, P. U., Nwalo, F. N., & Unachukwu, M. N. (2019). Mechanism and health effects of heavy metal toxicity in humans. In O. Karcioglu & B. Arslan (Eds.), Poisoning in the Modern World: New Tricks for an Old Dog? BoD–Books on Demand. doi: 10.5772/intechopen.82511.

Balali-Mood, M., Naseri, K., Tahergorabi, Z., Khazdair, M. R., & Sadeghi, M. (2021). Toxic Mechanisms of Five Heavy Metals: Mercury, Lead, Chromium, Cadmium, and Arsenic. Frontiers in Pharmacology, 12, 643972. doi: 10.3389/fphar.2021.643972

Batáriová, A., Spěváčková, V., Beneš, B., Čejchanová, M., Šmíd, J., & Černá, M. (2006). Blood and urine levels of Pb, Cd and Hg in the general population of the Czech Republic and proposed reference values. International Journal of Hygieneand Environmental Health, 209(4), 359-366. doi: 10.1016/j.ijheh.2006.02.005.

Cao, Z. R., Cui, S. M., Lu, X. X., Chen, X. M., Yang, X., Cui, J. P., & Zhang, G. H. (2018). Effects of occupational cadmium exposure on workers' cardiovascular system. Zhonghua Lao Dong Wei Sheng Zhi Ye Bing Za Zhi, 36(6), 474–477. doi: 10.3760/cma.j.issn.1001-9391.2018.06.025.

Carvalho Cdos, S., & Fernandes, M. N. (2008). Effect of copper on liver key enzymes of anaerobic glucose metabolism from freshwater tropical fish Prochilodus lineatus. Comparative Biochemistry & Physiology, 151, 437-442.

Djordjevic, V. R., Wallace, D. R., Schweitzer, A., Boricic, N., Knezevic, D., Matic, S., … & Buha, A. (2019). Environmental cadmium exposure and pancreatic cancer: evidence from case control, animal and in vitro studies. Environment International, 128, 353-361. doi: 10.1016/j.envint.2019.04.048.

Dongre, N. N., Suryakar, A. N., Patil, A. J., Ambekar, J. G., & Rathi, D. B. (2011). Biochemical effects of lead exposure on systolic &

diastolic blood pressure, heme biosynthesis and hematological parameters in automobile workers of north Karnataka (India). Indian Journal of Clinical Biochemistry, 26(4), 400-406. doi: 10.1007/s12291-011-0159-6.

Djuric, A., Begic, A., Gobeljic, B., Stanojevic, I., Ninkovic, M., Vojvodic, D., … & Djukic, M. (2015). Oxidative stress, bioelements and androgen status in testes of rats subacutely exposed to cadmium. Food and Chemical Toxicology, 86, 25-33.

Ellman, G. L. (1959). Tissue sulfhydryl groups. Archives of Biochemistry and Biophysics, 82(1), 70-77.

El Yamani, N., Collins, A. R., Runden-Pran, E., Fjellsbo, L. M., Shaposhnikov, S., Zienolddiny, S., & Dusinska, M. (2017). In vitro genotoxicity testing of four reference metal nanomaterials, titanium dioxide, zinc oxide, cerium oxide and silver: Towards reliable hazard assessment. Mutagenesis, 32, 117-126.

Fay, M. J., Alt, L. A. C, Ryba, D., Salamah, R., Peach, R., Papaeliou, A., … & Prozialeck, W. C. (2018). Cadmium nephrotoxicity is associated with altered microRNA expression in the rat renal cortex. Toxics, 6(1), 16. doi: 10.3390/toxics6010016.

Gavrilov, V. B., Gavrilov, A. R., & Khmara, N. F. (1988). Measurement diene conjugates in plasma by UV absorption heptane and isopropanol extract. Laboratornoe case, 2, 60-63.

Havezov, I., & Tsalev, D. (1983). Atomic absorption analysis. Leningrad: Chemistry.

Husak, V. V., Mosiichuk, N. M., Kubrak, O. I., Matviishyn, T. M., Storey, J. M., Storey, K. B., & Lushchak, V. I. (2018). Acute exposure to copper induces variable intensity of oxidative stress in goldfish tissues. Fish Physiology and Biochemistry, 44, 841-852.

Kim, J.-J., Kim, Y.-S., & Kumar, V. (2019). Heavy metal toxicity: An update of chelating therapeutic strategies. Journal of Trace Elements in Medicine and Biology, 54, 226-231. doi: 10.1016/j.jtemb.2019.05.003.

Kim, T. H., Kim, J. H., Le Kim, M. D., Suh, W. D., Kim, J. E., Yeon, H. J., … & Jo, G. H. (2020). Exposure assessment and safe intake guidelines for heavy metals in consumed fishery products in the Republic of Korea. Environmental Science and Pollution Research, 27, 33042-33051. doi: 10.1007/s11356-020-09624-0.

Koroliuk, M. A. (1988). Method for determining activity of catalase in biological material, 2, 31-34.

Kucherenko, M. E., Babenyuk, Y. D., & Voytsitskyy, V. M. (2001). Modern methods of biochemical research. Kyiv: Fitosotsiotsentr.

Kulshrestha, A., Jarouliya, U., Prasad, G., Flora, S., & Bisen, P. S. (2014). Arsenic-induced abnormalities in glucose metabolism: Biochemical basis and potential therapeutic and nutritional interventions. World Journal of Translational Medicine, 3(2), 96-111. doi: 10.5528/wjtm.v3.i2.96.

Kumar, S, & Sharma, A. (2019). Cadmium toxicity: effects on human reproduction and fertility. Reviews on Environmental Health, 34, 327-338.

Lech, T., & Sadlik, J. K. (2017). Cadmium concentration in human autopsy tissues. Biological Trace Element Research, 179(2), 172-177. doi: 10.1007/s12011-017-0959-5.

Li, H., Fagerberg, B., Sallsten, G., Borné, Y., Hedblad, B., Engström, G., Barregard, L., & Andersson, E.M. (2019). Smoking-induced risk of future cardiovascular disease is partly mediated by cadmium in tobacco: Malmö Diet and Cancer Cohort Study. Environmental Health, 18(1), 56. doi: 10.1186/s12940-019-0495-1.

Luo, L., Wang, B., Jiang, J., Huang, Q., Yu, Z., Li, H., … & Chen, S. (2021). Heavy metal contaminations in herbal medicines: determination. comprehensive risk assessments. Frontiers in Pharmacology, 11, 595335. doi: 10.3389/fphar.2020.595335.

Mannervik, B. (1985). Glutathione peroxidase. Methods in enzymology, 113, 490-495.

Ohta, H., & Ohba, K. (2020). Involvement of metal transporters in the intestinal uptake of cadmium. Journal of Toxicological Sciences, 45(9), 539-548. doi: 10.2131/jts.45.539.

Oluranti, O. I., Adeyemo, V. A., Achile, E. O., Fatokun, B. P., & Ojo, A. O. (2021). Rutin improves cardiac and erythrocyte membrane-bound ATPase activities in male rats exposed to cadmium chloride and lead acetate. Biological Trace Element Research, 1-10. doi: 10.1007/s12011-021-02711-4.

Orehovych, V. N. (1977). Modern methods in biochemistry. Moscow: Medicyna.

Patra, R. C., Swarup, D., & Dwivedi, S. K. (2001). Antioxidant effects of α tocopherol, ascorbic acid and l-methionine on lead induced oxidative stress to the liver, kidney and brain in rats. Toxicology, 162 (2), 81-88. doi: 10.1016/s0300-483x(01)00345-6.

Proshad, R., Zhang, D., Uddin, M., & Wu, Y. (2020). Presence of cadmium and lead in tobacco and soil with ecological and human health risks in Sichuan province, China. Environmental Science and Pollution Research, 27, 18355-18370. doi: 10.1007/s11356-020-08160-1.

Rani, A., Kumar, A., Lal, A., & Pant, M. (2014). Cellular mechanisms of cadmium-induced toxicity: a review. International Journal of Environmental Health Research, 24(4), 378-399. doi: 10.1080/09603123.2013.835032.

Saghazadeh, A., & Rezaei, N. (2017). Systematic review and meta-analysis links autism and toxic metals and highlights the impact of country development status: Higher blood and erythrocyte levels for mercury and lead, and higher hair antimony, cadmium, lead, and mercury. Progress in Neuro-Psychopharmacology & Biological Psychiatry, 79, 340-368.

Saha, P., & Paul, B. (2019). Assessment of heavy metal toxicity related with human health risk in the surface water of an industrialized area by a novel technique. Human and Ecological Risk Assessment Journal, 25, 966-987. doi: 10.1080/10807039.2018.1458595.

Severyn, S. E., & Soloveva, G. A. (1989). Praktikum on biochemistry. Moscow: MGU.

Sharifi-Rad, M., Anil Kumar, N. V., Zucca, P., Varoni, E. M., Dini, L., Panzarini, E., … & Sharifi-Rad, J. (2020). Lifestyle, Oxidative Stress, and Antioxidants: Back and Forth in the Pathophysiology of Chronic Diseases. Frontiers in Pharmacology, 11, 694. doi: 10.3389/fphys.2020.00694.

Singh, Y. P., Patel, R. N., Singh, Y., Butcher, R. J., Vishakarma, P. K., & Singh, R. K. B. (2017). Structure and antioxidant superoxide dismutase activity of copper(II)hydrazone complexes. Polyhedron, 122, 1-15. doi: 10.1016/j.poly.2016.11.013.

Stalnaya, Y. D., & Haryshvyly, T. G. (1977). Modern methods in biochemistry. Moscow: Medicyna.

Vlasova, S. N., Shabunyna, E. I., & Pereslehyna, A. I. (1990). Glutathione dependent activity of enzymes in red blood cells chronic disease liver in children. Laboratornoe case, 8, 19-21.

Wang, Y., Mandal, A. K., Son, Y.-O., Pratheeshkumar, P., Wise, J. T. F., Wang, L., … & Chen, Z. (2018). Roles of ROS, Nrf2, and autophagy in cadmium-carcinogenesis and its prevention by sulforaphane. Toxicology and Applied Pharmacology, 353, 23-30. doi: 10.1016/j.taap.2018.06.003.

Калінін І. В., Томчук В. А. , Грищенко В. А. (2021). ВПЛИВ ВАЖКИХ МЕТАЛІВ НА АНТИОКСИДАНТНУ СИСТЕМУ І БІОХІМІЧНІ ПОКАЗНИКИ У ЩУРІВ.
Ukrainian Journal of Veterinary Sciences, 12(4): 53–65, https://doi.org/10.31548/ujvs2021.04.004

Анотація. *Дослідження проводилося для вивчення впливу важких металів на антиоксидантну систему та біохімічні показники крові в організмі щурів. Встановлено вплив важких металів на показники антиоксидантної системи (активність ферментів антиоксидантної системи – глутатіонпероксидази, глутатіонредуктази, каталази та супероксиддисмутази) та процеси перекисного окиснення ліпідів (вміст гідропероксидів та продуктів тіобарбітурової кислоти) у щурів. Встановлено, що за дії важких металів у крові та печінці щурів інтенсивніше функціонує антиоксидантної системи. Дослідження активності ферментів показало активацію останніх в умовах інтоксикації важкими металами в 1,5–2,0 рази (залежно від важкого металу), порівнюючи з контролем. Встановлено, що в інтоксикованих щурів усіх дослідних груп підвищений рівень загального та прямого білірубіну, креатиніну, сечовини, порівнюючи з інтактними тваринами. Однак у всіх дослідних групах, порівнюючи з інтактними щурами, також виявлено зниження вмісту альбуміну, загального білка, холестеролу та тригліцеридів. За дії важких металів у крові щурів підвищується активність загальної α-амілази, лактатдегідрогенази та концентрації глюкози. За результатами досліджень у інтоксикованих тварин, порівнюючи з інтактною групою, спостерігалася зміна катіонно-аніонного пулу, зокрема, тенденція до зниження вмісту натрію та неорганічного фосфору, та збільшення вмісту хлоридів, магнію, кальцію та калію.*

Ключові слова: *щури, кров, печінка, мідь, цинк, кадмій, свинець, антиоксидантна система*

UDC 636.09:599.323.41]:615.2-034.1:616.12/.36 https://doi.org/10.31548/ujvs2021.04.003

MICROSCOPIC CHANGES IN THE INTERNAL ORGANS OF WHITE MICE DURING EXPERIMENTAL IRON (IV) CLATHROCHELATE TOXICOSISS

B. V. BORYSEVYCH,
Doctor of Veterinary Sciences, Professor, Academician Volodymyr Kasyanenko Department of Animal Anatomy, Histology and Pathomorphology
https://orcid.org/0000-0002-0015-6350
V. V. LISOVA,
PhD, Associate Professor, Academician Volodymyr Kasyanenko Department of Animal Anatomy, Histology and Pathomorphology
https://orcid.org/0000-0002-5169-4503
I. M. DERKACH,
PhD, Associate Professor, Department of Pharmacology, Parasitology and Tropical Veterinary Medicine
https://orcid.org/0000-0002-0149-7923
S. S. DERKACH,
PhD, Associate Professor, Department of Obstetrics, Gynaecology and Biotechniques of Animal Reproduction
https://orcid.org/0000-0002-6174-1377
V. B. DUKHNYTSKYI,
Doctor of Veterinary Sciences, Professor, Department of Pharmacology, Parasitology and Tropical Veterinary Medicine
https://orcid.org/0000-0002-9670-1244
A. M. TYSHKIVSKA,
Graduate Student, Department of Pharmacology, Parasitology and Tropical Veterinary Medicine
https://orcid.org/0000-0003-4419-2174
E-mail: Irina1215@ukr.net
National University of Life and Environmental Sciences of Ukraine, 15 Heroiv Oborony st., Kyiv 03041, Ukraine

Abstract. *Iron (IV) clathrochelate based on a macrobicyclic ligand of the hexahydrazide type is a unique compound that contains iron in a rare high valence IV. Preclinical and clinical studies of this complex, which were started for the first time in Ukraine, have an important theoretical and practical consequence as this complex can be recommended as an active substance in iron-containing drugs with antianemic action.*

In conducting preclinical studies of new drugs, pathomorphological studies are important because they are a necessary step in studying the biological response of animals to the action of test substances. It was found that some pathological changes develop

in the body of white mice under conditions of experimental acute and chronic iron (IV) clathrochelate intoxication. They correlated with the dose of the test compound. During chronic intoxication, the microscopic changes in the liver and kidney of white mice treated with iron (IV) clathrochelate at a dose of 1/10 DL50 were similar to the microscopic changes in the liver and kidney of mice treated with the experimental drug at a dose of 1/5 DL50. However, the severity of these changes was lower, reflecting a lower degree of organ damage. In the myocardium of mice treated with iron (IV) clathrochelate at a dose of 1/5 DL50, as during acute iron (IV) clathrochelate poisoning, only edema was recorded on the 10th day. The prospects for further research are the study of microscopic changes in the organs of laboratory animals of other species during experimental iron (IV) clathrochelate toxicosis.

Keywords: *iron, pathomorphological studies, liver, kidneys, heart, toxicity*

Introduction

During preclinical studies of a new drug, the microscopic research of the systems and organs of experimental animals enables studying the pathogenesis of intoxication with the studied drug (Kotsyumbas et al., 2006). We have previously reported the study of acute and chronic toxicity of iron (IV) clathrochelate (based on a macrocyclic ligand of the hexahydrazide type) for laboratory animals (Dukhnisky et al., 2018; 2019; 2020), but the microscopic changes in their internal organs under experimental toxicosis of the test compound remain unexplored.

Analysis of recent researches and publications

Iron is the second most common metal in nature (after aluminum) and occurs in valencies II and III, and only in the form of compounds. However, in recent decades, such data have expanded significantly and are deepening today. In particular, studies of iron in high valencies, IV, V, VI, have become relevant (Weiss et al., 2001; Krahe et al., 2014; Shylin et al., 2019; Prakash et al., 2020; Kloß et al., 2021). Thus, Hohenberger et al. (2012) prove that oxo and nitrido complexes of high-valent iron are active intermediates in many biological and chemical processes in nature. Nam et al. (2014) studied the reactionary ability and the mechanism of the reaction of mononuclear nonheme iron (IV) oxo complexes. Machalová Šišková et al. (2016) investigated ferrates of high-valent forms (Fe (VI), Fe (V), and Fe (IV)) in aquatic environment. Under ambient conditions, high-valent iron compounds (+4, +5, +6) are not able to form spontaneously, and the synthetically obtained ones are unstable in polar organic solvents, especially in aqueous solutions, which, in turn, limits their research and use.

However, several studies have been conducted, in which more stable compounds of high-valent iron have been synthesized. Thus, Tomyn et al. (2017) proposed the synthesis of complexes of iron (IV) hexahydrazide clathrochelate in an alkaline aqueous medium from salts of iron (III), oxalodihydrazide, and formaldehyde, accompanied by air oxidation. Such combinations can exist for a long time in the environment without any signs of decomposition in water, non-aqueous solutions, and in the solid state. According to the results of pre-

clinical studies conducted by us, it was found that iron (IV) clathrochelate corresponds to class III hazard according to the classification of chemicals by degree of danger (GOST 12.1.007-76), and class IV and degree of toxicity – "low toxicity" – according to the classification of substances for toxicity (Dukhnisky et al., 2018; 2019).

In acute experimental toxicosis, the average lethal dose of iron (IV) clathrochelate was found to be 764.3 ± 32.71 mg/kg body weight for quails and 1258.3 ± 144.87 mg/kg body weight for white mice (Dukhnisky et al., 2018). The effect of iron (IV) hexahydrazide clathrochelate solutions in the various concentrations on laboratory animals (white mice, white rats, and quails) was investigated in the study of chronic toxicity. In this case, the determination of the dynamics of body weight, the relative mass coefficients of their internal organs, blood morphological parameters, and biochemical indicators of serum with repeated administration of the test substance in different doses to animals of three species was conducted (Dukhnisky et al., 2019; 2020).

During toxicological studies of drugs for laboratory animals, pathomorphological studies are quite important among other methods. They are a necessary step in the research of the biological response of animals to the action of drugs and allow to describe the nature and severity of the pathological process under the action of the studied substances. Analysis of microscopic changes in organs and tissues facilitates to determine the cause of animal death during the experiment. In this case, morphological studies in the dynamics during the experiment are mandatory, it assists to trace the development of pathological and restorative processes, to understand their nature and significance (pathology, compensation, and adaptation).

The research material is organs and tissues from specially killed animals and those who died during the experiment. The results of the effect of the veterinary medicinal product are evaluated after macroscopic examination and microscopic examination of the organs in animals of the control and experimental groups. Morphological methods can be used to test changes in various organs and tissues from minimal to obvious. Thus, under the influence of chemicals of general toxic and hepatotropic action, a typical corresponding reaction of the body is most often observed: violation of the protein, lipid, and carbohydrate metabolism, changes in the biliary and vascular systems. In general, the process may be in the nature of acute toxic dystrophy, toxic persistent hepatitis, and hepatosis. In case of intoxication with cardiotropic substances, morphologically changes are mainly diffuse in nature. Changes in the myocardium are more often registered in the form of disorders of lipid, carbohydrate, and protein metabolism in the heart muscle, which are found in eosinophilic, fuchsinophilic foci of muscle fibers, myolysis, fine-grained fatty degeneration, and coagulation necrosis. With various intoxications in the heart, there is fatty degeneration. An increase in the number of histiocytes in the stroma is often noted, but interstitial myocarditis with cellular infiltrates is rare, and its detection indicates a severe degree of intoxication. It should be noted that conducting microscopic examinations of animals in a chronic toxicological experiment has difficulties due to the need to diagnose minimal structural, structural and functional abnormalities in the organs, as well as to determine their severity (Kotsyumbas et al., 2006).

Therefore, during preclinical studies of the new drug, a detailed microscopic study of the systems and organs in experimental animals enables studying the pathogenesis of intoxication under the influence of the test substance.

Purpose. The aim of the study was to investigate microscopic changes in the internal organs of white mice in the acute and chronic experimental toxicosis with iron (IV) clathrochelate.

Materials and methods of research

The study of chronic toxicity of iron (IV) clathrochelate Na2[Fe(L-6H)]·2H2O (L – macrobicyclic hexahydrazide ligand) was performed on white mice weighing 19–25 g, formed into three groups of 15 white mice each. Mice of the 1st group (control) received water; mice of the 2nd group – a solution of iron (IV) clathrochelate at the rate of 125.8 mg/kg body weight (1/10 DL50 of the test compound); mice of the 3rd group – a solution of iron (IV) clathrochelate at a rate of 251.6 mg/kg body weight (1/5 DL50 of the test compound).

The animals were kept in the vivarium of the Faculty of Veterinary Medicine of the National University of Life and Environmental Sciences of Ukraine, with a constant air temperature and humidity in the premises. Feeding mice provided a standard diet with constant access to water/aqueous solution of iron (IV) clathrochelate. Before the experiment, laboratory animals of all groups were kept in the adaptation period of 10 days. No deviations in the behavioral responses of white mice in both the experimental and control groups were observed.

All activities were carried out in accordance with the "General Ethical Principles of Animal Experiments" (Ukraine, 2001) and in accordance with the provisions of the European Convention for the Protection of Vertebrate Animals used for Experimental and other Scientific Purposes (Strasburg: Council of Europe 18.03.1986).

During the study of the acute toxicity of iron (IV) clathrochelate, the main stages of pathomorphological research were the following: white mice that died after euthanasia (at the end of the experiment) were dissected; the macroscopic examination was performed; the organs were excised; the pieces of internal organs for histological examination were weighed and fixed.

During the study of chronic toxicity of iron (IV) clathrochelate, white mice of experimental and control groups were euthanized on days 10, 20, and 30 of the experiment; the internal organs of white mice of the 1st group (control), 2nd experimental group (1/10 DL50 of test compound), and 3rd experimental group (1/5 DL50 of test compound) were subjected to histological examination.

Histological examinations were performed in the laboratory of histology of the Academician Volodymyr Kasyanenko Department of Animal Anatomy, Histology and Pathomorphology of Faculty of Veterinary Medicine, National University of Life and Environmental Sciences of Ukraine. From each group of white mice in the established terms of research, an autopsy of 5 animals was carried out by a method of partial evisceration (Zon et al., 2009). The pieces of the liver, heart, kidneys, lungs, spleen, and stomach were taken for histological examination after pathological autopsy. The selected pieces were fixed in a 10% solution of neutral formalin, dehydrated in ethanol of increasing concentration, and poured into paraffin

through chloroform. Sections 6 ± 2 mm thick were prepared using a sled microtome and stained with Carazzi's hematoxylin and eosin. Hydropic dystrophy was differentiated from fatty dystrophy by staining frozen histological sections with Sudan III (Goralskyi et al., 2005). The study of histopreparations and their photography was performed using an OLYMPUS CX41 microscope and an OLYMPUS C-5050 camera.

Results of the research and their discussion

Histological examination of the liver in mice during acute experimental toxicosis with iron (IV) clathrochelate revealed the fragmentation of a part of liver plates and the granular dystrophy of hepatocytes. In many hepatocytes, the presence of fluid-filled vacuoles in the cytoplasm was observed, these vacuoles were not painted over in the response to the detection of lipids, which indicated the beginning of the development of hydropic dystrophy (Fig. 1).

On the 20th day, an increase in hydropic dystrophy was registered, and part of the dystrophically altered hepatocytes was destroyed (Fig. 2).

On the 30th day, complete disorganization of the structure of the liver lobes was observed and all hepatocytes were at different stages of destruction, or in a state of necrosis (Fig. 3).

Histological studies of the liver of white mice during chronic iron (IV) clathrochelate poisoning at various doses also revealed the microscopic changes but they were not as pronounced as in acute toxicity of iron (IV) clathrochelate at any time in our studies.

In the liver of mice treated with 1/5 DL50 of iron (IV) clathrochelate, granular dystrophy of hepatocytes was registered on the 10th day and in some liver cells – fluid-filled vacuoles in the cytoplasm (hydropic dystrophy). However, fragmentation of the liver plates and disorganization of the structure of the liver lobes, as observed in acute poisoning, were not observed (Fig. 4).

On the 20th day, the progression of

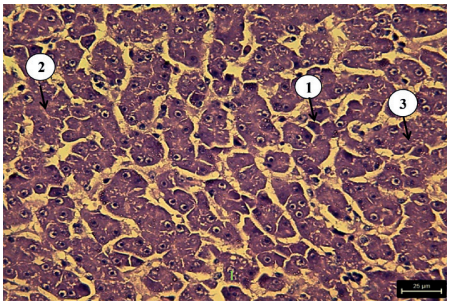

Fig. 1. The liver of a mouse during acute experimental toxicosis with iron (IV) clathrochelate on the 10th day: 1 – fragmentation of the liver plate; 2 – granular dystrophy of hepatocytes; 3 – fluid-filled vacuoles in the cytoplasm of the hepatocyte. Carazzi's hematoxylin and eosin, ×40

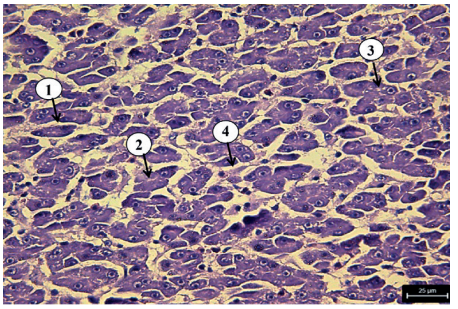

Fig. 2. The liver of a mouse during acute experimental toxicosis with iron (IV) clathrochelate on the 20th day: 1 – fragmentation of the liver plate; 2 – granular dystrophy of hepatocytes; 3 – fluid-filled vacuoles in the cytoplasm of the hepatocyte; 4 – destruction of the hepatocyte. Carazzi's hematoxylin and eosin, ×4

hydropic dystrophy in hepatocytes was detected (Fig. 5), which in some liver cells led to a complete lysis of the cytoplasm (Fig. 6).

On the 30th day, the number of hepatocytes in the state of hydropic dystrophy markedly increased but the fragmentation of liver plates and disorganization of the structure of liver lobes, as on day 10, was not detected (Fig. 7).

In the liver of mice treated with 1/10 DL50 of iron (IV) clathrochelate, granular dystrophy of hepatocytes and signs of hydropic dystrophy in some liver cells were registered on the 10th day, as well as with the use of iron (IV) clathrochelate at a dose of 1/5 DL50. However, the number of liver cells with signs of hydropic dystrophy was significantly lower (Fig. 8).

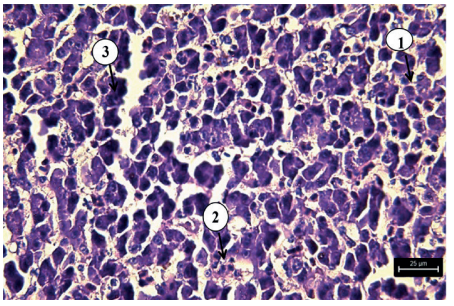

Fig. 3. The liver of a mouse during acute experimental toxicosis with iron (IV) clathrochelate on the 30th day: 1 – complete disorganization of the structure of the liver lobe; 2 – destruction of hepatocytes; 3 – necrosis of hepatocytes. Carazzi's hematoxylin and eosin, ×40

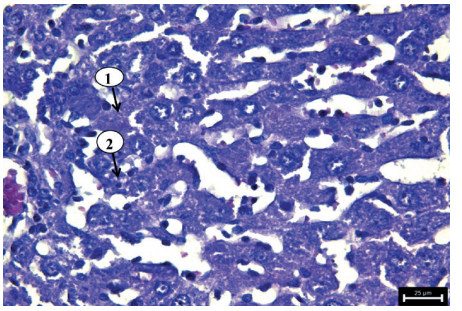

Fig. 4. The liver of a mouse during chronic experimental toxicosis with clathrochelate iron (IV) (1/5 DL50 of the test compound) on the 10th day: 1 – granular dystrophy of hepatocytes; 2 – fluid-filled vacuoles in the cytoplasm of the hepatocyte. Carazzi's hematoxylin and eosin, ×40

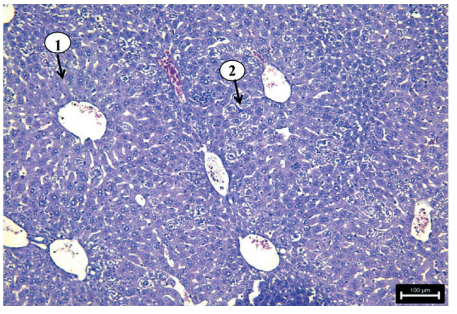

Fig. 5. The liver of a mouse during chronic experimental toxicosis with iron (IV) clathrochelate (1/5 DL50 of the test compound) on the 20th day: 1 – granular hepatocyte dystrophy; 2 – hydropic hepatocyte dystrophy. Carazzi's hematoxylin and eosin, ×10

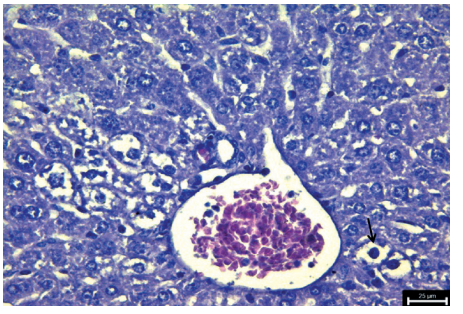

Fig. 6. The liver of a mouse during chronic experimental toxicosis with iron (IV) clathrochelate (1/5 DL50 of the test compound) on the 20th day: 1 – granular hepatocyte dystrophy; 2 – hydropic hepatocyte dystrophy. Carazzi's hematoxylin and eosin, ×40

On the 20th day, the number of cells with hydropic dystrophy increased slightly and on the 30th day, a small number of hepatocytes with complete lysis of the cytoplasm was detected (Fig. 9).

Thus, in the liver of mice treated with iron (IV) clathrochelate at a dose of 1/10 DL50 during chronic intoxication, the microscopic changes were similar to the microscopic changes in the liver of mice treated with the test drug at a dose of 1/5 DL50. However, the severity of these changes was lower, reflecting a lower degree of organ damage.

Histological examination of the kidneys of mice during acute experimental toxicosis with iron (IV) clathrochelate on the 10th day revealed granular dystrophy of the epithelial cells of the convoluted and straight tubules. In some tubules, the centers of the destruction of epitheliocytes were registered (Fig. 10).

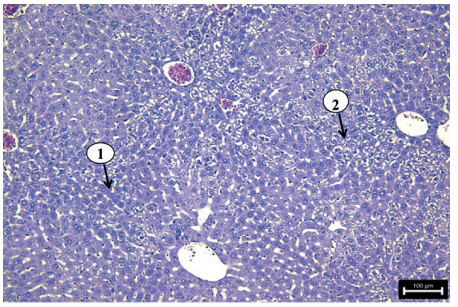

Fig. 7. The liver of a mouse during chronic experimental toxicosis with iron (IV) clathrochelate (1/5 DL50 of the test compound) on the 30th day: 1 – hepatic plate; 2 –hydropic hepatocyte dystrophy. Carazzi's hematoxylin and eosin, ×10

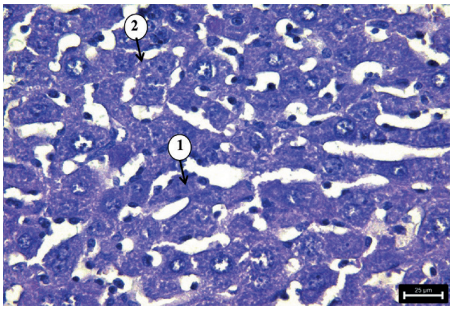

Fig. 8. The liver of a mouse during chronic experimental toxicosis with iron (IV) clathrochelate (1/10 DL50 of test compound) on the 10th day: 1 – granular dystrophy of hepatocytes; 2 – fluid-filled vacuoles in the cytoplasm of the hepatocyte. Carazzi's hematoxylin and eosin, ×40

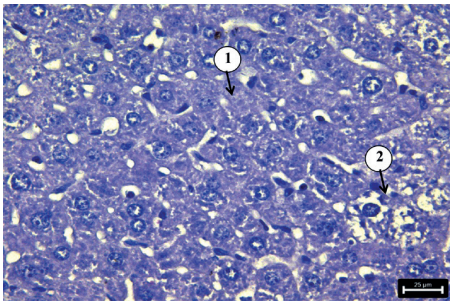

Fig. 9. The liver of a mouse during chronic experimental toxicosis with clathrochelate iron (IV) (1/10 DL50 of the test compound) on the 30th day: 1 – granular dystrophy of hepatocytes; 2 – hydropic hepatocyte dystrophy. Carazzi's hematoxylin and eosin, ×40

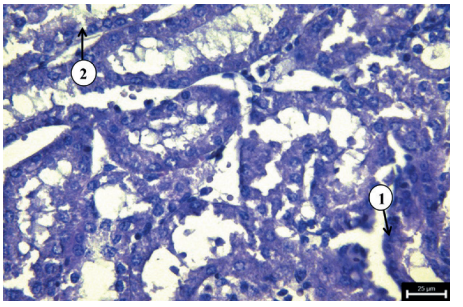

Fig. 10. The kidney of a mouse during acute experimental toxicosis with iron (IV) clathrochelate on the 10th day: 1 – granular dystrophy of the epithelium of the tortuous tubule; 2 – destruction of epithelial cells of the tortuous tubule. Carazzi's hematoxylin and eosin, ×40

On the 20th day, in addition to dystrophic changes and destruction of the epithelial cells of the renal tubules, serous extracapillary glomerulonephritis appeared (Fig. 11), and on the 30th day, necrosis of their epithelium was already registered in the tortuous tubules (Fig. 12).

Such microscopic changes indicated the rapid progression of significant renal damage in acute experimental toxicosis with iron (IV) clathrochelate.

Histological examinations of the kidneys of mice during chronic poisoning with iron (IV) clathrochelate at various doses also revealed microscopic changes but they were not as pronounced as with acute iron (IV) clathrochelate poisoning in any of the terms of research.

In the kidneys of mice treated with iron (IV) clathrochelate at a dose of 1/5 DL50 on the 10th day, as in acute poisoning, granular dystrophy of epithelial cells of tortuous and straight tubules was registered and the areas of epitheliocyte destruction were observed (Fig. 13).

On the 20th day, there was a serous extracapillary glomerulonephritis (Fig. 14).

However, later the nature of microscopic changes during chronic iron (IV) clathrochelate poisoning at a dose of 1/5 DL50 did not differ from that in acute poisoning. Necrosis of epithelial cells of the renal tubules did not develop (Fig. 15).

In the kidneys of mice treated with iron (IV) clathrochelate at a dose of 1/10 DL50, from days 10 to 30, only granular dystrophy and destruction of tubular epithelial cells were found (Fig. 16, 17).

Thus, during chronic poisoning in the kidneys of mice treated with iron (IV) clathrochelate at a dose of 1/10 DL50, the microscopic changes were similar to the microscopic changes in the kidneys of mice treated with iron (IV) clathrochelate at a dose of 1/5 DL50. However, the severity of these changes was less, reflecting a lower degree of organ damage.

Histological examinations of the heart of mice during acute experimental toxicosis with iron (IV) clathrochelate

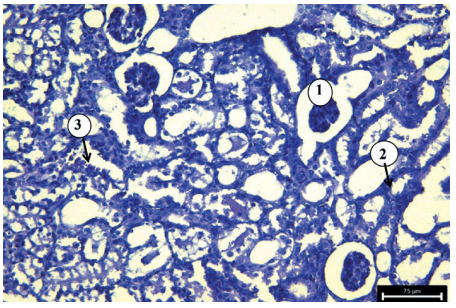

Fig. 11. The kidney of a mouse during acute experimental toxicosis with iron (IV) clathrochelate on the 20th day: 1 – serous extracapillary glomerulitis; 2 – granular dystrophy of the epithelium of the tortuous tubule; 3 – destruction of epithelial cells of the tortuous tubule. Carazzi's hematoxylin and eosin, ×20

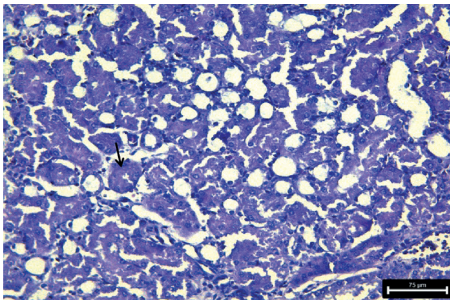

Fig. 12. The kidney of a mouse during acute experimental toxicosis with iron (IV) clathrochelate on the 30th day: necrosis of epithelial cells of the convoluted tubule (shown by the arrow). Carazzi's hematoxylin and eosin, ×20

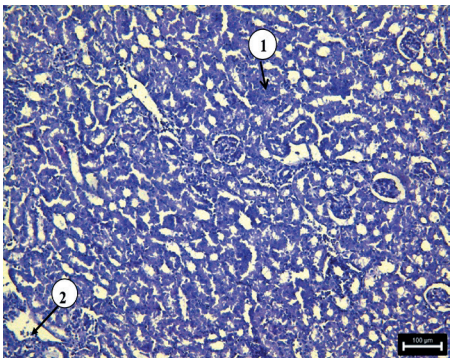

Fig. 13. The kidney of a mouse during chronic experimental toxicosis with iron (IV) clathrochelate (1/5 DL50 of the test compound) on the 10th day: 1 – granular dystrophy of the epithelium of the tortuous tubule; 2 – destruction of the epithelium of the tortuous tubule. Carazzi's hematoxylin and eosin, ×10

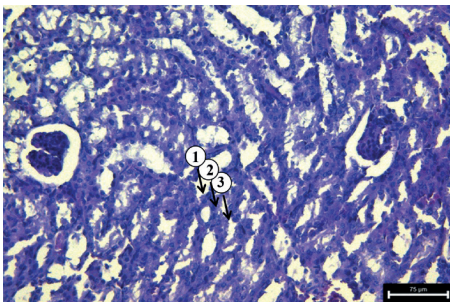

Fig. 14. The kidney of a mouse during chronic experimental toxicosis with iron (IV) clathrochelate (1/5 DL50 of the test compound) on the 20th day: 1 – serous extracapillary glomerulitis; 2 – granular dystrophy of the epithelium of the tortuous tubule; 3 – destruction of epithelial cells of the tortuous tubule. Carazzi's hematoxylin and eosin, ×20

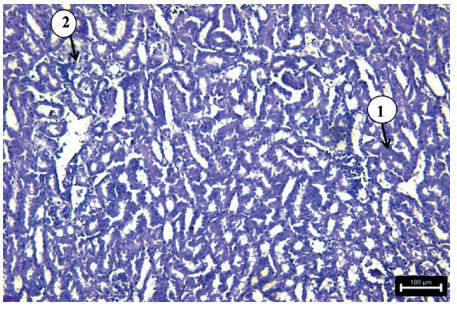

Fig. 15. The kidney of a mouse during chronic experimental toxicosis with iron (IV) clathrochelate (1/5 DL50 of the test compound) on the 30th day: 1 – granular dystrophy of the epithelium of the convoluted tubule; 2 – destruction of epithelial cells of the tortuous tubule. Carazzi's hematoxylin and eosin, ×10

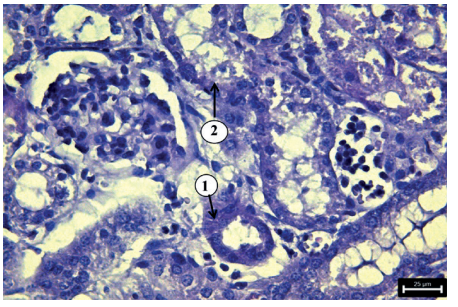

Fig. 16. The kidney of a mouse during chronic experimental toxicosis with iron (IV) clathrochelate (1/10 DL50 of the test compound) on the 10th day: 1 – granular dystrophy of the epithelium of the tortuous tubule; 2 – destruction of epithelial cells of the tortuous tubule. Carazzi's hematoxylin and eosin, ×40

revealed myocardial edema on the 10th day (Fig. 18).

On the 20th day, in addition to myocardial edema, granular dystrophy of myocardial cells was detected, and in part of the bundles of heart muscle fibers – granular decay of their sarcoplasm. Some of the dystrophically altered cells were destroyed (Fig. 19, 20).

On the 30th day, the presence of fairly large areas of myocardial necrosis was also found (Fig. 21).

In the epicardium and endocardium, we did not detect any microscopic

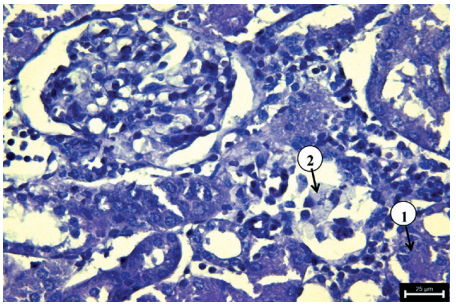

Fig. 17. The kidney of a mouse during chronic experimental toxicosis with iron (IV) clathrochelate (1/10 DL50 of the test compound) on the 30th day: 1 – granular dystrophy of the epithelium of the tortuous tubule; 2 – destruction of epithelial cells of the tortuous tubule. Carazzi's hematoxylin and eosin, ×40

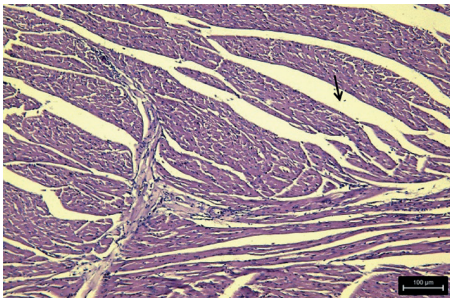

Fig. 18. The heart of a mouse during acute experimental toxicity of iron (IV) clathrochelate on the 10th day: edema between bundles of muscle fibers (shown by arrow). Carazzi's hematoxylin and eosin, ×10

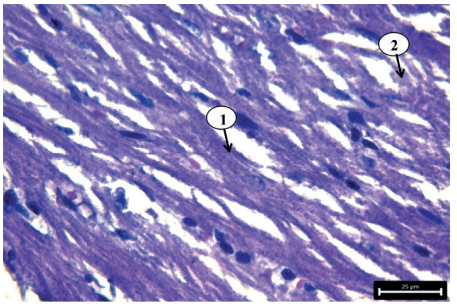

Fig. 19. The heart of a mouse during acute experimental toxicosis with iron (IV) clathrochelate on the 20th day: 1 – granular myocardial dystrophy; 2 – destruction of muscle fiber. Carazzi's hematoxylin and eosin, ×40

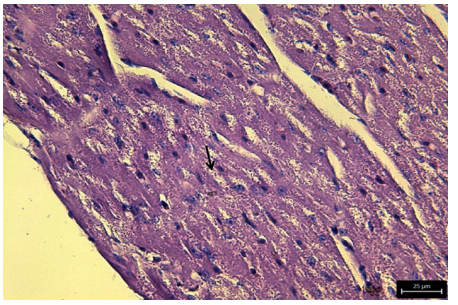

Fig. 20. The heart of mouse during acute experimental toxicosis with iron (IV) clathrochelate on the 20th day: granular disintegration of muscle fiber sarcoplasm (shown by arrow). Carazzi's hematoxylin and eosin, ×40

changes during acute experimental toxicosis with iron (IV) clathrochelate in any of our studies.

Histological examinations of mice hearts during chronic toxicosis caused by iron (IV) clathrochelate at various doses also revealed microscopic changes but they were not as pronounced as during acute poisoning with iron (IV) clathrochelate in our studies. In the myocardium of mice treated with iron (IV) clathrochelate at a dose of 1/5 DL50 on the 10th day, as in acute poisoning, edema was registered (Fig. 22).

On the 20th day, granular dystrophy of myocardial cells and destruction of some dystrophically altered cells were registered (Fig. 23), and on the 30th day, granular decay of sarcoplasm of muscle fibers was observed (Fig. 24).

On the 10th day, the myocardial edema was detected in mice treated with

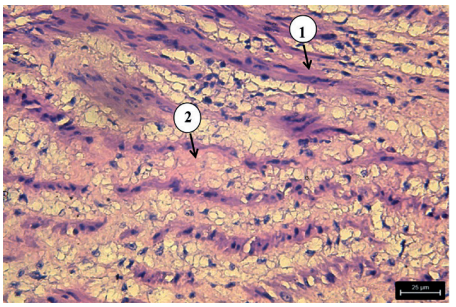

Fig. 21. The heart of a mouse during acute experimental toxicosis with iron (IV) clathrochelate on the 30th day: 1 – muscle fiber; 2 – necrosis of muscle fiber. Carazzi's hematoxylin and eosin, ×40

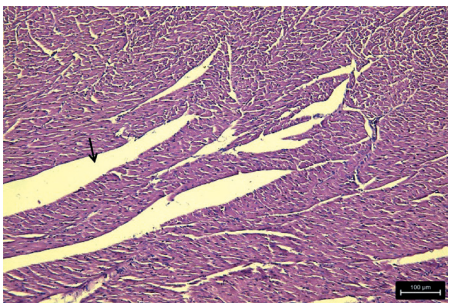

Fig. 22. The heart of a mouse during chronic experimental toxicosis with iron (IV) clathrochelate (1/5 DL50 of test compound) on the 10th day: edema (shown by arrow). Carazzi's hematoxylin and eosin, ×10

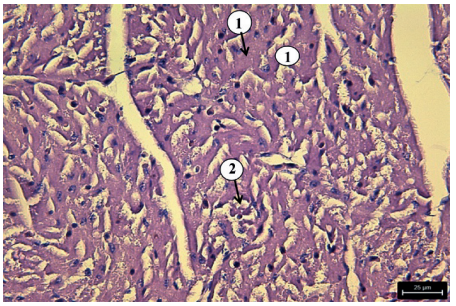

Fig. 23. The heart of a mouse during chronic experimental toxicosis with iron (IV) clathrochelate (1/5 DL50 of the test compound) on the 20th day: 1 – granular dystrophy of muscle fibers; 2 – destruction of muscle fibers. Carazzi's hematoxylin and eosin, ×40

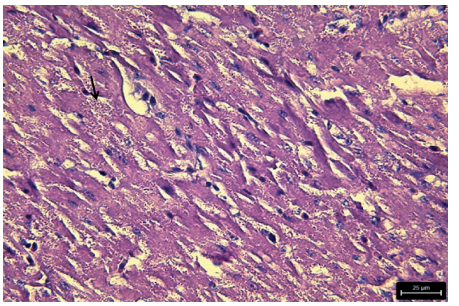

Fig. 24. The heart of a mouse during chronic experimental toxicosis with iron (IV) clathrochelate (1/5 DL_{50} of test compound) on the 30th day: granular disintegration of muscle fiber sarcoplasm (shown by arrow). Carazzi's hematoxylin and eosin, ×40

iron (IV) clathrochelate at a dose of 1/10 DL50, and on the 20th day – also granular dystrophy of myocardial cells (Fig. 25), and on the 30th day – the destruction of a part of the dystrophic altered heart muscle cells (Fig. 26).

As with acute poisoning, microscopic changes in the epicardium and endocardium during chronic intoxication were not found by us in any of the cases.

Thus, microscopic changes in the myocardium of mice treated with iron (IV) clathrochelate at doses of 1/5 and 1/10 DL50 during chronic intoxication were similar to microscopic changes in the myocardium of a mouse during acute poisoning with iron (IV) clathrochelate. However, the severity of these changes was lower, reflecting a lower degree of organ damage, and depended on the dose of iron (IV) clathrochelate that mice received. In the stomach, intestines, and

lungs, microscopic changes during both acute and chronic poisoning with iron (IV) clathrochelate were not detected in any of the cases (Fig. 27, 28).

In the spleen of all studied mice, the lymphoid nodules were small, fairly dense arrangement of lymphocytes, fuzzy borders, and did not contain light centers (Fig. 29), which indicated the absence of sufficiently strong antigenic stimulation.

This confirms that the animals in our studies were free of infectious agents. In addition, the red pulp had a microscopic structure characteristic of infectious diseases in mice (Fig. 30).

Therefore, the described changes indicated a violation of metabolic processes in the body of white mice. They are confirmed by previously obtained research results (Dukhnisky et al., 2019; 2020). Thus, the analysis of the coefficients of mass of the internal organs of white mice

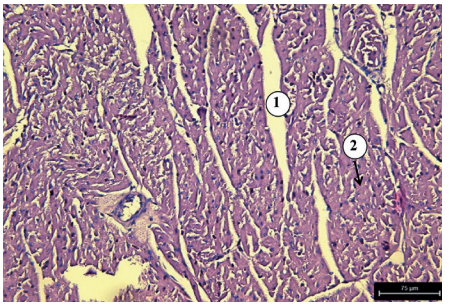

Fig. 25. The heart of a mouse during chronic experimental toxicosis with iron (IV) clathrochelate (1/10 DL50 of the test compound) on the 20th day: 1 – edema; 2 – granular dystrophy of myocardial cells. Carazzi's hematoxylin and eosin, ×20

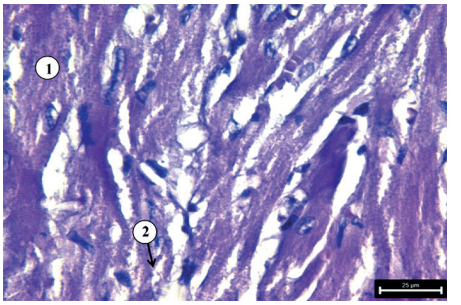

Fig. 26. The heart of a mouse during chronic experimental toxicosis with iron (IV) clathrochelate (1/10 DL_{50} of the test compound) on the 30th day: 1 – granular myocardial dystrophy; 2 – destruction of myocardial cells. Carazzi's hematoxylin and eosin, ×40

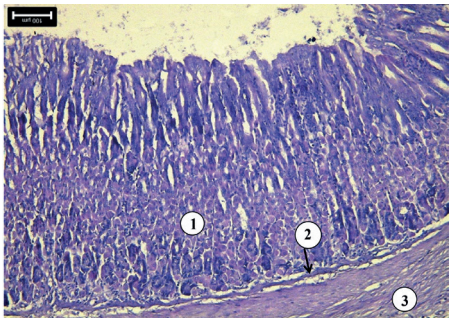

Fig. 27. The stomach of a mouse during acute experimental toxicosis with iron (IV) clathrochelate: 1 – gastric dimples; 2 – submucosal basis; 3 – muscular membrane. Carazzi's hematoxylin and eosin, ×10

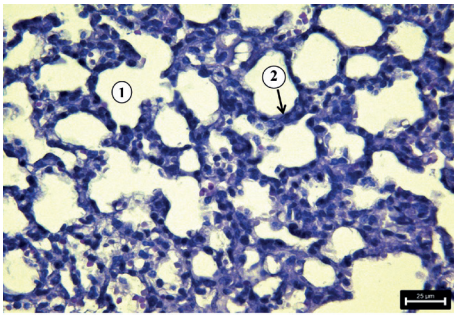

Fig. 28. The lungs of a mouse during acute experimental toxicosis with iron (IV) clathrochelate: 1 – lumen of the alveoli; 2 – the wall of the alveoli. Carazzi's hematoxylin and eosin, ×40

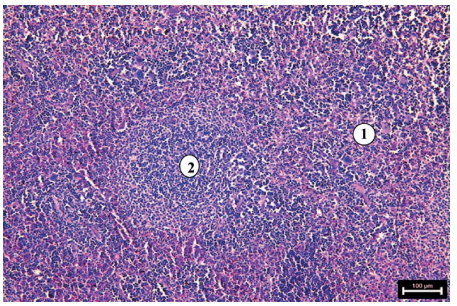

Fig. 29. The spleen of a mouse during acute experimental toxicosis with iron (IV) clathrochelate: 1 – red pulp; 2 – lymphoid nodule (white pulp). Carazzi's hematoxylin and eosin, ×10

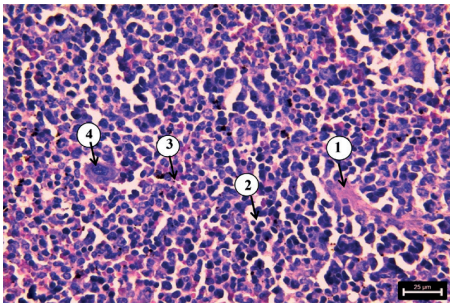

Fig. 30. The spleen of a mouse during acute experimental toxicosis with iron (IV) clathrochelate: 1 – trabeculae; 2 – lymphocyte; 3 – erythrocyte; 4 – macrophage. Carazzi's hematoxylin and eosin, ×40

on the 10th day shows an increase in the masses of all studied organs in animals of experimental groups. Moreover, under the influence of iron (IV) clathrochelate at a dose of 251.6 mg/kg body weight (3rd experimental group), these changes were more pronounced than under its influence at a dose of 125.8 mg/kg body weight. On the 20th day, only the decrease in the relative ratio of the weight of the liver by 6% and spleen by 30% ($P < 0.05$) was found in animals of the 3rd experimental group compared with animals in the control group. The indicators of relative coefficients of internal organs in mice of experimental groups on the 30th day tended to decrease compared with those of animals in the control group. The relative ratio of the weight of the liver was lower by 5% in mice of the 2nd experimental group (a dose of 125.8 mg/kg body weight) and by 13% in mice of the 3rd experimental group (a dose of 251.6 mg/kg body weight). The relative ratio of the mass of the heart was lower by 29% ($P < 0.001$) in mice of the 2nd experimental group and by 43% ($P < 0.001$) in mice of the 3rd experimental group compared with animals in the control group. The relative ratio of the mass of the kidney decreased sharply on the 30th day and was lower by 5% in mice of the 2nd experimental group and by 11% in mice of the 3rd experimental group compared with animals in the control group. The relative coefficient of the mass of the spleen was lower by 17% in mice of the 2nd experimental group and by 25% in mice of the 3rd experimental group. The described data indicate an excessive load of iron (IV) clathrochelate on these organs in white mice. Our previous results of the study of serum biochemical parameters in white mice showed that the greatest changes were in the metabolism of proteins and non-protein compounds of nitrogen, enzyme activity, glucose, and inorganic phosphorus.

Our data are confirmed by the results of studies by other researchers. Thus, the nanoparticles of iron (II) accumulate in target organs (heart, liver, and kidneys) during prolonged administration to the abdominal cavity and cause a wide range of structural and functional changes, which indicate their cardio-vasotoxic, hepatotoxic, and nephrotoxic effects. It was found that prolonged introduction of

these particles into the abdominal cavity of rats is accompanied by the accumulation of small crystalline inclusions in the cytoplasm of cardiomyocytes, hepatocytes, and nephrothelial cells. This indicates the accumulation of the nanoparticles of iron (II) in target organs, which leads to dystrophic and necrobiotic processes in cells and determines the effect of toxic action (Luhovskyi et al., 2019).

Since our studies were conducted for the purpose of preclinical studies of antianemic drugs with the active substance clathrochelate iron (IV), our attention was paid to the microscopic studies of the internal organs of animals using drugs of iron and to the microscopic changes in the body of animals suffering from the iron deficiency anemia. Antipov & Zharov (2013) established that alternative and compensatory processes develop in parenchymal and immunocompetent organs of animals suffering from iron deficiency anemia. The lesions of the liver have certain topical features that reflect the structural and functional heterogeneity of this organ. The most pronounced pathomorphological changes were observed in centrilobular hepatocytes, which were in a state of protein, fatty, and carbohydrate degeneration. Protein dystrophy develops in the epithelium of the kidney tubules. Alterative processes in the kidney tubules are accompanied by apical destruction and desquamation of nephrocytes. The results of studies of parenchymal organs indicate the initial processes of the formation of fibrosis with the possible development of renal and hepatic failure.

In the research of Chetverikova et al. (2006), the morphological studies of internal organs fully confirmed the lack of iron preserved in the body and the associated hypoxic and dystrophic phenomena. The liver had a pale color, hemosiderin was present in the form of traces diffusely, sometimes in the region of the vessels, in some sections, there were areas of necrosis of hepatocytes, the phenomena of protein and fatty degeneration were observed.

Conclusions and future perspectives

The severity of microscopic changes in the organs of white mice correlates with the dose of iron (IV) clathrochelate received by the animals. The histological changes in the liver of mice during acute experimental toxicosis with iron (IV) clathrochelate were characterized by fragmentation of a part of the liver plates, granular dystrophy of hepatocytes, and the presence of fluid-filled vacuoles was observed in the cytoplasm of many hepatocytes, and on the days 20 and 30, there was complete disorganization of the structure of the liver lobes, all hepatocytes were at different stages of destruction, or in a state of necrosis. During chronic poisoning with iron (IV) clathrochelate, microscopic changes in the myocardium of white mice were similar to microscopic changes in the myocardium of white mice during acute poisoning with iron (IV) clathrochelate. In the myocardium of mice treated with 1/10 DL50 of iron (IV) clathrochelate, only edema was detected on the 10th day, additional granular myocardial dystrophy on the 20th day, and destruction of some dystrophically altered cardiac cells on the 30th day. In the kidneys of white mice from the 10th to 30th days, we found granular dystrophy and destruction of tubular epithelial cells.

The future perspectives are the study of microscopic changes in the organs of laboratory animals of other species (white mice and quails) during experimental toxicosis with iron (IV) clathrochelate.

References

Antipov, A. A., & Zharov, A. V. (2013). Gistologicheskie i morfometricheskie izmenenija pecheni, pochek, selezenki i limfaticheskih uzlov u porosjat pri alimentarnoj zhelezodeficitnoj anemii [Histological and morphometric changes in the liver, kidney, spleen and lymph nodes of piglets with nutritional iron deficiency anemia]. Rossijskij veterinarnyj zhurnal [Russian veterinary journal], 1, 19-21. Retrieved from https://cyberleninka.ru/article/n/gistologicheskie-i-morfometricheskie-izmeneniya-pecheni-pochek-selezenki-i-limfaticheskih-uzlov-porosyat-pri-alimentarnoy

Chetverikova, T. D., Krasnikova, I. M., Medvedeva, S. A., Aleksandrova, G. P., Grishchenko, L. A., & Kuklina, L. V. (2006). Modelirovanie I korekchija alimentarnoj anemii [Modeling and correction of iron deficiency anemia]. Bulleten VSNC CO RAMN, 5, 246-251.

Dukhnitsky, V. B., Derkach, I. M., Plutenko, M. O., Fritsky, I. O., & Derkach, S. S. (2018). Determination of the accumulative toxicity parameters of iron (IV) on white mice. Ukrainian Journal of Ecology, 8(2), 308-312. doi: 10.15421/2018_343

Dukhnitsky, V. B., Derkach, I. M., Derkach, S. S., Fritsky, I. O., & Plutenko, M. O. (2019). Chronic toxicity of the Iron (IV) clathrochelate complexes for white rats. Scientific Messenger of LNU of Veterinary Medicine and Biotechnologies. Series: Veterinary Sciences, 21(95), 15-21. doi: 10.32718/nvlvet9503

Dukhnitsky, V. B., Derkach, I. M., Plutenko, M. O., Fritsky, I. O., & Derkach, S. S. (2019). Cumulative properties of ferrum (IV) clathrochelate in rats. Bulletin of Poltava State Agrarian Academy, (2), 238-246. doi: 10.31210/visnyk2019.02.32

Dukhnitsky, V. B., Derkach, I. M., Plutenko, M. O., Fritsky, I. O., & Derkach, S. S. (2019). Acute toxicity of the iron clathrochelate complexes. Regulatory Mechanisms in Biosystems, 10(3), 276-279. doi: 10.15421/021942

Dukhnitsky, V. B., Derkach, I. M., Derkach, S. S., Plutenko, M. O., & Fritsky, I. O. (2019). Influence of iron (IV) clathrochelate complex on quail blood parameters and weight characteristics. Ukrainian Journal of Ecology, 9(3), 126-131. doi: 10.15421/2019_719

Dukhnitsky, V. B., Derkach, I. M., Derkach, S. S., Fritsky, I. O., Plutenko, M. O., & Lozovy, V. M. (2020). Investigation of the irritant effects and allergenic properties of the Iron (IV) clathrochelate complexes. Scientific Messenger of LNU of Veterinary Medicine and Biotechnologies. Series: Veterinary Sciences, 22(97), 130-135. doi: 10.32718/nvlvet9721

Dukhnitsky, V. B., Kalachniuk, L. H., Derkach, I. M., Derkach, S. S., Plutenko, M. O., & Fritsky, I. O. (2020). Iron (IV) hexahydrazide clathrochelate complexes: the chronic toxicity study. Ukrainian Journal of Ecology, 9(3), 18-23. doi: 10.15421/2020_3

Goralskyi, L. P., Khomich, V. T., & Kononsky, O. I. (2005). Osnovy histolohichnoi tekhniky i morfofunktsionalni metody doslidzhennia u normi ta pry patolohii [Fundamentals of histological technique and morphofunctional research methods in normal and pathology]. Zhytomyr. Polissya.

Hohenberger, J., Ray, K., & Meyer, K. (2012). The biology and chemistry of high-valent iron-oxo and iron-nitrido complexes. Nature communications, 3, 720. doi: 10.1038/ncomms1718

Krahe, O., Bill, E., & Neese, F. (2014). Decay of iron(V) nitride complexes by a N-N bond-coupling reaction in solution: a combined spectroscopic and theoretical analysis. Angewandte Chemie (International ed. in English), 53(33), 8727-8731. doi:10.1002/anie.201403402

Kloß, S. D., Haffner, A., Manuel, P., Goto, M., Shimakawa, Y., & Attfield, J. P. (2021). Preparation of iron(IV) nitridoferrate Ca4FeN4 through azide-mediated oxidation under high-pressure conditions. Nature communications, 12(1), 571. doi: 10.1038/s41467-020-20881

Kotsyumbas, I. Ya., Malik, O. G., & Paterega, I. P. (2006). Doklinichni doslidzhennja veterynarnyh likars'kyh zasobiv [Preclinical studies of veterinary drugs]. Lviv: Triada pljus.

Luhovskyi, S. P., Dmytrukha, N. M., Didenko, M. M., Bakalo, L. V., Lahutina, O. S., & Melnyk, N. A. (2019). Morfofunktsionalni zminy vnutrishnikh orhaniv shchuriv za tryvaloho vvedennia v cherevnu porozhnynu nanochastynok oksydu zaliza (Fe2O3) [Morphofunctional changes in the internal organs of rats with prolonged introduction into the abdominal cavity of nanoparticles of iron oxide (Fe2O3)]. Ukrainskyi zhurnal z problem medytsyny, 15(3), 228-239. doi: 10.33573/ujoh2019.03.228

Machalová Šišková, K., Jančula, D., Drahoš, B., Machala, L., Babica, P., Alonso, P. G., Trávníček, Z., Tuček, J., Maršálek, B., Sharma, V. K., & Zbořil, R. (2016). High-valent iron (Fe(VI), Fe(V), and Fe(IV)) species in water: characterization and oxidative transformation of estrogenic hormones. Physical chemistry chemical physics, 18(28), 18802-18810. doi: 10.1039/c6cp02216b

Nam, W., Lee, Y. M., & Fukuzumi, S. (2014). Tuning reactivity and mechanism in oxidation reactions by mononuclear nonheme iron (IV)-oxo complexes. Accounts of chemical research, 47(4), 1146-1154. doi: 10.1021/ar400258p

Prakash, O., Cháber a, P., Rosemann, N. W., Huang, P., Häggström, L., Ericsson, T., ... & Wärnmark, K. (2020). A Stable Homoleptic Organometallic Iron(IV) Complex. Chemistry (Weinheim an der Bergstrasse, Germany), 26(56), 12728-12732. doi: 10.1002/chem.202002158

Shylin, S. I., Pavliuk, M. V., D'Amario, L., Fritsky, I. O., & Berggren, G. (2019). Photoinduced hole transfer from tris(bipyridine)ruthenium dye to a high-valent iron-based water oxidation catalyst. Faraday discussions, 215(0), 162-174. doi: 10.1039/c8fd00167g

Tomyn, S., Shylin, S. I., Bykov, D., Ksenofontov, V., Gumienna-Kontecka, E., Bon, V., & Fritsky, I. O. (2017). Indefinitely stable iron (IV) cage complexes formed in water by air oxidation. Nature Communications, 8, 1-8. doi: 10.1038/ncomms14099

Zon, G. A., Skrypka, M. B., & Ivanivska, L. B. (2009). Pathological autopsy of animals. Donetsk: PP Glazunov R. O.

Weiss, R., Bulach, V., Gold, A., Terner, J., & Trautwein, A. X. (2001). Valence-tautomerism in high-valent iron and manganese porphyrins. Journal of biological inorganic chemistry: JBIC: a publication of the Society of Biological Inorganic Chemistry, 6(8), 831-845. doi: 10.1007/s007750100277

Борисевич Б. В., Лісова В. В., Деркач І. М., Деркач С. С., Духницький В. Б., Тишківська А. М. (2021). МІКРОСКОПІЧНІ ЗМІНИ У ВНУТРІШНІХ ОРГАНАХ БІЛИХ МИШЕЙ ЗА ЕКСПЕРИМЕНАЛЬНОГО ТОКСИКОЗУ КЛАТРОХЕЛАТОМ ФЕРУМУ (IV).
Ukrainian Journal of Veterinary Sciences, 12(4): 36–52, https://doi.org/10.31548/ujvs2021.04.003

Анотація. *Клатрохелат Феруму (IV) на основі макробіциклічного ліганду гексагідразидного типу – унікальна сполука, до складу якої входить Ферум у рідкісній високій валентності IV. Вона характеризується високою стабільністю за високих температур та за різних значень pH тощо. Доклінічні та клінічні дослідження цього комплексу, які розпочаті вперше в Україні, мають важливе теоретичне та практичне значення для різних наук, зокрема для галузі ветеринарної медицини, оскільки цей комплекс може бути рекомендований як діюча речовина у ферумумісних лікарських засобах із протианемічною дією. Нами було досліджено гостру та хронічну токсичність Феруму (IV) для білих мишей,*

білих щурів та перепелів. Клатрохелат Феруму (IV) відповідає III класу небезпечності згідно з класифікацією хімічних речовин за ступенем небезпечності (ГОСТ 12.1.007-76), та IV класу і ступеню токсичності «малотоксичні речовини» відповідно до класифікації речовин за токсичністю. Встановлено, що середня смертельна доза клатрохелату Феруму (IV) для білих мишей за внутрішнього введення становить 1258,3 ± 144,87 мг/кг маси тіла. За проведення доклінічних досліджень нових лікарських засобів важливе місце займають патоморфологічні дослідження, які є необхідним етапом у вивченні біологічної реакції організму тварин на дію лікарських засобів. Вони дають змогу скласти точне уявлення про характер і важкість перебігу патологічного процесу за дії досліджуваних речовин, що суттєво доповнює характеристику загальної інтоксикації за експериментального токсикозу. Установлено, що за умов експериментальної інтоксикації клатрохелатом Феруму (IV) в організмі білих мишей розвиваються патологічні зміни, які корелюють із дозою досліджуваної сполуки: чим вищою є доза, тим більш тяжкі виникають ураження. За хронічної інтоксикації у печінці та нирках білих мишей, які одержували клатрофелат Феруму (IV) у дозі 1/10 DL50, мікроскопічні зміни були подібними до мікроскопічних змін у печінці та нирках мишей, які одержували досліджуваний препарат у дозі 1/5 DL50. Проте ступінь виразності цих змін була меншою, що відображало нижчий ступінь пошкодження органу. У міокарді мишей, які одержували клатрохелат Феруму (IV) у дозі 1/5 DL50, на 10 добу, як і за гострого отруєння, реєструвався лише набряк. Виявлені зміни вказували на порушення метаболічних процесів організмі білих мишей, що підтверджується результатами досліджень, отриманими нами раніше. Перспективою подальших досліджень є вивчення мікроскопічних змін в органах лабораторних тварин інших видів за експериментального токсикозу клатрохелатом Феруму (IV).

Ключові слова: *залізо, патоморфологічні дослідження, печінка, нирки, серце, токсичність*

UDC 619:612.315:636.52/.58 https://doi.org/10.31548/ujvs2021.04.005

MORPHOGENESIS OF THE WALL OF GLANDULAR PART OF THE STOMACH IN CHICKENS DURING POSTNATAL PERIOD OF ONTOGENESIS

N. V. DYSHLIUK,
Doctor of Veterinary Sciences, Associate Professor, Academician
V. G. Kasyanenko Department of Anatomy, Histology and Pathomorphology
https://orcid.org/0000-0003-4753-9356
E-mail: dushlyuk@ukr.net
National University of Life and Environmental Sciences of Ukraine,
15 Heroiv Oborony st., Kyiv 03041, Ukraine

Abstract. *Knowledge about the morphological features of the structure and functions of the digestive organs provides the basis for rational and effective use of feed, prevention and treatment of gastrointestinal diseases in poultry. In this regard, the study of the morphogenesis of the digestive system in birds and the mechanisms of their regulation is of great importance.*

The object of the study was the glandular part of the stomach (proventriculus) in chickens of Shaver 579 strain. The material for macro- and microscopic examinations was selected from birds at age of 1, 30, 60, 90, 120, 150, 180, 210, 240, 270, and 300 days and 1, 2, and 3 years; it was fixed in a 10% neutral formalin solution and embedded into paraffin according to conventional methods. For submicroscopic examinations, the material was selected from hens of this strain at age of 180 days. The structure of epitheliocytes in the superficial epithelium and secretory cells of the deep glands was studied in ultrathin sections. Digital indicators of research results were statistically processed by a personal computer using the Microsoft Excel program.

The glandular stomach in chickens is a direct extension of the esophagus and has the form of a thick-walled tube, the wall of which is formed by mucous, muscular, and serous membranes. The superficial epithelium of the mucosa is represented by cylindrical epithelial cells that are located within the basal membrane. They are linked to each other by different types of contacts and have a well-defined polar differentiation. The lobules of the deep glands are formed by cells with well-developed synthesizing organelles and secretory granules.

The morphogenesis of the glandular part of the stomach in chickens according to age aspect is manifested by changes in morphometric parameters of the thickness and the area of the membranes of its wall. The wall thickness increases (between the folds 4223.23 ± 189.25 and in the area of the folds 5561.32 ± 45.01 μm) unevenly in chickens up to the age of 240 days. The most developed membrane of the wall of the glandular stomach is the mucosa. Its area increases (by 82.14 ± 0.56%) in chickens up to the age of 180 days, and the area of muscular and serous membranes decreases (by 15.54 ± 0.65 and 2.32 ± 0.33%, respectively). In older birds, the thickness of the wall and the area of the membranes of the glandular stomach do not change significantly.

Keywords*: chickens, stomach, morphometric parameters, mucosa, muscular membrane, serosa*

Introduction

Poultry farming in Ukraine is the most efficient branch of animal husbandry, which provides opportunities for a short time to significantly increase the production of high-calorie dietary products – meat and eggs in order to provide the population with physiologically necessary nutrition. This is facilitated by climatic conditions and developed grain farming (Seliverstova, 2018). Knowledge of the structural and morphological features of the structure and functions of the digestive system form the basis for rational and effective use of feed, prevention and treatment of gastrointestinal diseases in poultry. In this regard, the study of the morphogenesis of the avian digestive system and the mechanisms of their regulation is of great importance.

Analysis of recent researches and publications

Birds capture with their beak and swallow unchewed feed (due to the absence of teeth), which from the esophagus enters directly into the glandular part of the stomach (Khomych et al., 2020). The latter is not clearly separated from the esophagus and differs only in thicker walls and a large number of glands that secrete digestive enzymes. The size and shape of the glandular part of the stomach depend on the amount and size of feed objects (trophic specialization) that are coming from the environment. Depending on the bird species, it can be spindle-shaped, barrel-shaped, or truncated cone-shaped (Kharchenko, 2014).

A typical feature for the mucosa in the glandular part of the avian stomach is the folding and the presence of superficial and deep glands. The superficial glands are simple tubular, located in the lamina propria of the mucosa, and the deep glands – in the submucosa. The deep glands form lobes with a central cavity, into which numerous secretory departments open (Nasrin et al., 2012; Abumandour, 2013; Naletova, 2013). In grain-eating, herbivorous, and omnivorous birds, these glands are multilobed with a complexly branched system of ducts, and in carnivorous and insectivorous birds, they are unilobed. The deep glands produce gastric juice, under the influence of which the chemical processing of feed occurs. The optimal environment in the glandular part of the stomach is provided by hydrochloric acid, which simultaneously causes the transition of inactive pepsinogen to active pepsin. There is a species difference in proteolytic activity and acidity of the juice in birds. The gastric juice in chickens and turkeys has the greatest digestive power and acidity, and the least – geese (Naletova, 2013).

Many scientific works are devoted to the glandular part of the stomach in birds, including chickens (Ahmed et al., 2011; Dahekar et al., 2014; Demirbag et al., 2015) but some inaccuracies remain in the morphogenesis of the gastric gland wall during the postnatal period of ontogenesis.

The purpose of the study is to determine the morphological features and to establish the morphometric indicators of the growth of the glandular part of the chicken stomach in the age aspect.

Materials and methods of research

Macroscopic, microscopic, and submicroscopic methods of morphological research were used in the study. All interventions and euthanasia of birds were performed by acute exsanguination after

ether anesthesia in compliance with the requirements of the European Convention for the Protection of Vertebrate Animals Used for Experimental and Other Scientific Purposes (Strasbourg, 1986), the First National Congress on Bioethics (Kyiv, 2001), and the Law of Ukraine On Protection of Animals from Brutal Treatment (2006).

The material for macro- and microscopic examinations (glandular part of the stomach) was selected from chickens of egg-laying cross Shaver 579 at age of 1, 30, 60, 90, 120, 150, 180, 210, 240, 270, and 300 days and 1, 2 and 3 years. The birds were clinically healthy and showed no signs of disease. The research was conducted in the Scientific Laboratory of Immunomorphology of the Academician V. G. Kasyanenko Department of Anatomy, Histology and Pathomorphology, the National University of Life and Environmental Sciences of Ukraine. The selected material was labeled and fixed in a 10% aqueous solution of neutral formalin. After fixation, the material was washed in running water, dehydrated in alcohols of increasing concentration, compacted, and embedded into paraffin according to conventional methods. The paraffin-embedded material was placed on wooden blocks, and histological sections 5–10 μm thick were made by the MPS-2 sled microtome. Sections were stained with Caracci's hematoxylin and eosin, according to the Weigert and Van Gieson methods (Goralskyi et al., 2005). The area of the membranes of the glandular part of the stomach was determined by the method of "point counting" using an MBS-2 binocular microscope and a measuring grid, which is included in its kit. The wall thickness was measured using an MBI-2 microscope and an MOV-1-15x eyepiece micrometer. The results of the studies were recorded in protocols and their figures were statistically processed using a personal computer by Microsoft Excel (Plokhinskyi, 1970; Goralskyi et al., 2005). The material for the illustrations was photographed using an Olympus microscope with a Nikon Coolpix S3100 camera.

The submicroscopic examination was performed to study the superficial epithelial cells and secretory cells of the deep glands of the glandular part of the stomach in 180-day-old chickens. The studies were performed in the Laboratory of Electron Microscopy of the Bogomolets National Medical University. The material was selected no later than 5 minutes after bird slaughter (Vlasov et al., 2011). The glandular part of the stomach was cut into pieces 1.5 mm^3 in size, fixed in 2.5% glutaraldehyde for 1 hour at a temperature of +40 °C, washed with 0.1 M Na-cocadylate buffer, and fixed again in 2% osmic acid solution. Then the pieces were dehydrated in ethanol of increasing concentration and acetone and poured into an Epon-Araldite mixture according to conventional methods. The samples were placed in capsules and filled with a mixture of epoxy resins (epon and araldite), which were polymerized for 24 hours at a temperature of +37 °C and 24 hours at a temperature of +60 °C. Ultrathin 50–90 nm sections were obtained on an LKB-III B ultramicrotome using disposable glass knives. Substrate films (collodion) were applied to the sections and transferred to support grids, contrasted with solutions of uranyl acetate and lead citrate, and examined under an electron transmission microscope (SELMI PEM-125K). Morphological subjects were photographed with a camera mounted in an electron microscope on black and white film and analyzed.

Results of the research and their discussion

Studies have confirmed that the glandular part of the stomach in chickens is a direct extension of the esophagus and occupies a position close to the middle sagittal plane (Langlois, 2019). It has the appearance of a thick-walled tube, which consists of the apex, the body, and the intermediate zone (isthmus), by which it is connected to the muscular part. The apex lies between the thoracic air sacs and the body lies between the lobes of the liver. The right surface of the glandular part of the stomach borders on the spleen and ileum, and the left – with the cecum. On the surface of the mucosa, the conical papillae limited by folds are visible. At their tops, the ducts of the deep glands of the stomach open.

In one-day-old chickens, the general plan of the microscopic structure of the glandular part of the stomach is the same as in adult birds. Its wall is formed by mucous, muscular, and serous membranes. The mucosa forms low longitudinal folds, which straighten when filled with feed and are represented by the epithelium, lamina propria, muscularis externa, and submucosa. The data of other researchers (Hassouna, 2001; Aksoy & Cinar, 2009; Akter et al., 2018) have been confirmed that the superficial epithelium is simple cylindrical glandular. It is formed by a single layer of epitheliocytes that lies on the basal membrane. These cells have a cylindrical shape, their height significantly exceeds the width (Fig. 1). Some of them reproduce by mitosis.

Epitheliocytes produce a mucous secret that covers the inner surface of the glandular part of the stomach. They are tightly arranged and connected by different types of contacts: simple, tight, interdigital, and desmosomes. In epitheliocytes, two poles are clearly expressed – apical (directed to the external environment) and basal (located on a basal membrane). The microvilli are visible on their apical pole. However, in epitheliocytes, which are overflowing with the secrets, the microvilli are solitary and the apical surface of these cells is almost smooth. The nucleus is single, located in the area of the basal pole, and has a predominantly rounded shape. It has one nucleolus; heterochromatin is mainly locally fixed to the nucleolemma and scattered in places in the nucleoplasm. The cytoplasm of epitheliocytes has medium electron density. Near the nucleus, the tubules of the granular and agranular endoplasmic reticulum, ribosomes, and their clusters, the polyribosomes, are clearly expressed. Mitochondria are mainly concentrated in the middle part of the cytoplasm and near the apical pole. They are oval, rod-shaped, round, spindle-shaped with a matrix of medium electron density. Above the nucleus, there is a peculiar round or oval zone, the

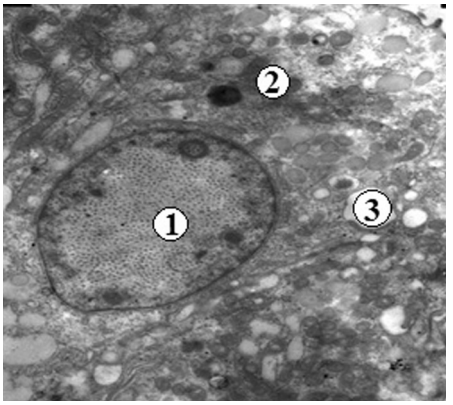

Fig. 1. The superficial epithelial cell of the mucosa of the glandular part of the stomach in a 180-day-old chicken. Electronogram: 1 – nucleus; 2 – cytoplasm; 3 – secretory granules. ×7000

contours of which are limited by mitochondria. There are noticeable elements of the Golgi complex, among which cisterns located among vacuoles and vesicles predominate. In the middle part of the cytoplasm of epitheliocytes, there are many secretory inclusions in the form of round, elongated-oval, spindle-shaped granules with different electron densities. They are located freely. Secretory granules are bounded by a membrane. Some of them, many of which are in the area of the apical pole, merge with each other or connect with the cell membrane. They released the secrets into the lumen of a stomach. In areas of the cytoplasm, which has no secretory inclusions, single tonofibrils are well visible, which intertwine with each other and rarely form bundles.

The lamina propria of the mucosa is formed by the loose fibrous connective tissue. It contains blood vessels and numerous superficial tubular glands, the ducts of which open on the surface of the mucosa (Fig. 2, 3). Mucus is found in the glands. Due to the numerous glands that are located vertically to the surface of the mucosa, its relief has a peculiar appearance on histopreparations. It seems that the epithelium and lamina propria form papillae. The muscularis externa of the mucosa is an extension of the muscularis externa of the esophagus and is formed by smooth muscle tissue. It is not always well expressed, has an intermittent appearance. Its bundles of smooth muscle cells do not have a clear orientation.

The thickest layer of the mucosa is the submucosa, which is formed by the loose fibrous connective tissue with blood vessels and nerves. It contains complex (deep) glands, which are grouped into lobes. They correspond to the mammalian stomach glands (Matsumoto & Hashimoto, 2000). The particles of the deep glands are mostly polygonal, rarely rounded and are located in several layers (Fig. 4). Their typical feature is a complex system of excretory ducts. Each lobe has a collecting cavity into which the ducts of individual glands open. The collecting cavity is covered with a simple glandular epithelium, which in some

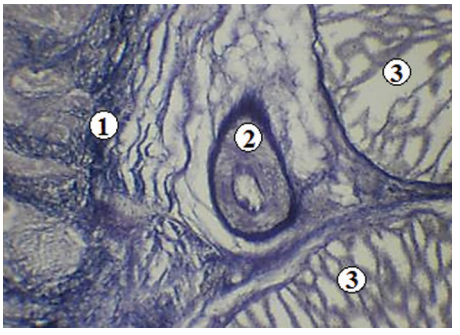

Fig. 2. The blood vessel in the lamina propria of the mucosa of the glandular part of the stomach in a 90-day-old chicken. Histopreparation: 1 – lamina propria; 2 – blood vessel; 3 – lobules of deep glands. Weigert staining, ×90

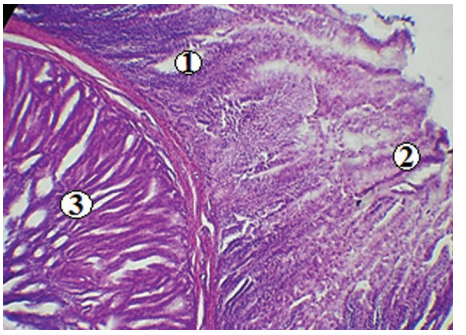

Fig. 3. Superficial tubular glands in the lamina propria of the mucosa of the glandular part of the stomach in a 90-day-old chicken. Histopreparation: 1 – lamina propria; 2 – superficial tubular glands; 3 – lobules of the deep gland. Staining with hematoxylin and eosin, ×63

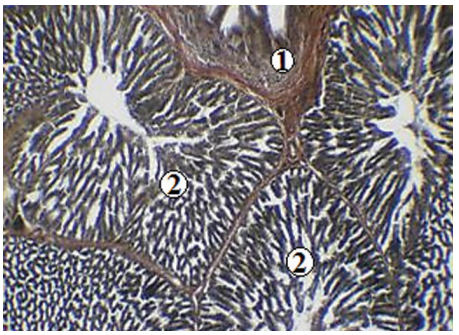

Fig. 4. The lobules of the deep glands of the glandular part of the stomach in a 30-day-old chicken. Histopreparation: 1 – lamina propria of the mucosa; 2 – lobules of deep glands. Van Gieson's staining, ×63

lobes passes into the epithelial layer of the mucosa. The glands in the lobes are tightly adjacent to each other, and are located radially around the collecting cavity. From the latter originates the common excretory duct, which opens on the surface of mucosal elevation. These elevations are visible macroscopically and are called glandular sacs, or papillae. In the intermediate zone of the glandular part of the stomach, the deep glands are absent, the submucosa thins. In the lamina propria of the mucosa of this zone, the glands inherent in the muscular part of the stomach appear, the secretion of which forms a thin cuticle, as a result of which the color of the mucosa becomes yellowish (Naletova, 2013).

Submicroscopic studies have shown that the lobules of the deep glands of the submucosa are formed by glandular cells (glandulocytes) with light and dark cytoplasm (Fig. 5, 6). Glandular cells have a single nucleus, in which chromatin clumps are well expressed. Synthesizing organelles, such as the granular endoplasmic reticulum, ribosomes, and the Golgi complex, are well developed among general-purpose organelles. Numerous mitochondria with a significant number of densely spaced cristae and numerous secretory granules are also visible in the cytoplasm. The secretory granules have a rounded shape, different sizes, and dif-

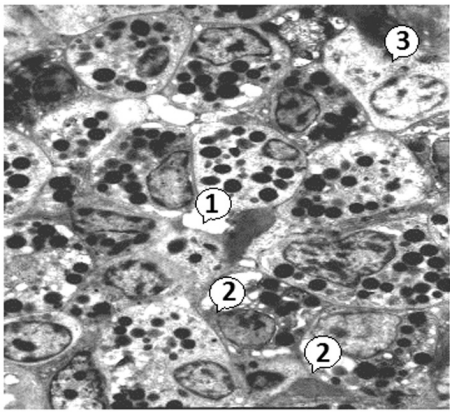

Fig. 5. The cellular composition of the submucosal lobule of the glandular part of the stomach in a 180-day-old chicken. Electronogram: 1 – lumen of the gland; 2 – glandular cells; 3 – plasma cell. ×3000

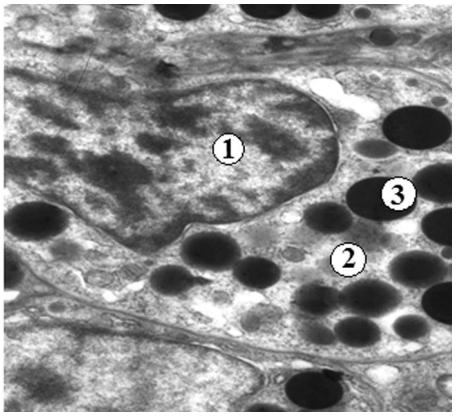

Fig. 6. The deep gland cell of the glandular part of the stomach in a 180-day-old chicken. Electronogram: 1 – nucleus; 2 – cytoplasm; 3 – secretory granules. ×8000

ferent color intensities (black, gray, and gray with black areas).

According to some authors, glandulocytes combine the secretion of pepsinogen and hydrochloric acid (in birds, in contrast to mammals, these glands are not differentiated into major and parietal), which gave rise to calling them oxyntopeptic. Moreover, the synthesis of hydrochloric acid occurs in the apical pole of the glandular cell, and pepsinogen – in the basal (Mabelebele et al., 2014; Zhang et al., 2016). In the layers of the loose fibrous connective tissue that surrounds the lobules of the deep glands, there are well-defined blood vessels, including capillaries (Fig. 7).

The muscular membrane of the glandular part of the stomach is formed by smooth muscle tissue and is divided into three layers: inner and outer longitudinal and middle circular, of which the best developed is middle layer, and the least – the outer longitudinal layer (Fig. 8). According to some researchers, this membrane in birds is two-layered: the inner longitudinal and outer – circular (Catroxo et al., 1997; Sayrafi & Aghagolzadeh, 2020), or vice versa inner circular and outer – longitudinal (Jeurissen et al., 1989; Kadhim et al., 2011). The serosa consists of loose fibrous connective tissue with blood vessels and nerve bundles, which is covered with mesothelium (simple squamous epithelium).

According to Naletova (2013), the muscularis externa of the mucosa of the intermediate zone connects with the muscular membrane and together they form an annular sphincter, which regulates the flow of feed into the muscular part of the stomach.

Morphogenesis of the glandular part of the stomach in chickens in the age aspect is manifested by changes in morphometric parameters of the thickness and the area of the membranes of its wall. Indicators of wall thickness between folds and in the area of mucosal folds increase from 1-day-old to 240-day-old (Table 1).

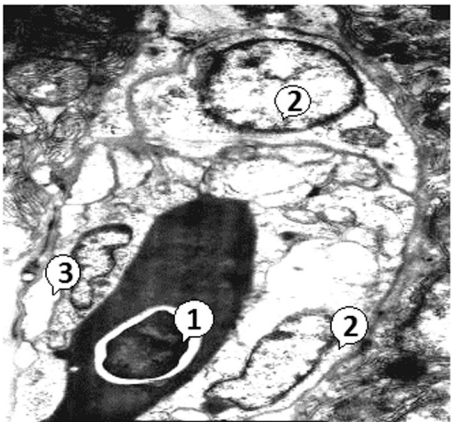

Fig. 7. Blood capillary in the submucosa of the glandular part of the stomach in a 180-day-old chicken. Electronogram: 1 – erythrocyte in the lumen of the capillary; 2 – endotheliocytes; 3 – pericyte. × 8000

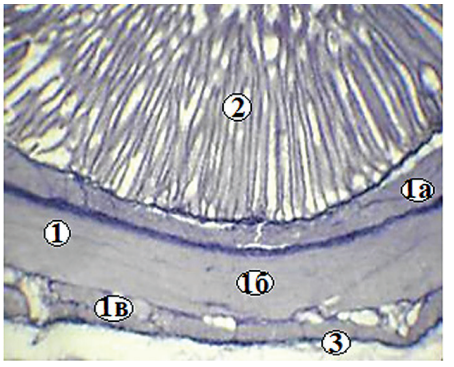

Fig. 8. The muscular membrane of the glandular part of the stomach in a 120-day-old chicken. Histopreparation: 1 – muscular membrane: 1a – inner longitudinal layer, 1b – middle – circular layer, 1c – outer longitudinal layer; 2 – lobule of the deep gland; 3 – serosa. Weigert staining, ×90

1. The wall thickness in the glandular part of the stomach in chickens (M ± m, μm)

Age of chickens	Thickness	
	between the folds of the mucosa	in the area of the folds of the mucosa
1 day	1295.32 ± 37.27	1604.89 ± 46.29
30 days	2495.93 ± 197.45***	3323.84 ± 134.67***
60 days	3192.47 ± 148.37**	4124.25 ± 154.08**
90 days	3583.51 ± 92.44*	4536.67 ± 54.78*
120 days	3733.21 ± 101.58	4613.05 ± 102.72
150 days	3965.39 ± 162.07	5092.68 ± 108.42**
180 days	4127.30 ± 186.61	5156.84 ± 146.09
210 days	4218.95 ± 135.82	5553.99 ± 41.09
240 days	4223.23 ± 189.25	5561.32 ± 45.01
270 days	4219.56 ± 139.64	5531.99 ± 56.95
300 days	4212.23 ± 122.18	5509.10 ± 178.22
1 year	4204.90 ± 189.25	5502.66 ± 90.95
2 years	4201.24 ± 194.76	5506.33 ± 90.03
3 years	4208.57 ± 127.69	5524.62 ± 159.85

Note: * $P < 0.05$; ** $P < 0.01$; *** $P < 0.001$ compared with the indicator in previous group.

Thus, in one-day-old birds, this indicator between the folds of the mucosa is 1295.32 ± 37.27 μm and in the area of their folds –1604.89 ± 46.29 μm, and in 240-day-old – 4223.23 ± 189.25 and 5561.32 ± 45.01 μm, respectively. That is, during this period, the wall thickness between the folds increases by 226.04% and in the area of folds – by 246.52%. The most intense wall thickness of the glandular part of the stomach increases in chickens from 1 to 30 days of age (92.69 and 107.11%, respectively). In chickens aged 270 days and older, this figure between the folds and in the area of the folds of the mucosa is almost unchanged and ranges from 4201.24 ± 194.76 to 4219.56 ± 139.64 μm between the folds and from 5502.66 ± 90.95 to 5531.99 ± 56.95 μm in the area of folds.

The most developed membrane of the wall of the glandular part of the stomach, as noted above, is the mucosa (Table 2). Its area grows from the daily age (79.60 ± 0.90%) to the age of 180 days (82.14 ± 0.56%) by 3.19%. This indicator increases most intensively in chickens aged from one to 30 days (by 1.23%). In birds aged 210 days – 3 years, the area of the mucosa is almost unchanged and varies between 81.04 ± 0.47 and 82.01 ± 0.51%.

2. The area of the mucous, muscular, and serous membranes of the glandular part of the stomach in chickens (M ± m, %)

Age of chickens	Mucous membrane	Muscular membrane	Serous membrane
1 day	79.60 ± 0.90	17.07 ± 0.70	3.33 ± 0.22
30 days	80.58 ± 0.21	16.24 ± 0.36	3.18 ± 0.30
60 days	80.97 ± 0.84	16.20 ± 0.95	2.83 ± 0.45
90 days	81.38 ± 0.57	16.15 ± 0.59	2.47 ± 0.31
120 days	81.45 ± 0.43	16.09 ± 0.65	2.46 ± 0.32
150 days	81.48 ± 0.38	16.03 ± 0.43	2.49 ± 0.46
180 days	82.14 ± 0.56	15.54 ± 0.65	2.32 ± 0.33
210 days	82.01 ± 0.51	15.55 ± 0.46	2.44 ± 0.47
240 days	81.08 ± 0.36	16.46 ± 0.71	2.46 ± 0.38
270 days	81.27 ± 0.76	16.50 ± 0.76	2.23 ± 0.79
300 days	81.15 ± 0.31	16.35 ± 0.95	2.50 ± 0.66
1 year	81.27 ± 0.12	16.65 ± 0.58	2.08 ± 0.46
2 years	81.05 ± 0.38	16.71 ± 0.54	2.24 ± 0.70
3 years	81.04 ± 0.47	16.51 ± 0.59	2.45 ± 0.51

The area of muscular and serous membranes, on the contrary, decreases in birds aged from one (17.07 ± 0.70 and 3.33 ± 0.22%) to 180 days (15.54 ± 0.65 and 2.32 ± 0.33%) by 8.96 and 30.33%. A particularly sharp decrease in the area of the muscular membrane was registered in chickens from one to 30 days (by 4.86%), and serosa – from 30 to 60 days (by 11.01%). In birds aged 210 days – 3 years, the area of the muscular membrane varies between 15.55 ± 0.46 and 16.71 ± 0.54%. The area of the serosa in 210-day-old birds and older does not change and varies between 2.08 ± 0.46 and 2.50 ± 0.66%.

As noted above, lobules of deep glands are located in the submucosa of the glandular part of the stomach. Their number increases from one day of age (22.40 ± 0.46) to 120 days (36.70 ± 0.76) by 63.84% (Table 3).

The most intense number of lobules of the deep glands increases in chickens from 30 to 60 days of age (by 20.96%). In 150-day-old chickens and older, the number of lobules practically does not change and varies between 34.80 ± 0.58 and 36.10 ± 0.71. The diameter of the lobules of the deep glands increases in chickens from the one-day (789.49 ± 31.30 μm) to 240-day (2990.41 ± 68.96 μm) age by 278.78%. This indicator increases most intensively in birds aged from 30 to 60 days – by 58.40%. In 270-day-old birds and older, the diameter of the lobules of the deep glands remains almost unchanged and ranges from 2921.01 ± 103.84 to 2945.89 ± 135.20 μm.

3. The number of lobules of the deep glands of the glandular part of the stomach and their diameter in chickens (M ± m)

Age of chickens	Number of lobes	Diameter, microns
1 day	22.40 ± 0.46	789.49 ± 31.30
30 days	27.20 ± 0.91***	1440.73 ± 94.69***
60 days	32.90 ± 0.55***	2282.08 ± 109.97***
90 days	33.70 ± 0.71	2541.32 ± 33.60*
120 days	36.70 ± 0.76*	2791.39 ± 103.35*
150 days	35.80 ± 0.68	2822.82 ± 177.68
180 days	35.50 ± 0.79	2876.50 ± 146.83
210 days	36.00 ± 0.75	2931.49 ± 75.91
240 days	36.10 ± 0.71	2990.41 ± 68.96
270 days	34.80 ± 0.58	2935.41 ± 104.68
300 days	35.20 ± 0.75	2921.01 ± 103.84
1 year	36.00 ± 0.75	2945.89 ± 135.20
2 years	35.10 ± 0.72	2936.72 ± 149.75
3 years	35.40 ± 0.93	2944.58 ± 168.32

Note: * $P < 0.05$; ** $P < 0.01$; *** $P < 0.001$ compared with the previous group.

Conclusions and future perspectives

The glandular part of the stomach in chickens has the form of a thick-walled tube, in which the mucosa is best developed. The superficial epithelium of this membrane is represented by cylindrical epithelial cells that lie on the basal membrane. They are interconnected by different types of contacts and have a well-defined polar differentiation. The lobules of the deep glands of the mucosa are formed by cells with well-developed synthesizing organelles and secretory granules.

Morphogenesis of the glandular part of the stomach in chickens in the age aspect is manifested by changes in morphometric parameters of the thickness and the area of the membranes of its wall. The wall thickness increases in chickens up to 240 days of age, the area of the mucosa – up to 180 days, while the muscular and serous membranes decrease. In older birds, the thickness of the wall and the area of the esophageal membranes do not change significantly.

Further research should focus on the microstructure of the muscular part of the stomach in chickens in the age aspect.

References

Abumandour, M. (2013). Morphological studies of the stomach of falcon. Scientific Journal of Veterinary Advances, 2(3), 30-40.

Ahmed, Y., Kmel, G., & Ahmad, A. (2011). Histomorphological studies on the stomach of the Japanese quail. Asian Journal

of Poultry Science, 5, 56-67. doi: 10.3923/ajpsaj.2011.56.67

Aksoy, A., & Cinar, K. (2009). Distribution and ontogeny of gastrin and serotonin-immunoreactive cells in the proventriculus of developing chick, Gallus gallus domesticus. Journal of Veterinary Science, 10(1), 9-13. doi: 10.4142/jvs.2009.10.1.9

Akter, K., Mussa, T., Sayeed, A., & Hai, M. A. (2018). Proventriculus of digestive tract of broiler. Bangladesh Journal of Veterinary Medicine, 16(1), 7-11. doi: 10.3329/bjvm.v16i1.37367

Catroxo, M. H. B., Lima, M. A. I., & Cappellaro, C. E. (1997). Histological aspects of the stomach (proventriculus and gizzard) of the red-capped cardinal (Paroaria gularis gularis), Linnaeus, 1766). Revista chilena de anatomia, 15(1), 19-27. doi: 10.4067/S0716-98681997000100003

Hassouna, E. M. A. (2001). Some anatomical and morphometrical studies on the intestinal tract of chicken, duck, goose, turkey, pigeon, dove, quail, sparrow, heron, jackdaw, hoopoe, kestrel and owl. Assiut Veterinary Medical Journal, 44, 47-78.

Horalskyi, L. P., Khomych, V. T., & Kononskyi, O. I. (2005). Osnovy histolohichnoyi tekhniky i morfofunktsional'ni metody doslidzhen' u normi ta pry patolohiyi [Fundamentals of histological technique and morphofunctional methods of research in norm and in pathology]. Zhytomyr: Polissia.

Jeurissen, S. H. M., Janse, E. M., Koch, G., & De Boer, G. F. (1989). Postnatal development of mucosa-associated lymphoid tissues in chickens. Cell and Tissue Research, 258, 119-124.

Dahekar, N. M., Mamde, C. S., John, M. A., & Rohankar, R. U. (2014). Gross anatomical and histomorphological studies on proventriculus of Japanese quail. Indian Journal of Veterinary Anatomy, 26(1), 62-63.

Dashiyeva, T. O. (1982). Morfologiya organov pishchevareniya domashney utki v postnatal'nom ontogeneze [The morphology of the digestive organs of domestic ducks in postnatal ontogenesis]. (Abstaract of dissertation of Candidate of Veterinary Sciences). Ulan–Ude.

Demirbag, E., Cinar, K., Tabur, M. A., & Asti, R. N. (2015). Histochemical structure of stomach (Proventriculus and Gizzard) in some bird species. Journal of Natural and Applied Science, 19(2), 115-122. doi: 10.19113/sdufbed.48385

Kadhim, K. K., Zuki, A. B., Noordin, M. M., & Babjee, S. M. (2011). Histomorphology of the stomach, proventriculus and ventriculus of the red jungle fowl. Anatomia, Histologia Embryologia, 40(3), 226-233. doi: 10.1111/j.1439-0264.2010.01058.x

Kharchenko, L. P. (2014). Makroskopichna budova shlunka ptakhiv riznykh trofichnykh spetsializatsiy [Macroscopic structure of the stomach of birds of different trophic specializations]. Biolohiya ta valeolohiya, 16, 62-70.

Khomych, V. T., Usenko S. I., & Dyshliuk, N. V. (2020). Morphofunctional features of the esophageal tonsil in some wild and domestic bird species. Regulatory Mechanisms in Biosystems, 11(2), 207-213. doi: 10.15421/022030

Langlois, I. (2019). The anatomy, physiology, and diseases of the avian proventriculus and ventriculus. Veterinary Clinics: Exotic Animal Practice, 6(1), 85-111. doi: 10.1016/S1094-9194(02)00027-0

Mabelebele, M., Alabi, O. J., Ng`ambi, J. W., Norris, D., & Ginindza, M. M. (2014). Comparison of gastrointestinal tracts and pH values of digestive organs of Ross 308 broiler and indigenous. Venda chickens fed the same diet. Asian Journal of Animal and Veterinary Advances, 9, 71-76. doi: 10.3923/ajava.2014.71.76

Matsumoto, R., & Hashimoto, Y. (2000). Distribution and developmental change of lymphoid tissues in the chicken proventriculus. Journal of Veterinary Medical Science, 62(2), 161-167. doi: 10.1292/jvms.62.161

Naletova, L. A. (2013). Anatomical and histological characteristics of the glandular stomach of chickens and geese. Bulletin of the Buryat State University, 4, 186-188.

Naletova, L. A. (2013). Anatomo-gistologicheskaya kharakteristika zhelezistogo zheludka kur i gusey [Anatomical and histological characteristics of the glandular stomach of chickens and geese]. Bulletin of the Buryat State University, 4, 186-188.

Nasrin, M., Siddiqi, M. N. H., Masum, M. A., & Wares, M. A. (2012). Gross and histological studies of digestive tract of broilers during postnatal growth and development. Journal of the Bangladesh Agricultural University, 10(1), 69-77. doi: 10.3329/jbau.v10i1.12096

Plokhinskyi, N. A. (1970). Biometriya [Biometrics]. Novosibirsk.

Sayrafi, R., & Aghagolzadeh, M. (2020). Histological and histochemical study of the proventriculus (Ventriculus glandularis) of common starling (Sturnus vulgaris). Anatomia, Histologia, Embriologia, 49(1), 105-111. doi: 10.1111/ahe.12495

Seliverstova, L. S. (2018). Tendentsiyi rozvytku ta efektyvnosti funktsionuvannya rynku produktsiyi ptakhivnytstva v Ukrayini [Development tendencies and peculiarities of functioning of the poultry market in Ukraine]. Efektyvna ekonomika, 1. Retrieved from http://www.economy.nayka.com.ua/?op=1&z=6368

Vlasov, A. I., Yelsukov, K. A., & Kosolapov I. A. (2011). Elektronnaya mikroskopiya [Electron microscopy]. Moscow: MGTU im. Baumana.

Zhang, H., Peng, T. Ge. S., Zhong, S., & Zhou, Z. (2016). Microstructure features of proventriculus and ultrastructure of the gastric gland cells in chinese taihe black-bone silky fowl (Gallus gallus domesticus Brisson). Anatomia, Histologia, Embriologia, 45(1), 1-8. doi: 10.1111/ahe.12164

Дишлюк Н. В. (2021). МОРФОГЕНЕЗ СТІНКИ ЗАЛОЗИСТОЇ ЧАСТИНИ ШЛУНКУ КУРЕЙ У ПОСТНАТАЛЬНОМУ ПЕРІОДІ ОНТОГЕНЕЗУ

Ukrainian Journal of Veterinary Sciences, 12(4): 66–78, https://doi.org/10.31548/ujvs2021.04.005

Анотація. *Знання морфологічних особливостей будови і функцій органів травлення створюють основу раціонального та ефективного використання кормів, профілактики та лікування шлунково-кишкових захворювань свійської птиці. У зв'язку з цим, великого значення набуває вивчення морфогенезу травної системи птахів та механізмів їхньої регуляції.*

Об'єктом дослідження була залозиста частина шлунку (proventriculus) курей кросу Шевер 579. Для макро- і мікроскопічних досліджень матеріал відібрали від птиці віком 1, 30, 60, 90, 120, 150, 180, 210, 240, 270 і 300 діб та 1, 2 і 3 роки, який фіксували в 10% розчині нейтрального формаліну й заливали в парафін відповідно до загальноприйнятої методики. Для субмікроскопічних досліджень матеріал відібрали від курей цього ж кросу віком 180 діб. На ультратонких зрізах вивчали будову епітеліоцитів поверхневого епітелію й секреторних клітин глибоких залоз. Цифрові показники результатів досліджень обробляли статистично за допомогою персонального комп'ютера з використанням програми Microsoft Excel.

Залозиста частина шлунку курей є безпосереднім продовженням стравоходу й має вигляд товстостінної трубки, яка утворена слизовою, м'язовою й серозною оболонками. Поверхневий епітелій слизової оболонки представлений епітеліоцитами циліндричної форми, які лежать на базальній мембрані. Вони з'єднані між собою різними типами

контактів і мають добре виражену полярну диференціацію. Часточки глибоких залоз утворені клітинами із добре розвиненими синтезуючими органелами та секреторними гранулами.

Морфогенез залозистої частини шлунку курей у віковому аспекті проявляється змінами морфометричних показників товщини і площі оболонок її стінки. Товщина стінки нерівномірно збільшується до 240-добового віку курей (між складками 4223,23 ± 189,25 і в ділянці складок 5561,32 ± 45,01 мкм). Найбільш розвиненою оболонкою стінки залозистої частини шлунку є слизова. Її площа збільшується (на 82,14 ± 0,56%) до 180-добового віку курей, а м'язової й серозної оболонок зменшується (відповідно на 15,54 ± 0,65 і 2,32 ± 0,33%). У птиці старшого віку показники товщини стінки і площі оболонок залозистої частини шлунку суттєво не змінюються.

Ключові слова: *кури, шлунок, морфометричні показники, слизова оболонка, м'язова оболонка, серозна оболонка*

UDC 612.014: 576.3:602.018.26.9 https://doi.org/10.31548/ujvs2021.04.006

BIOLOGICAL PECULIARITIES OF ADIPOSE TISSUE-DERIVED MESENCHYMAL STEM CELLS AT DIFFERENT PASSAGES OF CULTIVATION

L. V. KLADNYTSKA[1],
Doctor of Veterinary Sciences, Associate Professor
Department of Biochemistry
and Physiology of Animals named after Academician M. F. Gulyi
https://orcid.org/0000-0002-9360-0587
E-mail: kladlarisa@ukr.net
A. Y. MAZURKEVYCH[1],
Doctor of Veterinary Sciences, Professor
Department of Surgery and Pathophysiology
named after Academician I. O. Povazhenko
https://orcid.org/0000-0002-2409-7703
S. V. VELYCHKO[2],
Candidate of Biological Sciences
https://orcid.org/0000-0003-1842-5114
L. V. GARMANCHUK[3],
Doctor of Biological Sciences, Professor
https://orcid.org/0000-0002-1527-2346
M. O. MALYUK[1],
Doctor of Veterinary Sciences, Associate Professor
Department of Surgery
and Pathophysiology named after Academician I. O. Povazhenko
https://orcid.org/0000-0003-3019-6035
T. A. MAZURKEVYCH[1],
Doctor of Veterinary Sciences, Associate Professor
Academician V. G. Kasyanenko Department of Anatomy,
Histology and Pathomorphology
https://orcid.org/0000-0002-1294-5939
V. V. KOVPAK[1],
Doctor of Veterinary Sciences, Associate Professor
Gynecology and Biotechnology of Animal Reproduction
https://orcid.org/0000-0003-2419-1246
E-mail:kovpak8887@gmail.com
T. V. KOZYTSKA[4],
Candidate of Veterinary Sciences, Associate Professor
https://orcid.org/ 0000-0002-7554-0808

Yu. O. KHARKEVYCH[1],
Candidate of Veterinary Sciences, Associate Professor
Department of Surgery and Pathophysiology named after Academician I. O. Povazhenko
https://orcid.org/0000-0002-7877-8272
R. R. BOKOTKO[1],
Candidate of Veterinary Sciences, Associate Professor
Department of Surgery and Pathophysiology named after Academician I. O. Povazhenko
https://orcid.org/0000-0002-6217-5266
T. L. SAVCHUK[1],
Candidate of Veterinary Sciences, Associate Professor
Department of Surgery and Pathophysiology named after Academician I. O. Povazhenko
https://orcid.org/0000-0002-7351-5684
E-mail: kladlarisa@ukr.net
[1]National University of Life and Environmental Sciences of Ukraine,
15 Heroyiv Oborony st., Kyiv 03041, Ukraine
[2]Hospital of Veterinary Medicine, Holosiivskyi Avenue, 105 b, Kyiv 03127, Ukraine
[3]Taras Shevchenko National University of Kyiv, Educational and Scientific
Center Institute of Biology and Medicine, 2 Hlushkova Avenue, Kyiv 03127, Ukraine
[4]Bogomolets National Medical University, 13 Shevchenko blvr., Kyiv 01601, Ukraine

Abstract. *The studies were conducted on 2–3-months-old males of C57BL/6 mice weighing 20–24 g. Obtaining and operating with adipose tissue-derived mesenchymal stem cell (MSC) culture was performed in a sterile laminar box under conditions of asepsis and antiseptics. The adipose tissue-derived MSC of the 2, 4, 7 and 12 passages were analyzed. Morphometric analysis was performed using a light microscopy. Morphometric parameters such as cell and nucleus area or nuclear-cytoplasmic ratio were calculated using the Axiovision light microscope (Carl Zeiss, Germany) and Image J 1.45 software. Trypan blue dye used for investigation of the viability of MSC.*

The morphological characteristics of adipose tissue-derived MSC during the process of cultivation changes: at the first passages of cultivation, the cells are spindle-shaped with two, at least three, long cytoplasmic processes, which are located bipolar. Near the nucleus, the Golgi complex is clearly visible – a sign of active cells. At later passages, cells have a small cytoplasmic processes and the bipolar arrangement of processes changes by stellar arrangement. Golgi complex is also clearly visualized. The indicator of the nuclear-cytoplasmic ratio in MSC from adipose tissue is significantly reduced at the 7th passage to 0.2189 ± 0.0122 ($P < 0.01$), and at the 12th passage to 0.1111 ± 0.0086 ($P < 0.001$) compared to the 2nd passage. The coefficient of proliferation of adipose tissue-derived MSC is significantly reduced at 12th passage. The viability of MSC from adipose tissue with an increasing of a number of passages significantly reduces and at the 12th passage of cultivation reaches 84.67 ± 1.36 ($P < 0.05$). The content of apoptotic cells that exhibited sensitivity to serum-free cultivation significantly increased at the 7th and 12th passages and was 21.33 ± 1.36 ($P < 0.05$) and 23.67 ± 0.97% ($P < 0.05$), respectively.

Keywords: *adipose tissue mesenchymal stem cells, nucleus, nuclear-cytoplasmic ratio, coefficient of proliferation, viability, apoptosis, early passages, late passages*

Introduction

It is known that mesenchymal stem cells (MSC) in the bone marrow are from 0.001% to 0.01% of the total fraction of mononuclear cells, and bone marrow aspiration is an invasive procedure and has a significant effect on the donor after the surgical period (Dmitrieva et al., 2012). Therefore, other sources of stem cells, in particular, umbilical cord blood and placenta, are used in modern human and veterinary medicine (Ning et al., 2012). The adipose tissue is also an excellent alternative source of MSC, since it contains approximately 500 times more MSC in compare with bone marrow. It should be noted that the process of obtaining of adipose tissue is quite simple and does not harm the body. Some data are already known about biological properties of adipose-derived MSC (AD-MSC). In particular, it is known about high differential potential of MSC from adipose tissue in animals of different species, their immunomodulatory property. Some authors emphasize that they exhibit stronger immunomodulatory effects, due to the fact that they are characterized by a higher level of cytokine secretion (Arnhold & Wenisch, 2015).

Analysis of recent researches and publications

Certain specific morphological features of stem cells, which were determined by light microscopy, are known. In particular, it was found that MSC with high proliferative activity were thick, and those that had low proliferative activity were thin, even if these MSC were cells of early passages. The diameter of the nucleus of MSC from the dog and the horse is determined. Also the individual morphological parameters of the feline MSC in early passages were investigated (Grzesiak et al., 2011; Maciel et al., 2014). It was investigated that MSC from the umbilical cord at the 15th passage age due to the decrease in metabolism and proliferation activity (Katsube et al., 2008).

There are reports about some morphological characteristics of stem cells. In the study of MSC from horses and dogs, it was found that in the first passages of cultivation, mitochondries are localized pericentrically and there are endosomal vesicles in the cell cytoplasm (Otsu et al., 2009). They were mostly found in the perinuclear zone, but before cell proliferation they moved to the opposite pole. In the non-proliferation cells, there were endoplasmic vesicles that moved intensively inside the cell. It was found that the cultivation process affects the change of morphological parameters of stem cells. In particular, it was investigated that MSC from dogs and horses changed their length and diameter, as evidenced by the authors of the publication. According to these studies, stem cells at the 19–20th passages changed their adhesive properties in the direction of reduction, were more flattened and "took up more space". The number of cells decreased to 1.9 × 106 per cup, indicating a change in their proliferative activity. Their functional state also changed, which was confirmed by a decrease in viability to 56% (Grzesiak et al., 2011; Otsu et al., 2009).

A team of other researchers found that stem cells from the same culture had morphological and functional differences. In particular, in stem cell culture, there are cells of different thickness, and the proliferative activity of stem cells depends on their thickness. Thicker cells had higher proliferative activity. Cells,

being small in thickness, expressed genes associated with cell aging and had low proliferative activity (Nagano et al., 2019).

Parallel studies indicate that the morphological parameters of MSC in different passages of cultivation have significant differences. It was found that MSC from feline bone marrow had a spindle-shaped shape, a significant amount of cytoplasm, a length of 106.97 ± 38.16 and 177.91 ± 71.61 μm in the first and third passages, respectively. The cell width was 30.79 ± 16.75 μm and 40.18 ± 20.46 μm in the first and third passages, respectively. The length of feline bone marrow MSC in the first passage was 16.28 μm after 24 hours of cultivation and 21.29 μm after 120 hours of cultivation, and in the third – significantly increased and amounted to 26.35 μm after 24 hours of cultivation and 25.22 μm after 120 hours of cultivation (Maciel et al., 2014).

Thus, the **purpose** of our work was to determine in vitro the morphological parameters and functional state of MSC from adipose tissue of C57Bl/6 mices during the early and late passages.

Materials and methods of research

The studies were conducted on 2–3-months-old males of C57BL/6 mice weighing 20–24 g. All studies were conducted in accordance with the Rules of Good Laboratory Practice and Use of Experimental Animals and in accordance to Compliance with the Law of Ukraine "On the Protection of Animals from BrutalCruel Treatment" and the "International European Convention on the Protection of Animals Used for Experimental and Other Scientific Purposes".

MSCs obtaining from mice adipose tissue of mice (Kladnytska et al., 2016). Obtaining and processingprocessing of adipose tissue were carried out in a sterile laminar box with compliance of conditions of asepsis and antiseptics. The mice were euthanized, their adipose tissue removed, and washed three times with sterile phosphate buffer solution with the addition of 1% antibiotic-antimycotic solution (Sigma-Aldrich, USA). Adipose tissue was added to culture dishes filled with DMEM, 10-–15% of fetal bovine serum, 1% of antibiotic-antimycotic solution (Sigma-Aldrich, USA) and cultured in a CO_2 incubator at 37 °C and 5% CO_2. The culture medium was partially or completely changed by fresh medium every 3 days during cultivation. After formation of cells monolayer at 80–90 %, cells were removed with trypsin-ethylenediaminetetraacetic acid solution (EDTA), washed with phosphate buffer and placed in Petri dishes for cultivation. Passaging the adipose derived mesenchymal stem cells (AD- MSCs) provided a reduction of heterogeneity of cell culture and the development of biological material for transplantation.

AD- MSCs of the 2nd, 4th, 7th, and 12th passages were analyzed.

Cells counting was performed using a light-optical microscope with a magnification an increase of 200 times in all squares and is calculated by the formula:

$$X=A\times1000\div0.9 \quad (1)$$

X = A x 1000 / 0,9, where
X – number of cells in 1 cm^3;
A – number of cells in all squares;
1000 – number of mm^3 in cm^3;
0.9 – the volume of the Goriaev chamber camera Goryaev in mm^3.

Calculation of the cell proliferation index was carried out according to the formula:

$$X=a\div b \quad (2)$$

X = a/b, where:
a – the final concentration of the cell/ cm^3;
b – seeded cell concentration / cm^3.

Morphometric analysis was performed using a light microscopy. For this purpose, the cells were stained with Carazzi's hematoxylin Karatci and eosin dyes (Alfarus, Ukraine). Morphometric parameters such as cell and nucleus area or nuclear-cytoplasmic ratio (NCR) were calculated using the Axiovision light microscope (Carl Zeiss, Germany) and ImageJ 1.45 (National Institutes of Health, USA) software.

The viability of the bone marrow MSCs was assessed using trypan blue dye, which is unable to penetrate the cytoplasm of living cells (Shakhov et al., 2004). For this purpose, equal volumes of suspension of bone marrow MSCs and 0.16–0.20% trypan blue, prepared in physiological solution, were mixed. The cells were incubated for 10 minutes at 37 ° C, and the percentage of uncolored nucleated cells from the total number of cell elements were counted in the Goriaev chamber.

Evaluation of the level of apoptosis of in MSC caused by their cultivation in serum-free medium. The MSC at the 2nd, 4rd, 7th and 12th passages were seeded in a quantity of 2×10^3 cells in wells of a 96-well plate, and cultivated during 72 hours in a serum-free medium. Apoptotic cells were revealed by using a trypan blue dye. The method is based on the ability of inanimate cells to absorb the dye. The percentage of colored (dead) cells was calculated in the Goryaev Goriaev chamber.

The statistical analysis of the obtained results was achieved by using Statistica 6.0 (StatSoft, USA) and OriginLab (OriginLab Corporation, USA) software. Normality of data distribution was determined by the Kolmogorov-Smirnov test. In order to assess the validity of the revealed changes, parametric (Student t-test for two-samples) and non-parametric (Mann-Whitney U-test for the independent groups) methods of variation statistics were used, the difference was significant at p $P < 0.05$. The obtained results were presented as the mean ± SD mean error (mean M ± standard deviationm).

Results of the research and their discussion

The cells changed morphology during cultivation. Cells at the 2nd and 4th passages have pronounced morphology of fibroblasts with two or three long cytoplasm processes. Cell nucleus was bean-shaped. Near the nucleus in the zone of enlightenment, the Golgi complex is clearly defined, which is well developed in proliferative cells. A small number of cells with an oval cytoplasm and a round nucleus were recorded (Fig. 1).

At the later passages, the morphology of MSC from adipose tissue has changed. MSC had more processes, they had smaller length, the area of the cell, which was adhered to the culture plastic, was increased. A Golgi complex was registered near the nucleus, indicating that cell proliferation remain at the high level (Fig. 2).

This is confirmed by morphometric indices and functional activity of AD-MSC at different passages (Table 1).

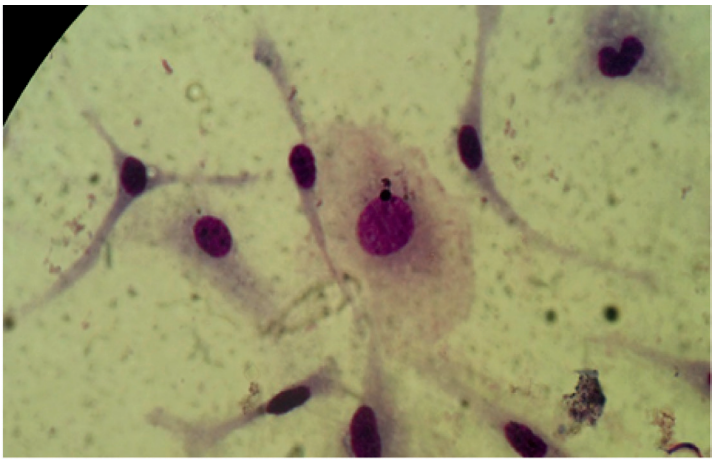

Fig. 1. Mesenchymal stem cells of mouse adipose tissue culture, 2nd passage. Painting according to Carazzi's hematoxylin and eosin. Micropreparation, × 900.

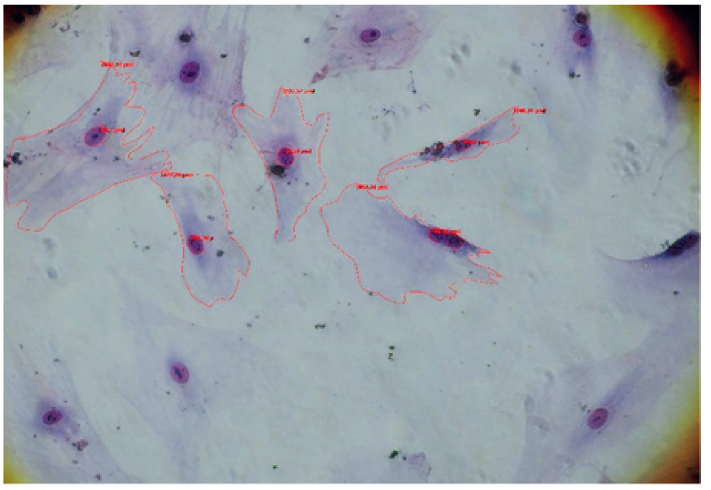

Fig. 2. Mesenchymal stem cells from mouse adipose tissue culture at the 12th passage of cultivation with the calculation of the nucleus area and cell area using the program Axio visine. Pappenheim staining. Micropreparation, × 320.

As can be seen from the Table 1, the area of the nucleus at the 2nd and 4th passages did not significantly changed. At the 7th passage, there can be seen a tendency to reduce the area of the nucleus. At the 12th passage, a significant decrease to 135.78 ± 11.21 μm^2 ($P < 0.05$) was recorded in the area of the nucleus compared to the MSC of the 2nd passage.

During the cultivation, the area of the cytoplasm has no significant differences at the 2nd and 4th passages, and a tendency to increase it can be seen at

1.The morphometric indices and functional activity of adipose-derived mesenchymal stem cells at different passages (M ± m, n = 5)

Parameters	Passages			
	2	4	7	12
Nucleus area (μm^2)	161.11 ± 5.65	161.56 ± 5.48	151.67 ± 3.51	135.78 ± 11.21*
Cells area (μm^2)	759.56 ± 28.42	748.11 ± 25.90	841.56 ± 46.96	1416.90 ± 151.97***
NCR	0.2689 ± 0.0046	0.2756 ± 0.0042	0.2189 ± 0.0122**	0.1111 ± 0.0086***
Coefficient of proliferation	2.92 ± 0.02	3.02 ± 0.03	2.79 ± 0.09	2.55 ± 0.01***
Viability (%)	96.33 ± 1.36	96.67 ± 0.97	93.67 ± 0.97	84.67 ± 1.36*
Serum deprivation-induced apoptosis, %	14.33 ± 1.94	18.67 ± 0.77	21.33 ± 1.36*	23.67 ± 0.97 *

Note: * P < 0.05, ** P < 0.01, *** P < 0.001 in comparison with the 2nd passage.

the 7th passage. At later passage, a significant increase in the area of the cell to 1416.90 ± 151.97 μm^2 (P < 0.001) was recorded.

During the cultivating, the primary material from adipose tissue, unequal proliferative activity of MSC and the rate of the monolayer formation at different passages were registered (Table 1). The monolayer formation depends on many soluble factors, in particular, from those that synthesize cells themselves in the culture medium. Since the primary material was processed with new technique, it can be assumed that a significant amount of cytokines and growth factors have been introduced into the culture medium from adipose tissue, which cause a high rate of proliferation. This coincides with the studies of many authors, which emphasize the fact that adipose tissue contain a lot of soluble growth factors.

During cultivation, the rate of a monolayer formation decreases and, in our opinion, it is explained exactly by the reduction in the synthesis of soluble stimulating factors, which are excreted by cells in the culture medium. The coefficient of proliferation with the increase of a number of passages decreases, and at the 12th passage, this indicator is significantly lower in compare with the 2nd passage (P < 0.001), although it remains high (2.55 ± 0.01).

The viability of MSC from adipose tissue during cultivation reaches high rates, but with an increase in a number of passages, it significantly reduces. At the 12th passage of cultivation, viability reaches 84.67 ± 1.36% (P < 0.05), but remains high. In our opinion, this may be due to the biological aging of the cells and the influence of chemical reagents on them.

Cell resistance to apoptosis induced by cultivation in the serum-free medium decreases with the increase of a number of passages. A significant increase in the number of apoptotic cells has been registered at the 7th passage – 21.33 ± 1.36 (P < 0.05), and at the 12th passage their number has increased to 23.67 ± 0.97% (P < 0.05).

Thus, during the cultivation of MSC from adipose tissue, there are significant changes in morphological parameters of cells, which are reflected in their func-

tional state. In particular, the changes in cell morphology are accompanied by a decrease in the nuclear-cytoplasmic ratio by increasing the area of the cytoplasm. Also, a significant decrease in the cell proliferation coefficient and the viability of MSC at later cultivation passages were determined. The content of apoptotic cells that exhibited sensitivity to cultivation in serum-free medium was significantly increased at the 7th and 12th passages.

Considerable attention was paid to the morphology of MSC. It is known that today there are two main morphological forms of MSC: small, round or spindle-shaped, rapidly proliferating cells and large spreading cells (mature, slowly proliferating cells). That is, differences were observed depending on the rate of MSC proliferation (Grzesiak et al., 2011; Cheng et al., 2012). At the same time, such patterns were inherent in MSC of different origin and no significant differences depending on the species and tissue origin of MSC were found (Martin et al., 2002; Webb et al., 2012).

Several researches have been conducted to study age-related changes in the morphology and functions of human MSC both in vivo and in vitro. Most authors focused on the influence of donor age on the morphofunctional properties of MSC. It was found that MSC from older donors have significantly worse characteristics, including proliferative activity, rate of population doubling, the efficiency of colony formation and the ability to differentiate (Baxter et al., 2004; Miyoshi, 2016; Yang et al., 2018; Yamazaki et al., 2020).

In the cultivation of MSCs of various origins in the second passage, the cells adapted to in vitro conditions, formed a monolayer at the bottom of the culture vessel, dead cells and cells that did not belong to the mesenchymal stems were eliminated. The shape of the vast majority of cells was spindle-shaped with a small volume of cytoplasm, which formed long thin outgrowths. During further cultivation, the morphology of the cells changed in the direction of increasing cell size and cytoplasm size, the appearance of spread cells with a large number of cytoplasmic outgrowths. This coincides with the data of the vast majority of researchers. Thus, Maciel et al. (2014) when culturing MSC from feline bone marrow when comparing cells of the 1st and 3rd passages, an increase in length from 106.97 ± 38.16 μm to 177.91 ± 71.61 μm and width from 30.79 ± 16.7 μm to 40.18 ± 20.48 μm.

Morphofunctional properties of MSC from bone marrow and adipose tissue cultures at different passages of cultivation in combination with other obtained data testified in favor of their gradual replication aging. It was manifested by an increase in cytoplasmic volume $r = 0.73$ ($P = 0.01$); decrease in the nuclear-cytoplasmic ratio $r = -0.87$; ($P = 0.001$); increasing the number of growths of the cytoplasm; decrease in the proliferation coefficient ($P < 0.01$) and cell viability ($r = -0.70$; $P < 0.05$); gradual decrease in the number of cells in the phases G2/M and S of the cell cycle ($P < 0.001$); increased sensitivity to apoptosis induced by the absence of growth factors $r = 0.81$; ($P = 0.001$); increasing the level of secretion of IL-6 ($P < 0.01$). The number of diploid cells decreased, although in all cases it was not less than 95%. It is known that significant MSC aneuploidy is associated with an increased risk of malignant transformation (Ben-David et al., 2018; Saalbach & Anderegg, 2019). The data obtained in the complex indicate in fa-

vor of replicative aging of cultures and determine the feasibility of using in subsequent experiments MSC cultures from adipose tissue and bone marrow in the early stages of cultivation (Kladnytska et al., 2020). Similar results were obtained by Yang et al. (2018) in the study of morphological features and proliferative activity of bone marrow MSC at the 4th and 8th passages of cultivation. The problem of replicative aging is an important obstacle to the application of MSC of late cultivation passages. Therefore, there are attempts to delay the development of this process (Yang et al., 2018). For example, Heo et al. (2016) indicate a significant delay in the aging of MSC cultures when cultured on plates coated with poly-L-lysine, other authors – when neutralizing IL-6 (O'Hagan-Wong et al., 2016).

Conclusions and future perspectives

1. The morphological characteristics of mesenchymal stem cells from adipose tissue during the process of cultivation changed: the cells at the first passages of cultivation are spindle-shaped with two, at least three, long cytoplasmic processes, located bipolar. Near the nucleu,s the Golgi complex is clearly visible – a sign of active cells. At later passages, cells have a small cytoplasmic processes and the bipolar arrangement of processes changes by stellar arrangement. The Golgi complex is also clearly visualized.

2. The indicator of the nuclear-cytoplasmic ratio in MSC from adipose tissue is significantly reduced to 0.2189 ± 0.0122 ($P < 0.01$) at the 7th passage and at the 12th passage to 0.1111 ± 0.0086 ($P < 0.001$) compared to the 2nd passage.

3. The coefficient of proliferation of MSC from adipose tissue is significantly reduced at the 12th passage.

4. The viability of mesenchymal stem cells from adipose tissue with an increasing of a number of passages significantly reduces and at the 12th passage of cultivation reaches 84.67 ± 1.36 ($P < 0.05$).

5. The content of apoptotic cells that exhibited sensitivity to serum-free medium significantly increased at the 7th and 12th passages and was 21.33 ± 1.36 ($P < 0.05$) and $23.67 \pm 0.97\%$ ($P < 0.05$), respectively.

References

Arnhold, S., & Wenisch, S. (2015). Adipose tissue derived mesenchymal stem cells for musculoskeletal repair in veterinary medicine. American journal of stem cells, 4(1), 1-12.

Baxter, M. A., Wynn, R. F., Jowitt, S. N., Wraith, J. E., Fairbairn, L. J., & Bellantuono, I. (2004). Study of telomere length reveals rapid aging of human marrow stromal cells following in vitro expansion. Stem cells, 22(5), 675-682.

Ben-David, U., Gan, Q. F., Golan-Lev, T., Arora, P., Yanuka, O., Oren, Y. S., ... & Benvenisty, N. (2013). Selective elimination of human pluripotent stem cells by an oleate synthesis inhibitor discovered in a high-throughput screen. Cell stem cell, 12(2), 167-179.

Maciel, B. B., Rebelatto, C. L., Brofman, P. R., Brito, H. F., Patricio, L. F., Cruz, M. A., & Locatelli-Dittrich, R. (2014). Morphology and morphometry of feline bone marrow-derived mesenchymal stem cells in culture. Pesquisa Veterinária Brasileira, 34, 1127-1134.

Cheng, C. C., Lian, W. S., Hsiao, F. S. H., Liu, I. H., Lin, S. P., Lee, Y. H., ... & Wu, S. C. (2012). Isolation and characterization of novel murine epiphysis derived mesenchymal stem cells. PloS one, 7(4), e36085, 360-385.

Dmitrieva, R., Minullina, I. R., Bilibina, A. A., Tarasova, O. V., Anisimov, S. V., & Zaritskey, A. Y. (2012). Bone marrow- and subcutaneous adipose tissue-derived mesenchymal stem cells differences and similarities. Cell Cycle, 11(2), 377-383.

Grzesiak, J., Marycz, K., Czogala, J., Wrzeszcz, K., & Nicpon, J. (2011). Comparison of behavior, morphology and morphometry of equine and canine adipose derived mesenchymal stem cells in culture. International Journal of Morphology, 29(3), 1012-1017. doi: 10.4067/S0717-95022011000300059

Heo, J. S., Kim, H. O., Song, S. Y., Lew, D. H., Choi, Y., & Kim, S. (2016). Poly-L-lysine prevents senescence and augments growth in culturing mesenchymal stem cells ex vivo. BioMed research international, 2016, e8196078.

Katsube, Y., Hirose, M., Nakamura, C., & Ohgushi, H. (2008). Correlation between proliferative activity and cellular thickness of human mesenchymal stem cells. Biochemical and biophysical research communications, 368(2), 256-260. doi: 10.1016/j.bbrc.2008.01.051.

Kladnytska, L., Mazurkevych, A., Bezdieniezhnykh, N., Melnyc, O., Velychko, S., Malyuk, M., ... & Gryzinska, M. (2020). The Expression of Cytoplasmic and Membrane Proteins in Dog Adipose-Derived Stem Cells on Different Passages During Cultivation in Vitro. Pakistan Journal of Zoology, 52(4), 1547.

Martin, D. R., Cox, N. R., Hathcock, T. L., Niemeyer, G. P., & Baker, H. J. (2002). Isolation and characterization of multipotential mesenchymal stem cells from feline bone marrow. Experimental hematology, 30(8), 879-886.

Yamazaki, M., Kojima, H., & Miyoshi, H. (2020). Morphology and differentiation of human mesenchymal stem cells cultured on a nanoscale structured substrate. Electronics and Communications in Japan, 103(9), 23-28. doi: 10.1002/ecj.12260

Miyoshi, H. (2016). Exogenous control of intracellular forces in regulation of selective gene expression. The Japanese Society for Biomaterials, 34(2), 132-137.

Nagano, T., Katsurada, M., Dokuni, R., Hazama, D., Kiriu, T., Umezawa, K., ... & Nishimura, Y. (2019). Crucial role of extracellular vesicles in bronchial asthma. International journal of molecular sciences, 20(10), 2589.

Ning, X., Li, D., Wang, D. K., Fu, J. Q., & Ju, X. L. (2012). Changes of biological characteristics and gene expression profile of umbilical cord mesenchymal stem cells during senescence in culture. Zhongguo shi yan xue ye xue za zhi, 20(2), 458-465.

O'Hagan-Wong, K., Nadeau, S., Carrier-Leclerc, A., Apablaza, F., Hamdy, R., Shum-Tim, D., ... & Colmegna, I. (2016). Increased IL-6 secretion by aged human mesenchymal stromal cells disrupts hematopoietic stem and progenitor cells' homeostasis. Oncotarget, 7(12), 13285.

Otsu, K., Das, S., Houser, S. D., Quadri, S. K., Bhattacharya, S., & Bhattacharya, J. (2009). Concentration-dependent inhibition of angiogenesis by mesenchymal stem cells. Blood, The Journal of the American Society of Hematology, 113(18), 4197-4205.

Saalbach, A., & Anderegg, U. (2019). Thy-1: more than a marker for mesenchymal stromal cells. The FASEB Journal, 33(6), 6689-6696.

Webb, T. L., Quimby, J. M., & Dow, S. W. (2012). In vitro comparison of feline bone marrow-derived and adipose tissue-derived mesenchymal stem cells. Journal of feline medicine and surgery, 14(2), 165-168.

Yang, Y. H. K., Ogando, C. R., See, C. W., Chang, T. Y., & Barabino, G. A. (2018). Changes in phenotype and differentiation potential of human mesenchymal stem cells aging in vitro. Stem cell research & therapy, 9(1), 1-14.

Yang, Y. Z., Zhang, X. Y., & Li, J. (2018). MSC Senescence-related signaling pathway-Review. Zhongguo shi yan xue ye xue za zhi, 26(1), 307-310.

Yang, Y. H. K., Ogando, C. R., See, C. W., Chang, T. Y., & Barabino, G. A. (2018). Changes in phenotype and differentiation potential of human mesenchymal stem cells aging in vitro. Stem cell research & therapy, 9(1), 1-14.

Kladnytska, L. V., Mazurkevych, A. Y., & Velychko, S. V. (2016). The method of obtaining mesenchymal stem cells from adipose tissue of the dog. Patent 109148 Ukraine. Kyiv: State Patent Office of Ukraine.

Кладницька Л. В., Мазуркевич А. Й., Величко С. В., Гарманчук Л. В., Малюк М. О., Мазуркевич Т. А., Ковпак В. В., Козицька Т. В., Харкевич Ю. О., Бокотько Р. Р., Савчук Т. Л. (2021). БІОЛОГІЧНІ ОСОБЛИВОСТІ МЕЗЕНХІМАЛЬНИХ СТОВБУРОВИХ КЛІТИН ІЗ ЖИРОВОЇ ТКАНИНИ ЗА РІЗНИХ ПАСАЖІВ КУЛЬТИВУВАННЯ *Ukrainian Journal of Veterinary Sciences, 12(4): 79–89, https://doi.org/10.31548/ujvs2021.04.006*

Анотація. *Дослідження проводили на самцях мишей C57BL/6 вагою 20–24 г віком 2–3 місяці. Обробку первинного матеріалу та роботу з мезенхімальними стовбуровими клітинами культури жирової тканини проводили в стерильному ламінарному боксі з дотриманням умов асептики та антисептики. Культивування проводили у CO_2 інкубаторі за температури 37 °С та вмісту CO_2 5%. Проводили дослідження мезенхімальних стовбурових клітин культури жирової тканини 2, 4, 7 та 12 пасажів. Морфометричний аналіз проводили за допомогою світлової мікроскопії. Морфометричні параметри, такі, як площа клітини, ядра визначали за допомогою світлового мікроскопа Axiovision (Carl Zeiss, Німеччина) та програмного забезпечення ImageJ 1.45. Для прижиттєвого фарбування мезенхімальних стовбурових клітин використовували барвник трипановий синій для дослідження їхньої життєздатності.*

Морфологічна характеристика мезенхімальних стовбурових клітин культури жирової тканини в процесі культивування змінюється: на перших пасажах культивування клітини мають веретеноподібну форму з двома, щонайменше трьома довгими цитоплазматичними відростками, розташованими біполярно. Біля ядра добре видно комплекс Гольджі – ознака активних клітин. За пізніх пасажів клітини мають велику кількість коротких цитоплазматичних відростків із зірчастим розташуванням. У них також чітко візуалізується комплекс Гольджі. Показник ядерно-цитоплазматичного співвідношення в мезенхімальних стовбурових клітинах культури жирової тканини значно знижується на 7 пасажі до 0,2189 ± 0,0122 ($P < 0,01$), а на 12 пасажі – до 0,1111 ± 0,0086 ($P < 0,001$) порівнюючи з 2 пасажем. Коефіцієнт проліферації мезенхімальних стовбурових клітин із жирової тканини значно знижується на 12 пасажі до 2,55 ($P < 0,001$). Життєздатність мезенхімальних стовбурових клітин із жирової тканини за пізніх пасажів культивування значно знижується й на 12 пасажі культивування досягає 84,67 ± 1,36 ($P < 0,05$). Вміст апоптотичних клітин, які виявляли чутливість до безсироваткового культивування, достовірно збільшувався на 7 та 12 пасажах і становив відповідно 21,33 ± 1,36 ($P < 0,05$) та 23,67 ± 0,97% ($P < 0,05$).

Ключові слова: *мезенхімальні стовбурові клітини культури жирової тканини, ядерно-цитоплазматичне співвідношення, коефіцієнт проліферації, життєздатність, апоптоз, ранні пасажи, пізні пасажи*

UDC: 636.5.09:616.15/.8:577.112 https://doi.org/10.31548/ujvs2021.04.007

DYNAMICS OF SERUM PROTEIN CONTENT AND PRODUCTIVITY OF CHICKENS WITH DIFFERENT TONUS OF THE AUTONOMOUS NERVOUS SYSTEM

A. A. STUDENOK,
Graduate Student, Department of Biochemistry and Physiology of Animals named after Academician M. F. Gulyi
https://orcid.org/0000-0002-0740-3609
E-mail: artemstudenok@gmail.com
E. O. SHNURENKO,
Graduate Student, Department of Biochemistry and Physiology of Animals named after Academician M. F. Gulyi
https://orcid.org/0000-0002-1121-4106
V. O. TROKOZ,
Doctor of Agricultural Sciences, Professor, Department of Biochemistry and Physiology of Animals named after Academician M. F. Gulyi
https://orcid.org/0000-0001-8619-195X
V. I. KARPOVSKYI,
Doctor of Veterinary Sciences, Professor, Department of Biochemistry and Physiology of Animals named after Academician M. F. Gulyi
https://orcid.org/0000-0003-3858-0111
National University of Life and Environmental Sciences of Ukraine, 15 Heroyiv Oborony st., Kyiv 03041, Ukraine

Abstract. *The main role in maintaining the functioning of the body, its growth, and its development belongs to protein. It is involved in the formation of the muscular skeleton and is s part of enzymes, neurotransmitters, hormones. The effect of the autonomic nervous system on total protein metabolism has not been sufficiently studied. It is known that the autonomic nervous system is a structure that is responsible for the homeostasis and stability of the whole organism. It participates in the regulation of the heart, endocrine and external secretion glands, gastrointestinal tract, excretory organs, and more.*

In our studies, it was found that in chickens of Cobb 500 strain with different tones of the autonomic nervous system during the growing period from the 35th to the 60th day, different contents of total protein, albumin, and globulins were observed and different body weights were recorded. Vagotonic chickens showed the lowest protein metabolism at the age of 35 and 45 days ($P < 0.05–0.001$) compared with sympathicotonics and normotonics, which tended to increase between 35 and 60 days of rearing compared with other groups of birds, where the studied protein fractions on the contrary decreased.

Correlations between total protein, albumin, and bird body weight had a high linear relationship in all groups of chickens ($P < 0.05–0.001$) and a negative relationship

between the 45th and 60th days of rearing in sympathicotonics and normotonics. In birds with a predominance of the parasympathetic tone of the autonomic nervous system, this correlation maintained its direction with high reliability (P < 0.05) between body weight and total protein on the 60th day of rearing.

Keywords: *sympathicotonia, vagotonia, normotonia, protein metabolism, albumin, globulin*

Introduction

The study of the dynamics of the influence of different tones of the autonomic nervous system on the metabolism of total protein and its components in the serum of chickens has not been thoroughly studied. Its fluctuations are influenced by numerous factors, such as age, diet, keeping animals, their genetic characteristics. In recent decades, breeders have bred high-yielding poultry crosses that have high feed conversion, rapid growth, and development. Therefore, the study of the peculiarities of the metabolic processes of protein as a major component involved in the growth of the organism is an extremely important issue today.

Analysis of recent researches and publications

Serum protein is a central link in all biochemical processes in animals and humans (Derho & Sereda, 2016). Albumin and globulins that are part of it are synthesized directly in the liver and immune organs (globulins). The functions of these proteins are difficult to overestimate because they provide transport of metabolites, biologically active substances, are a plastic material for the needs of the body, there are protective immune complexes, etc. (Gotovsky et al., 2018). The content of these proteins in the body depends on the state and activity of the immune system (Filipović et al., 2007), nutritional feed and content of all necessary substances, synthesizing capacity of the liver (Zaefarian et al., 2019), and directly the needs of the body (Filipović et al., 2007).

Effective metabolism of various compounds in animals is ensured by numerous biochemical processes that occur and are regulated under the influence of neuro-humoral factors (Postoi et al., 2020; Reutov & Chertok, 2016). The autonomic nervous system (ANS) through its numerous array of reflexes is able to regulate the work of almost all physiological functions of the body (Abboud & Singh, 2017). It consists of three divisions – sympathetic, parasympathetic (Wehrwein et al., 2016), and enteral (intestinal) (Volkova, 2015). Their centers are located at different levels of the nervous system – the cortex of the large hemispheres, hypothalamus, cerebellum, basal ganglia, and spinal cord (Gibbons, 2019). The activity of the sympathetic and parasympathetic divisions mostly has different directions, which allows them to precisely regulate any processes in the body of living beings (McCorry, 2007). For example, increased activity of the sympathetic branch of the ANS causes an increase in glucose output and utilization (Karpovskyi et al., 2013), the development of anti-inflammatory response in the body by activating T and B lymphocytes, and NO secretion (Padro & Sanders, 2014; Abboud & Singh,

2017), increased antibacterial and lysozyme activity of the blood (Karpovskyi et al., 2016). The sympathetic system directly affects the growth of bone tissue. Strengthening of the alveolar bone of the upper jaw and a decrease in tooth mobility was observed in rats treated with selective β-blockers (Uchibori et al., 2020). The increased influence of the sympathetic system provides a decrease in osteoblast activity, which may lead to a decrease in skeletal strength (Elefteriou, 2008; Dimitri & Rosen, 2017). Studies (Postoi et al., 2019) found that pigs with a different tone of the ANS have varying degrees of the intensity of protein metabolism in the body. Animals with a predominance of sympathetic and parasympathetic divisions had a higher urea content and a decrease in total serum protein during the first seven days after exposure to technological stress. Also, pigs with balanced ANS tone took less time to establish baseline levels of test substances in serum compared to other groups. Other studies have shown the effect of the ANS on the state of the antioxidant system in pigs. Animals dominated by the sympathetic branch had significantly higher superoxide dismutase activity compared to other groups. The ratios of antioxidants superoxide dismutase to catalase (SOD/CAT) and superoxide dismutase to glutathione peroxidase (SOD/GPO) were lower in vagotonic pigs and sympathicotonics (Skrypkina et al., 2016). Determination of the influence of the ANS on the activity of the enzymatic link of antioxidant protection showed a significant effect in sympathicotonic pigs (Skrypkina et al., 2016).

One of the main functions of the ANS is the implementation of precise regulation of the cardiovascular system. The activity of the heart as the main target of the sympathetic and parasympathetic divisions is provided by regulating the rhythm and heart rate, vascular tone, and blood supply, which is necessary for the needs of the body (Albarado-Ibañez, 2019). Such control is not a simple predominance of sympathetic or parasympathetic influence but is a complex interaction of circulatory reflexes, the functioning of baro- and chemoreceptor zones in the vessel walls, as well as various molecular and hormonal factors (Taralov et al., 2016). The effect of the ANS on the cardiovascular system can be described as maintaining balance with various changes in the external and internal environment of the body, as confirmed by numerous studies. For example, in rats and weather-sensitive humans, reduced atmospheric pressure and hypoxia increase the parasympathetic effect on the vessels of the brain, which is necessary to maintain oxygen homeostasis and maintain energy-dependent processes in nerve cells (Volkova, 2015). In waterfowl, there is a well-defined evolutionary antagonism of the mechanism of action of the parasympathetic system. During immersion under water and emergence of reflex apnea, there is a blocking of a sympathetic branch of the ANS with the subsequent decrease in heart rate. This allows birds to spend more energy on swimming and oxygen for the body's biochemical needs (Shereshkov et al., 2010). Studies in rats have shown that early experimental desympathization leads to an increase in the diameter of blood vessels, delays the formation of their multidimensional structure, and the preservation of a predominantly linear orientation, which is characteristic of early development. There is also a decrease in the distance between the vascular wall and the area of the neuromuscular synapse, which

indicates a change in the level of metabolic reactions (Kovrigina & Filimonov, 2013). Identical data on vascular diameter were obtained in heifers with different ANS tones. They increased the Kernogan index (the ratio of the thickness of the middle membrane of the vascular wall to the width of the lumen of the vessel) in parallel with the growth of sympathicotonia in animals and vice versa (Demus, 2010).

The inter regulatory work of the sympathetic and parasympathetic divisions of the ANS ensures the precise functioning of tissues and the regulation of the metabolism of proteins, carbohydrates, fats, minerals, and biologically active substances. The ANS provides constant adaptation to changes in the internal and external environment. As a result of violation or imbalance of these departments of the ANS in the body, there are persistent disorders of hemodynamics, functioning of endocrine organs, catabolic or anabolic processes begin to predominate (Wehrwein et al., 2016; Zhukov et al., 2020). At present, the effect of the ANS on protein metabolism has not been sufficiently studied (McCorry, 2007; Postoi et al., 2019). Therefore, research in this direction is relevant.

Purpose. To determine the effect of different ANS tones on serum protein metabolism in chickens during the period of their rearing.

Materials and methods of research

Studies of protein metabolism depending on the tone of the ANS were performed on broiler chickens Cobb 500 strain, aged 35, 45, and 60 days in accordance with international bioethical requirements set out in Directive 86/609/EEC on the Protection of Animals Used for Experimental and Other Scientific Purposes (Louhimies, 2002) and the Law of Ukraine On Protection of Animals from Cruelty (Law of Ukraine, 2006). Determination of the ANS tone was performed by the method of variation pulsometry (Tybinka, 2011). At least 100 consecutive cardio intervals were recorded for 20–30 s with a portable electrocardiograph (EK3T 01-RD, Russia) (Studenok et al., 2020). Alligator electrodes were placed according to standard electrocardiography (ECG) protocols in poultry in the shoulders and legs (Tybinka, 2011; Reddy et al., 2016). Experimental animals, depending on the tone of the ANS were divided into 3 groups: sympathicotonics, in which the indicators of the mode of the duration of the cardiac cycle (Mo) were 0.14–0.16 s, the amplitude of the mode (Amo) – > 45%; normotonics (Mo – 0.16–0.17 s, Amo – 40–45%); vagotonics (Mo – 0.18–0.21 s, Amo – < 40%) (Studenok et al., 2020). Venous blood for biochemical studies was taken from the subcutaneous vein of the shoulder after a 2-hour fasting diet (Bayer et al., 2012). The venipuncture site was cleaned of dirt, disinfected with 70% aqueous solution of ethyl alcohol, skin anesthesia was performed with gel (Kategel, Austria) based on lidocaine (Bayer et al., 2012). The content of total protein in blood serum was determined by biuret reaction (Levchenko et al., 2002), albumin-method with bromocresol green (Levchenko et al., 2002) on a semi-automatic biochemical analyzer (Biosystems A15, Spain) using a set of reagents (Pointer Scientific, USA) according to the manufacturer's instructions, and the content of globulins – by calculating the difference between the content of total protein and albumin. Statistical processing of the results was performed in the Statistica 6 program

with the determination of averages and their errors, the probability of difference between groups, correlation (Pearson's method) and analysis of variance of the data (one-way analysis of variance) was performed in Microsoft Excel.

Results of the research and their discussion

The dynamics of the content of total protein and its fractions in blood serum of chickens with balanced ANS tone in the period of 35–60 days of rearing was characterized by a decrease (Fig. 1–3). In particular, the content of total protein (Fig. 1) decreased by 2.20 g/L (3.0%), albumin – by 1.10 g/L (5.5%), globulins – by 1.05 g/L (4.4%) within the trend.

A similar pattern was observed in chickens with a predominance of the sympathetic tone of the ANS. The content of total protein was the same for 35- and 60-days-old with a slight increase at the age of 45 days (1.50 g/L; 3.6%). The content of globulin fraction (Fig. 3) at the age of 45 days also increased by (1.20 g/L; 5.2%) with a subsequent decrease to the 60th day. The content of albumins (Fig. 2) increased slightly by 0.60 g/L (3.1%).

With age, there is a balance of metabolic processes, the transition from intensive growth, and an increase in muscle mass in the plateau of stable indicators (Filipović et al., 2007; Pi-

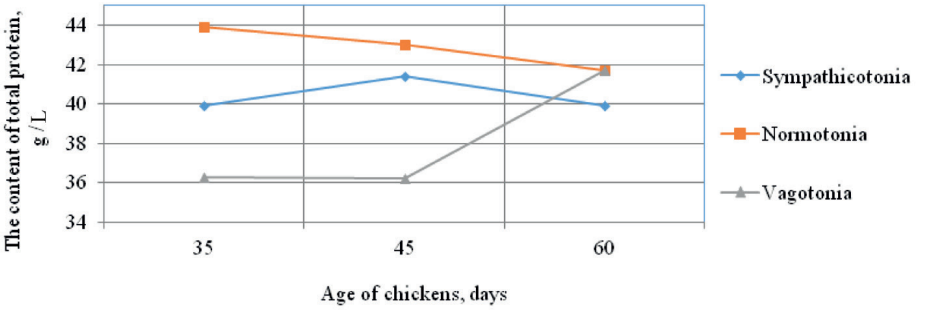

Fig. 1. Dynamics of the total protein content in serum of chickens with different tones of the autonomic nervous system, n = 8

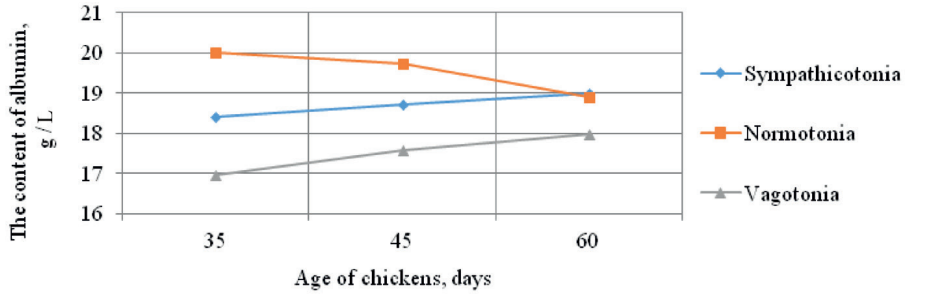

Fig. 2. Dynamics of albumin content in serum of chickens with different tones of the autonomic nervous system, n = 8

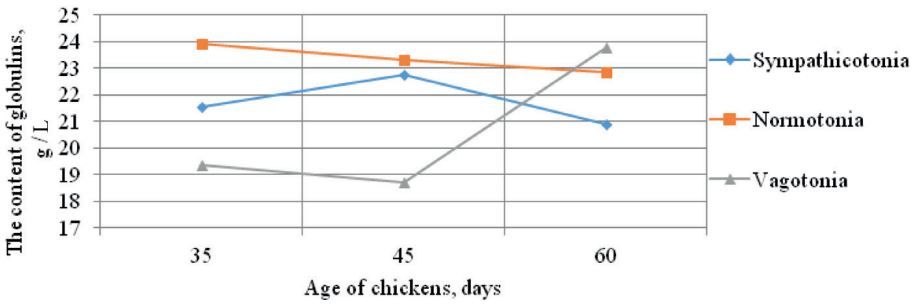

Fig. 3. Dynamics of globulin content in serum of chickens with different tones of the autonomic nervous system, n = 8

otrowska et al., 2011). This is especially noticeable in chickens with a predominance of the parasympathetic tone of the ANS, in which protein metabolism gradually increased and at the 60th day of age approached the results of animals with a dominant sympathetic and balanced tone of the ANS.

Vagotonic chickens had a steady increase in the content of total protein and its fractions. Thus, between the 45- and 60-day period, the content of total protein and globulins increased rapidly by 5.50 g/L (13.1%; $P < 0.001$) and 5.10 g/L (21.3%; $P < 0.001$), respectively. The albumin fraction showed only a tendency to increase the content by 1.00 g/L (5.6%).

It should be emphasized that at the age of 35 and 45 days normotonic chickens compared to vagotonic had a significantly higher content of total protein ($P < 0.001$); albumins ($P < 0.01$–0.001), and globulins ($P < 0.01$–0.001) in serum. A similar pattern concerning these proteins was observed in sympathicotonic chickens compared with vagotonics at the age of 35 ($P < 0.05$) and 45 ($P < 0.001$) days. Chickens with a predominance of parasympathetic tone compared with sympathicotonic had a significantly higher content of globulins only at the age of 60 days ($P < 0.01$).

The content of total protein and its fractions in different periods of rearing may depend on many factors: the level of feeding, protein content in feed, intensity and rate of growth and development of the organism (Filipović et al., 2007; Piotrowska et al., 2011), age of the animal (Kuznyak & Savchuk, 2017). Different ANS tone, in our opinion, also affects the fluctuations of total protein, albumin, and globulins because the dominant effect of the sympathetic branch of the ANS is accompanied by an increase in catabolic processes in animals and humans (Morozova et al., 2016), which may cause statistical differences between indicators. The authors (Morozova et al., 2016) note that in vagotonic animals, due to rapid growth, weight gain, and trophic effects of parasympathicotonia, registered a decrease in total protein and its components in serum. Similar data were obtained in vagotonic chickens at the 35th and 45th days of age (Fig. 1–3).

Note that our results correlate with studies to determine the effect of different ANS tones on the intensity of growth of chickens, which revealed the relationship between the dominance of the parasympathetic system of higher

productivity of chickens during the period of its rearing. A bird with a balanced tone, on the contrary, had the lowest absolute and average daily weight gain (Shnurenko et al., 2020). Vagotonics and sympathicotonics in comparison with normotonics are characterized by a higher content of essential and non-essential amino acids in blood serum (Studenok et al., 2020; Studenok et al., 2021). It should be noted that the globulin fractions, which consist of α-, β-, and γ-globulins can also increase due to chronic and acute inflammatory processes, changes in the environment, and the body's adaptation to them (Tothova et al., 2019). Some authors report a physiologically low level of γ-globulin fraction in chickens, which usually increases during the growth of poultry with other peptides (Povoznikov & Pustovaya, 2013). Similar studies have shown an increase in total protein, albumin, and globulin levels by day 32–42 of meat-fattening poultry, which occurs during periods of intense growth (Filipović et al., 2007; Piotrowska et al., 2011). Other publications suggest that fluctuations in the content of protein fractions in serum of chickens depend on the needs of the body and the period of their rearing. According to the author (Repko, 2015), the protein content increased during the period of intensive egg-laying and tended to decrease after it.

Interactions between the content of total protein, albumin, globulins and body weight of chickens in all experimental groups had a rectilinear relationship at the 35th day of age with a predominance in vagotonic chickens (Table 1).

They showed a close correlation between the content of total protein, albumin, and body weight ($P < 0.001$). Sympathicotonic chickens aged 45 and 60 days showed a sharp change in the direction of the correlation, mostly in the negative direction compared to the previous period. Normotonics at the age of 45 days had a significant ($P < 0.01–0.001$) close correlation between the content of total protein, globulins, and body weight, which changed to negative on the 60th day of life. In contrast, in birds with a predominance of excitability of the parasympathetic division of the ANS, a significant positive correlation was observed between the content of to-

1. Correlation of the content of protein fractions in serum with body weight of chickens in different age periods of rearing, r (n = 8)

Indexes	35 days			45 days			60 days		
	Total protein	Albumin	Globulins	Total protein	Albumin	Globulins	Total protein	Albumins	Globulins
Body weight (sympathicotonics)	0.792*	0.768*	0.690	-0.473	-0.513	0.240	-0.212	-0.262	-0.083
Body weight (normotonics)	0.789*	0.497	0.716*	0.908**	0.205	0.936***	-0.441	-0.473	-0.414
Body weight (vagotonics)	0.927***	0.886**	0.699	0.260	-0.103	0.385	0.707*	0.230	0.809*

Note: * $P < 0.05$; ** $P < 0.01$; *** $P < 0.001$ – reliability of correlation coefficients.

tal protein, globulins, and body weight at the age of 60 days.

The concentration of protein fractions in serum of chickens and their interaction with weight gain over the entire study period, in our opinion, depends on the neuro-humoral effect on the metabolism of these compounds, the intensity of animal growth, and diet. Similar results were obtained in studies (Demus, 2010; Demus, 2013), where animals with a predominance of the parasympathetic ANS tone had higher measurements, body weight, and size of individual heart structures compared to sympathicotonics. In fish (rainbow trout Oncorhynchus mykiss) the positive effect of the vagus nerve on the hypothalamic protein AMPKα2, which participates in the control of energy homeostasis throughout the body by regulating feed intake (increased productivity), thermogenesis, metabolism in the liver and muscles (Conde-Sieira et al., 2020). Other studies have shown a direct effect of vagotonia on weight gain and hunger due to the action of neuropeptides Y and AgRP on nutrient-sensitive areas of the hypothalamus and subsequent hyperphagia (Grechko et al., 2018).

The effect of different ANS tones on the content of protein components depending on the age of the bird is diverse and has a general tendency to decrease depending on the growth of chickens. This is evidenced by the results of analysis of variance with the definition of the main indicator of the force of influence η2x (Table 2).

The growing period of 35 days was characterized by a significant effect of vagotonia and normotony on the content

2. The effect of different ANS tones on the content of protein fractions in serum of chickens, η2x (n = 8)

Indexes	35 days		
	Sympathicotonia	Normotonia	Vagotonia
Total protein	0	0.39**	0.37**
Albumin	0	0.26*	0.25*
Globulins	0	0.37**	0.35**
Indexes	45 days		
	Sympathicotonia	Normotonia	Vagotonia
Total protein	0	0.32**	0.65***
Albumin	0	0.19*	0.19*
Globulins	0.1	0.22*	0.61***
Indexes	60 days		
	Sympathicotonia	Normotonia	Vagotonia
Total protein	0.08	0	0
Albumin	0.04	0	0.12
Globulins	0.24*	0	0.15

Note: * $P < 0.05$; ** $P < 0.01$; *** $P < 0.001$ – reliability of the main indicator of the force of influence η^2_x.

of all fractions of protein in serum ($P < 0.05–0.01$) and the complete absence of such effects in sympathicotonics with a subsequent slight increase to the 60th day and a significant effect on the content globulins ($P < 0.05$). In contrast, the period of 45 and 60 days in vagotonic animals differed in the pronounced effect of the parasympathetic branch of the ANS on the content of blood proteins ($P < 0.05–0.001$).

The ratio of albumin to globulin (A/G) in 35-day-old chickens did not differ much in different experimental groups with a slight predominance in vagotonics by 3.4%. Chickens of 45-days-old with a predominance of the parasympathetic ANS tone had a significantly higher A/G ratio compared to sympathicotonics by 13.7% ($P < 0.05$) and within the trend – with normotonics by 9.5%. The 60-days-old bird had opposite ratios of protein fractions. In sympathicotonic chickens, A/G ratio was statistically higher than in normotonics by 8.8% ($P < 0.05$) and vagotonics by 16.5% ($P < 0.01$) (Fig. 4).

The authors (Taldykina & Semenyutin, 2021) in their research claim that the decrease in the albumin fraction of proteins may be associated with their use as a plastic material during the intensive growth of chickens. Instead, there are conflicting data that suggest that based on the detected increase in the ratio of albumin to globulins due to the former, we can indirectly talk about increased meat productivity, and globulins – increased egg production (Povoznikov & Pustovaya, 2013; Pushkarev et al., 2021). After all, the higher the value of A/G, the more intense the protein metabolism, which, in turn, affects the state of the whole organism (Pushkarev et al., 2021).

It should be noted that protein metabolism also depends on higher nervous activity, which performs the finest regulation of physiological processes in the body, including through the ANS. Studies by domestic authors have established a direct effect of different types of higher nervous activity on protein metabolism and productivity of pigs and cattle (Danchuk et al., 2020). Animals with a strong balanced higher nervous activity type had a higher content of total protein and albumin compared to a weak one; productivity in these animals also prevailed over the latter. The content of essential amino acids (valine, proline,

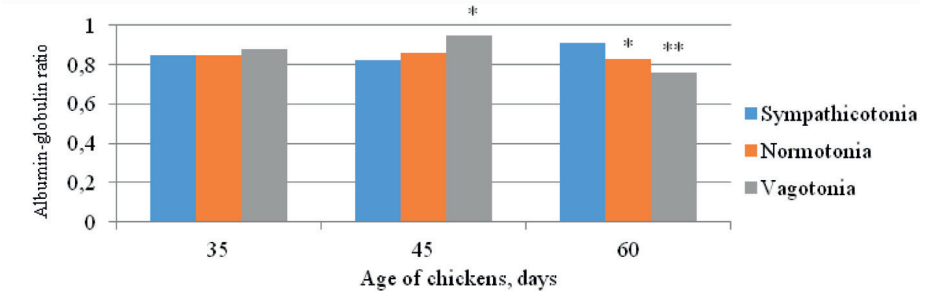

Fig. 4. Albumin-globulin ratio in different periods of rearing in chickens with different tones of the autonomic nervous system, n = 8

Note: * $P < 0.05$; ** $P < 0.01$ – compared with sympathicotonics.

and glycine) in individuals with a weak type of higher nervous activity was lower compared to other groups (Vasyliv et al., 2020).

It should be noted that the justification of these observations is based on the statement about the multifunctionality of blood proteins (Derho & Sereda, 2016). Their concentration in serum directly depends on the intensity of metabolism and the needs of other tissues. Proteins are also used as carriers of biologically active substances, from which hormones and enzymes are synthesized (Filipović et al., 2007; Piotrowska et al., 2011).

Thus, the studies found a relationship between different ANS tones and poultry productivity, total protein, albumin, and globulins in serum. The highest positive effect of parasympathicotonia on the content of test substances and weight gain in the period of 35–60 days of age was noted.

Conclusions and future perspectives

A significant difference in the content of total protein, albumin, and serum globulins in chickens with different tones of the autonomic nervous system in different periods of rearing is a manifestation of the influence of the autonomic nervous system on protein metabolism.

The influence of the dominant tone of the parasympathetic division of the autonomic nervous system is characterized by an increase in total protein and its fractions in the period from the 35th to the 60th day of growing chickens. In normotonics, the studied indicators, on the contrary, tend to decrease. In sympathicotonic chickens, significant fluctuations in the content of serum proteins are mostly absent.

The established correlation between the content of total protein, albumin, globulins and body weight of chickens indicates a direct relationship between protein metabolism and productivity of chickens, which depends on the tone of the autonomic nervous system in different periods of rearing.

A significant effect of parasympathetic and balanced autonomic nervous system tone on the content of protein fractions in serum of chickens aged 35 and 45 days, as evidenced by the albumin-globulin ratio, which decreases to the 60th day of rearing with a parallel significant correlation of total protein and albumin, body weight of the bird.

In the future, it is planned to investigate the effect of different autonomic nervous system tones on the content of micro- and macroelements, hormones in serum of chickens.

References

Abboud, F. M., & Singh, M. V. (2017). Autonomic regulation of the immune system in cardiovascular diseases. Advances in physiology education, 41(4), 578-593. doi: 10.1152/advan.00061.2017

Albarado-Ibañez, A., Arroyo-Carmona, R. E., Sánchez-Hernández, R., Ramos-Ortiz, G., Frank, A., García-Gudiño, D., &Torres-Jácome, J. (2019). The role of the autonomic nervous system on cardiac rhythm during the evolution of diabetes mellitus using heart rate variability as a biomarker. Journal of diabetes research, 10. doi: 10.1155/2019/5157024

Bayer, D. M., Mohan, K., Jayakumar, K., Manafi, M., & Pavithra, B. H. (2012). Simple cannulation procedure for serial blood sampling through cutaneous ulnar vein in chickens. Journal of Applied Animal Welfare Science, 15(1), 91-100. doi: 10.1080/10888705.2012.624925

Conde-Sieira, M., Capelli, V., Álvarez-Otero, R., Díaz-Rúa, A., Velasco, C., Comesaña, S., López, M., & Soengas, J. L. (2020). Hypothalamic AMPKα2 regulates liver energy metabolism in rainbow trout through vagal innervation. American Journal of Physiology-Regulatory, Integrative and Comparative Physiology, 318(1), 122-134. doi: 10.1152/ajpregu.00264.2019

Danchuk, O. V., Karposvkyi, V. I., Tomchuk, V. A., Zhurenko, O. V., Bobrytska, O. M., & Trokoz, V. O. (2020)a. Temperament in cattle: a method of evaluation and main characteristics. Neurophysiology, 1(52), 73-79. doi: 10.1007/s11062-020-09853-6

Danchuk, O. V., Broshkov, M. M., Karpovskyi, V. I., Bobrytska, O. M., Tsvivlikhovskyi, M. I., Tomchuk, V. A., ... & Kovalchuk, I. I. (2020) b. Types of Higher Nervous Activity in Pigs: Characteristics of Behavior and Effects of Technological Stress. Neurophysiology, 5(52), 358-366. doi: 10.1007/s11062-021-09892-7

Demus, N. V. (2010). Zakonomirnosti rostu i rozvytku telychok zalezhno vid typu avtonomnoi rehuliatsii sertsevoho rytmu [Regularities of growth and development of heifers depending on the type of autonomous regulation of heart rhythm]. Scientific bulletin of LNUVMBT named after Stepan Gzhytskyi, 2(12)(44)2)), 54-59.

Demus, N. V. (2013). Morfometriia vnutrishnikh struktur livoho shlunochka sertsia telychok zalezhno vid typu avtonomnoi rehuliatsii [Morphometry of the internal structures of the left ventricle of the heart of heifers depending on the type of autonomous regulation]. Herald of ZHNAEU, 2(1), 129-136.

Derho, M. A., & Sereda, T. I. (2016). Sopryazhennost metabolicheskikh funktsiy pecheni s sokhrannostyu ptits [The relationship of the metabolic functions of the liver with the safety of birds]. Innovative technologies for scientific development, International scientific and practical conference. Ufa, 39-42.

Dimitri, P., & Rosen, C. (2017). The Central Nervous System and Bone Metabolism: An Evolving Story. Calcified tissue international, 100(5), 476-485. doi: 10.1007/s00223-016-0179-6

Elefteriou, F. (2008). Regulation of bone remodeling by the central and peripheral nervous system. Archives of biochemistry and biophysics, 473(2), 231-236.

Filipović, N., Stojević, Z., Milinković-Tur, S., Ljubić, B. B., & Zdelar-Tuk, M. (2007). Changes in concentration and fractions of blood serum proteins of chickens during fattening. Veterinarski arhiv, 77(4), 319-326.

Grechko, A. V., Kiryachkov, Y. Y., & Petrova, M. V. (2018). Sovremennyye aspekty vzaimosvyazi funktsionalnogo sostoyaniya avtonomnoy nervnoy sistemy i kliniko-laboratornykh pokazateley gomeostaza organizma pri povrezhdeniyakh golovnogo mozga [Modern aspects of interconnection of functional state of autonomous nervous system and clinical and laboratory indicators of body homeostasis in brain damage]. A. I. Saltanov Intensive Care Bulletin, (2), 79-86.

Gibbons, C. H. (2019). Basics of autonomic nervous system function. Handbook of clinical neurology, 160, 407-418. doi: 10.1016/B978-0-444-64032-1.00027-8

Gotovsky, D. G., Sobolev, D. T., & Gisko, V. N. (2018). Pokazateli belkovogo obmena remontnogo molodnyaka kur pri ego vyrashchivanii v usloviyakh s razlichnym mikrobnym zagryazneniyem vozdukha [Indicators of protein metabolism in replacement chickens when they are grown in conditions with various microbial air pollution]. Veterinary Journal of Belarus, 2(9), 6-8.

Ivchuk, V. V., & Kovalchuk, T. A. (2019). Oksydantno-antyoksydantna systema pry khronichnomu obstruktyvnomu zakhvoriuvanni lehen profesiinoi etiolohii [Oxidant-antioxidant system in chronic obstructive pulmonary disease of occupational etiology]. Medical and Clinical Chemistry, 2(21), 61-67. doi: 10.11603/mcch.2410-

681X.2019.v.i2.10295

Karpovskyi, P. V., Postoi, R. V., Krivoruchko, D. I., Karpovskyi, V. I., Trokoz, V. O., Danchuk, O. V., ... Vasiliev, A. P. (2013). Deiaki pokaznyky obminu vuhlevodiv v syrovattsi krovi svynei z riznym tonusom avtonomnoi nervovoi systemy [Some indicators of carbohydrate metabolism in the serum of pigs with different tones of the autonomic nervous system]. Scientific Messenger of Lviv National University of VeterinaryMedicine and BiotechnologiesS.Z. Gzhytsky, 15(3(2)), 101-105.

Karpovskyi, V. I., Trokoz, V. A., Karpovskyi, P. V., Kryvoruchko, D. I., & Postoi, R. V. (2016). Vplyv tonusu avtonomnoi nervovoi systemy svynei na bakterytsydnu ta lizotsymnu aktyvnist syrovatky krovi [Influence of the tone of the autonomic nervous system of pigs on the bactericidal and lysozyme activity of blood serum]. Scientific Messenger of Lviv National University of VeterinaryMedicine and Biotechnologies S. Z. Gzhytsky, 18(1(2)), 69-73.

Kovrigina, T. R., & Filimonov, V. I. (2013). Reaktsiya mikrotsirkulyatornogo rusla skeletnoy myshtsy na defitsit simpaticheskoy innervatsii [The reaction of the microcirculatory tract of skeletal muscle to the deficit of sympathetic innervations]. Astrakhan Medical Journal, 8(1), 131-133.

Kuznyak, G., & Savchuk, L. (2017). Proteinove zhyvlennia ptytsi ta yoho zalezhnist vid viku [Protein nutrition of poultry and its dependence on age]. Agrarian Science and Education of Podillya, 334-336.

Law of Ukraine On protection of animals from brutal treatment № 3447-IV (2006). Vidomosti Verkhovnoi Rady Ukrainy, (27), 230.

Levchenko, V. I., Vlizlo, V. V., Kondrakhin, I. P., ... & Tsvilikhovskyi, M. V. (2002). Veterynarna klinichna biokhimiia [Veterinary clinical biochemistry]. Bila Tserkva: BSAU.

Louhimies, S. (2002). Directive 86/609/EEC on the protection of animals used for experimental and other scientific purposes. Alternatives to Laboratory Animals, 30(2_suppl), 217-219. doi: 10.1177/026119290203002S36

McCorry, L. K. (2007). Physiology of the autonomic nervous system. American Journal of Pharmaceutical Education, 71(4), 11. doi: 10.5688/aj710478

Morozova, O. H., Yaroshevskyi, A. A., Zdybskyi, V. I., Lipinska, Y. V., & Logvynenko, A. V. (2016). Vehetatyvna dysfunktsiia v zahalnoterapevtychnii praktytsi: shliakhy optymizatsii terapii [Autonomic dysfunction in general therapy practice: ways to optimize therapy]. Medicines of Ukraine, (5-6(201-2), 39-44. doi: 10.37987/1997-9894.2016.5-6(201-2).204799

Padro, C. J., & Sanders, V. M. (2014). Neuroendocrine regulation of inflammation. Semin Immunol 26, 357-368. doi: 10.1016/j.smim.2014.01.003.

Piotrowska, A., Burlikowska, K., & Szymeczko, R. (2011). Changes in blood chemistry in broiler chickens during the fattening period. Folia biologica, 59(3-4), 183-187. doi: 10.3409/fb59_3-4.183-187

Postoi, R., Karpovskyi, V., Cherepnina, A., & Postoi, V. (2020). Cortical and vegetative regulation of aminotransferase activity in blood serum of dry sows under exposure to a technological stimulus. Scientific Reports of NULES of Ukraine, (5(87)). doi: 10.31548/dopovidi2020.05.013

Postoi, R. V., Karpovskyi, V. I., Danchuk, O. V., & Kryvoruchko, D. I. (2019)a. Dynamika vmistu sechovyny v krovi svynomatok zanepadaie vid osoblyvostei diialnosti nervovoi systemy [The dynamics of urea in the blood of sows decreases due to the peculiarities of the nervous system]. Scientific Horizons, (6), 77-82. doi: 10.33249/2663-2144-2019-79-6-77-82

Postoi, R. V., Karpovskyi, V. I., Danchuk, O. V., & Kryvoruchko, D. I. (2019)b. Dynamika vmistu zahalnoho bilka v krovi svynomatok zalezhno vid osoblyvostei diialnosti nervovoi systemy [The dynamics of the content of

total protein in the blood of sows depending on the characteristics of the nervous system]. Scientific bulletin of LNUVMBT named after Stepan Gzhytskyi, 21(94), 51-56. doi: 10.32718/nvlvet9409

Tothova, C., Sesztakova, E., Bielik, B., & Nagy, O. (2019). Changes of total protein and protein fractions in broiler chickens during the fattening period, Veterinary World, 12(4), 598-604. doi: 10.14202/vetworld.2019.598-604

Povoznikov, N. G., & Pustovaya, N. V. (2013). Produktivnost i biokhimicheskiy sostav krovi kur [Productivity and biochemical composition of the blood of chickens]. Actual problems of intensive development of animal husbandry, 16(2), 206-219.

Pushkarev, I. A., Kureninova, T. V., Shanshin, N. V., & Belyaeva, N. Yu. (2021). Otsenka effektivnosti primeneniya tkanevogo biostimulyatora v raznykh dozakh dlya aktivizatsii belkovogo obmena u remontnogo molodnyaka krupnogo rogatogo skota [Evaluation of the effectiveness of the use of tissue biostimulants in different doses to activate protein metabolism in replacement young cattle]. Bulletin of NSAU (Novosibirsk State Agrarian University), (4), 131-137. doi: 10.31677/2072-6724-2020-57-4-131-137

Reddy, B. S., Reddy, P. A., Venkatasivakumar, R., Reddy, B. S. S., & Reddy, E. T. (2016). A study on electrocardiographic patterns in turkeys (Meleagris gallopavo). International Journal of Veterinary Science, 5(2), 79-82.

Repko, E. V. (2015). Metabolicheskiy profil pri gepatodistrofii i mochekislom diateze u kur yaichnykh krossov [Metabolic profile in hepatodystrophy and uric acid diathesis in chickens, egg crosses]. Actual problems of the humanities and natural sciences, (4-4), 7.

Reutov, V. P., & Chertok, V. M. (2016). Novyye predstavleniya o roli vegetativnoy nervnoy sistemy i sistem generatsii oksida azota v sosudakh mozga [New ideas about the role of the autonomic nervous system and systems for generating nitric oxide in the cerebral vessels]. Pacific Medical Journal, 2(64), 10-19.

Shereshkov, V. I., Shumilova, T. E., & Yanvareva, I. N. (2010). Vidovyye osobennosti khronotropnoy reaktsii serdtsa u vodoplavayushchikh ptits pri pogruzhenii v vodu [Specific features of the chronotropic reaction of the heart in waterfowl when immersed in water]. Biological Communications, (2), 107-113.

Shnurenko, E., Studenok, A., Karpovskyi, V., Trokoz, V., & Postoi, R. (2020). Vplyv tonusu avtonomnoi nervovoi systemyna intensyvnist rostu u kurei [Influence of tone of autonomous nervous system on growth intensity in chickens]. Scientific Horizons, 7(92), 14-18. doi: 10.33249/2663-2144-2020-92-7-14-18

Skrypkina, V. M., Karpovskyi, V. I., Danchuk, O. V., Postoy, R. V., Kryvoruchko, D. I., & Ukrainec, M. (2016). Aktyvnist ta zbalansovanist fermentatyvnoi systemy antyoksydantnoho zakhystu v orhanizmi svynei iz riznym tonusom avtonomnoi nervovoi systemy [Activity and balance of enzymatic antioxidant defense system in the body of pigs with different tone of autonomic nervous system]. Scientific bulletin of LNUVMBT named after Stepan Gzhytskyi, 18(1), 145-148.

Studenok, A. A., Shnurenko, E. O., Karpovskyi, V. I., Zhurenko, O. V., Kryvoruchko, D. I., Gutyj, B. V., & Trokoz, V. O. (2021). Interactions of productivity, content of separate amino acids, the general protein in blood serum of chickens and the tone of the autonomic nervous system. Regulatory Mechanisms in Biosystems, 12(3). doi: 10.15421/022177

Studenok, A. A., Shnurenko, E.O., Trokoz, V.O., Karpovsky, V.I., Zhurenko, O.V., & Krivoruchko, D. I. (2020)a. A method of assessing the tone of the autonomic nervous system in chickens. Patent 142943 Ukraine. Kyiv: State Patent Office of Ukraine.

Studenok, A., Radchikov, V., & Trokoz, V. (2020) b. Soderzhaniye arginina i gistidina v syvorotke krovi kur s raznym tonusom nervnoy

sistemy [The content of arginine and histidine in the blood serum of chickens with different tone of the nervous system]. Zootechnical science of Belarus, 55(2), 359-367.

Taralov, Z. Z., Terziyski, K. V., & Kostianev, S. S. (2016). Heart rate variability as a method for assessment of the autonomic nervous system and the adaptations to different physiological and pathological conditions. Folia medica, 57(3-4), 173-180. doi: 10.1515/folmed-2015-0036

Taldykina, A. A., & Semenyutin, V. V. (2021). Dinamika morfologicheskikh i biokhimicheskikh pokazateley krovi tsyplyat-broylerov pri ispolzovanii kompleksa organicheskikh kislot [Dynamics of morphological and biochemical parameters of the blood of broiler chickens using a complex of organic acids]. Scientific notes of the Kazan State Academy of Veterinary Medicine. N.E. Bauman, 246(2), 214-221.

Tybinka, A. M. (2011). Osoblyvosti variatsiino-pulsometrychnykh pokaznykiv kurei [Indicators of variation pulsometry of chickens of different types of autonomic tone]. Scientific bulletin of LNUVMBT named after Stepan Gzhytskyi, 4(13)(1), 446-449.

Uchibori, S., Sekiya, T., Sato, T., Hayashi, K., Takeguchi, A., Muramatsu, R., ... Goto, S. (2020). Suppression of tooth movement-induced sclerostin expression using β-adrenergic receptor blockers. Oral diseases, 26(3), 621-629. doi: 10.1111/odi.13280

Vasyliv, A. P., Karpovskyi, V. I., & Danchuk, O. V. (2017). Kortykalna rehuliatsiia obminu bilkiv u svynei [Cortical regulation of protein metabolism in pigs: a monograph]. Kyiv: NULES.

Volkova, N. M. (2015)a. Vplyv blokuvannia M1-kholinoretseptoriv asotsiatyvnoi kory doroslykh shchuriv na avtonomnu rehuliatsiiu sertsevoho rytmu pry hipoksychnomu vplyvi [The effect of blocking the M1-cholinoreceptors of the associative cortex of adult rats on the autonomic regulation of heart rate under hypoxic exposure]. Achievements of clinical and experimental medicine, (4), 8-11. doi: 10.11603/1811-2471.2015.v24.i4.5797

Volkova, N. M. (2015)b. Doslidzhennia avtonomnoi rehuliatsii sertsevoho rytmu molodykh shchuriv pry poiednanomu vplyvi hipoksychnoi atmosfery y melatoninu [Study of autonomic regulation of heart rate of young rats under the combined influence of hypoxic atmosphere and melatonin]. Medical Informatics and Engineering, (3), 62-65.

Wehrwein, E. A., Orer, H. S., & Barman, S. M. (2016). Overview of the anatomy, physiology, and pharmacology of the autonomic nervous system. Comprehensive Physiology, 6(3), 1239-1278. doi: 10.1002/cphy.c150037

Zaefarian, F., Abdollahi, M. R., Cowieson, A., & Ravindran, V. (2019). Avian Liver: The Forgotten Organ. Animals, 15(9)(2)), 63. doi: 10.3390/ani9020063

Zhukov, M. S., Alekhin, Yu. N., & Morgunova, V. I. (2020). The state of the autonomic nervous system of calves with different body weights at birth. Veterinarian, 6, 28-37. doi: 10.33632/1998-698X.2020-6-28-37

Студенок А. А., Шнуренко Е. О. , Трокоз В. О., Карповський В. І. (2021).
ДИНАМІКА ВМІСТУ БІЛКА В СИРОВАТЦІ КРОВІ ТА ПРОДУКТИВНОСТІ КУРЕЙ ІЗ РІЗНИМ ТОНУСОМ АВТОНОМНОЇ НЕРВОВОЇ СИСТЕМИ
Ukrainian Journal of Veterinary Sciences, 12(4): 90–104,
https://doi.org/10.31548/ujvs2021.04.007

Анотація. *Головна роль у підтриманні функціонування організму, його рості та розвитку належить білку. Він бере участь у формуванні м'язового каркасу та входить до складу ферментів, нейромедіаторів, гормонів. Вплив автономної нервової системи на ме-*

таболізм загального білка вивчений не достатньо. Відомо, що автономна нервова система – це структура, яка відповідає за гомеостаз та сталість усього організму. Вона бере участь у регулюванні роботи серця, залоз внутрішньої та зовнішньої секреції, травного тракту, органів виділення тощо.

У проведених нами дослідженнях було встановлено, що в курей кросу Кобб 500 в різним тонусом автономної нервової системи впродовж періоду вирощування з 35 до 60 доби спостерігався різний вміст загального білка, альбуміну, глобулінів та реєструвалася неоднакова маса тіла. Кури-ваготоніки демонстрували найнижчі показники білкового обміну у віці 35 та 45 діб ($P < 0,05–0,001$) порівнюючи з симпатикотоніками та нормотоніками, які мали тенденцію до зростанняи в період між 35 та 60 добою вирощування порівнюючи з іншими групами птиці, де досліджувані білкові фракції навпаки знижувались.

Кореляційні взаємозв'язки між загальним білком, альбуміном та масою тіла птиці мали високу лінійну залежність в усіх групах курей ($P < 0,05–0,001$) та негативну залежність у період між 45 та 60 добою вирощування в симпатикотоніків та нормотоніків. У птиці із домінуванням парасимпатичного тонусу автономної нервової системи така кореляція зберегла своє направлення із високою достовірністю ($P < 0,05$) між масою тіла та зальним білком на 60 добу вирощування.

Ключові слова: *симпатикотонія, ваготонія, нормотонія, метаболізм білка, альбумін, глобуліни*

UDC: 636.09:59461699:504.5:628.4.047 https://doi.org/10.31548/ujvs2021.04.008

LARVAL STAGES OF TREMATODES IN FRESHWATER SNAILS OF THE CHORNOBYL ZONE OF RADIOACTIVE CONTAMINATION

***V. I. STOROZHUK*[1],**
Graduate Student, Department of Pharmacology, Parasitology and Tropical Veterinary Medicine
https://orcid.org/0000-0003-1763-5742
***D. O. VYSHNEVSKYI*[2],**
Department of Ecology of Flora and Fauna
https://orcid.org/0000-0002-7824-5812
***V. F. GALAT*[1],**
Doctor of Veterinary Sciences, Professor, Department of Pharmacology, Parasitology and Tropical Veterinary Medicine
https://orcid.org/0000-0002-3844-2475
***O. V. SEMENKO*[1],**
Candidate of Veterinary Sciences, Associate Professor, Department of Pharmacology, Parasitology and Tropical Veterinary Medicine
https://orcid.org/0000-0002-6453-6192
***M. V. GALAT*[1],**
Doctor of Veterinary Sciences, Associate Professor, Department of Pharmacology, Parasitology and Tropical Veterinary Medicine
https://orcid.org/0000-0001-8881-0865
E-mail: galat_mv@nubip.edu.ua
[1]National University of Life and Environmental Sciences of Ukraine, 15 Heroiv Oborony st., Kyiv 03041, Ukraine
[2]Chornobyl Radiation and Ecological Biosphere Reserve, 6-b Staronavodnytska st., Kyiv 01015, Ukraine Kyiv, Ukraine

Abstract. *In 1986, at the Chornobyl Nuclear Power Plant in the Exclusion Zone after an industrial accident, ecosystems began to have several features that distinguish them from the objects of the natural reserve fund. Parasitic systems are an informative indicator of the state of the ecosystem, which is now sporadically applied in the Exclusion Zone. Any change in the parasite population can lead to changes in the host population. The degree of imbalance in the "parasite-host" system depends on the strength and nature of the influence of external factors. At the same time, the presence of mutual adaptations of parasitic organisms and snails gives grounds to consider the "parasite-host" system comprehensively.*

Freshwater gastropod snails of various systematic groups, which can be intermediate and secondary hosts for trematode agents, were selected as an object of the study.

In order to study freshwater gastropod snails for the presence of larval stages of helminths, snails were collected from such locations as Krasne Lake, Ilya River, Chernobyl Nuclear Power Plant cooling pond, bypass channel of the Chernobyl Nuclear Power Plant cooling pond, left bank of the Prypiat floodplain, Koshevka oxbow lake, Hrubchanskyi canal in the Meshevo village.

Based on the results of the research, the presence of larval stages of trematode agents at different stages of their development (redia and metacercaria) parasitizing in the freshwater snails Lymnae stagnalis and Radix auricularia was established.

Keywords: *freshwater snails, trematodes, larval stages, Chornobyl Exclusion Zone*

Introduction

Trematodes are flatworms that belong to phylum Platyhelminthes with a leaf-like unsegmented body and flattened dorsal-ventrally. They have a complicated life cycle, which comprises adult and several developing stages, such as egg, miracidium, sporocyst, redia, cercaria, and metacercaria (cyst). Trematodes are an important component of natural ecosystems (Curtis, 2002; Curtis, 2009; Rastyazhenko et al., 2015; Brian & Aldridge, 2020; Mouritsen & Elkjær, 2020; Wiroonpan et al., 2021).

The life cycle of these internal parasites constantly includes parthenogenetic and hermaphroditic generations. The effect of the diversity is formed by a wide set of numerous biological and morphological adaptations, existing at different stages of the development of these parasites, i.e., a great variety of animal hosts (both vertebrates and invertebrates) and a broad range of eco-systems and biotopes (Galaktionov et al., 2003; Kołodziejczyk et al., 2016). Trematodes are heterogeneous with a multiple host life cycle and require snails as their first or/and second intermediate host (Zbikowska & Nowak, 2009; Zhytova et al., 2017).

In rapport to modern taxonomy, there are known more than 18000 species of trematodes (Bray et al., 2008). In the Ukrainian Polissia forest zone, more than 166 species of trematodes of animals are known (Iskova et al., 1995). Furthermore, in Ukraine, trematode circulation ways from reservoirs of forestries of Polissia Nature Reserve (Rivne, Volyn, and Zhytomyr Regions). In this research, 26 species of trematodes from 14 families were found (Zhytova et al., 2019). On the previous stage of our snail investigation from the Chornobyl Exclusion Zone, the intensity of invasion by larvae of trematodes in *Lymnaea stagnalis* was 83%, in *Lymnaea (Radix) auricularis* – 50% and *Viviparus viviparus* – 75% (Semenko et al., 2020).

Like other parasitic organisms, trematodes negatively affect organisms, populations, animal groups, and food chains in general (Kuris et al., 2008; Magalhães et al., 2015; Żbikowska & Żbikowski, 2015; Moema et al., 2019; Paviotti-Fischer et al., 2019).

Studying trematodes and their circulation ways is necessary for the successful management of hunting farms, in particular, for breeding wild animals in enclosures.

The present study was carried out for identification and determination of the prevalence and intensity of parasite stages in freshwater snails collected from several water bodies of the Chornobyl Exclusion Zone.

Analysis of recent researches and publications

Freshwater snails are known to host a wide variety of parasites. They have received considerable attention because of their involvement with some species as intermediate hosts for trematodes. This has become an issue of significant medical and/or veterinary importance with regard to the cause of parasitic diseases in people and animals, and is especially true in diseases associated with various food-borne trematodes (Faltýnková & Haas, 2006; Wang et al., 2017; Dellagnola et al., 2019; Gilardoni et al., 2019; Chantima & Rika, 2020). Many trematode species, especially from the Echinostomatidae family, require 1 or 2 snail hosts to finish their life cycles. The Echinostomatidae is the largest family within the class Trematoda. Over 60 species of echinostomatid flukes are spread worldwide (Sorensen et al., 1998; Moraes et al., 2009). Members of this family, in their adult stage, can infect a far-ranging dimension of vertebrates (predominantly birds) such as poultries, migratory birds, and sometimes mammals, including humans. The zoonotic potential of this family of parasites is associated with the ingestion of raw fishes, amphibians, and snails, which can harbor the infective stage, metacercaria (Chantima et al., 2013; Nguyen et al., 2021).

Echinostomes are morphologically distinct from other trematodes by the presence of spines around the oral sucker, forming collar spines. The number and arrangement of these spines are the basis of genus identification. Their complex life cycle involves three categories of hosts. Among them definitive, first intermediate, and second intermediate hosts in which develop seven different stages (adult specie/species, eggs, miracidia, sporocysts, redia, cercaria, and metacercaria) (Toledo et al., 2014; Fernández et al., 2016; Horák et al., 2019). Also, in several trematode species that have the rediae stage, the latter comes in two distinct morphs (Poulin et al., 2019). The experimental study showed the possibility of native metacercariae (*Echinostoma revolutum, Echinoparyphium aconiatum*, and *Hypoderaeum conoideum*) settlement in non-specific snail species (*Potamopyrgus antipodarum*) (Zbikowski & Zbikowska, 2009).

Furthermore, there are cases in which trematoda, developing in gastropod snails, exploits first host for metacercarial encystment (Van den Broek & de Jong, 1979; Chai et al., 2011; Chantima et al., 2013; Sohn et al., 2017).

The shape of metacercarial cysts is variable and may be spherical (e.g. *Echinostoma trivolvis*), hemispherical (e.g. *Fasciola hepatica* or *Zygocotyle lunata*), flask-shaped (e.g. *Philophthalmus hegeneri*), ovoidal (e.g. *Parorchis acanthus*). Ventral lid or mucus plug may be present in a specific area of the cyst wall (e.g. *Fasciola hepatica*). During excystation, the ventral lid opens or the mucus plug is dissolved. Mechanisms of these processes are not fully explored. The structure of encysted metacercaria is differ from one species to another. Numerous histochemical, histological, and ultrastructural studies show that appreciable specific variation exists in both the chemical composition and their number of cyst layers (Fried et al., 1994).

Echinostome cercaria and furcocercous cercaria commonly develop in the body of viviparid and plumonate snails (*Lymnaea spp., Filopaludina spp.*) (Chontananarth & Wongsawad, 2013). *Echinostoma revolutum* and other similar species (*Ec. trivolvis* and *Ec. robus-*

tum) are possible to reveal via molecular genetic analyses (Pantoja et al., 2021). Cercarial numbers are known to vary both spatially and temporarily in aquatic ecosystems influenced by a range of factors, such as wind, water currents, and the specific geomorphology and biota of a habitat (Morley & Lewis, 2013).

Materials and methods of research

Collection of snails was carried out in the period from August 2021 till September 2021 using a simple random sampling approach and with the help of a strainer or net. Snails were collected in the following waterbodies as Krasne Lake, Ilya River, Chornobyl NPP cooling pond, bypass channel of the Chornobyl NPP cooling pond, left bank of the Pripyat floodplain, Koshevka oxbow lake, and Hrubchansky canal in the Meshevo village.

Then the research was conducted at the laboratory of the Department of Pharmacology, Parasitology and Tropical Veterinary Medicine of the Faculty of Veterinary Medicine of the National University of Life and Environmental Sciences of Ukraine.

In the laboratory, snails were placed in glass jars with tap water until they were identified. Identification was performed according to conchological characteristics and also based on morphological features (Brandt, 1974 (Fig. 1); Stadnichenko, 1990, 2006; Kruglov, 2005).

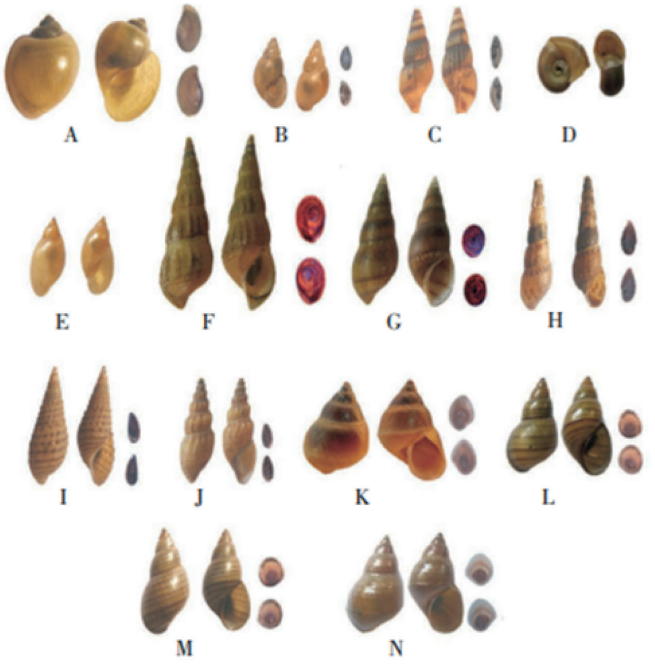

Fig. 1. Shell and operculate characteristics of snails collected from the collecting sites. A: *Pila polita*; B: *B. siamensis*; C: *Clea helena*; D: *I. exustus*; E: *Lymnaea auricularia rubiginosa*; F: *B. crostula crostula*; G: *Brotia wycoffi*; H: *M. tuberculata*; I: *T. granifera*; J: *T. scabra*; K: *E. eyriesi*; L: *Filopaludina dorliaris*; M: *Filopaludina sumatrensis polygramma*; N: *Filopaludina martensi* (Chontananarth & Wongsawad, 2013)

Subsequently, snails were examined using the compressorium technique for the detection of different stages of the development of trematoda species.

Results of the research and their discussion

Altogether 30 freshwater snails were collected, transported, and then identified and examined in the laboratory. On the basis of the shell morphology, the snail species were classified into 3 species. They included *Planorbis corneus, Lymnea stagnalis,* and *Radix auricularis* (Fig. 2–4).

In order to detect parasitic organisms, the liver and pancreas of the snails were examined under a microscope (Fig. 5–6).

Among 8 snails of the specie *Lymnea stagnalis*, 1 of them had larval stages of trematodes. The stage of the development was redia. Among the 9 studied snails of the specie *Radix auricularia*, all had a significant infestation with metacercariae. Metacercariae were morphologically classified echinostomatid species.

Among 13 snails of the species *Planorbis corneus*, no parasitic organisms were found.

So, the overall prevalence of trematodes infection in investigated snails was 33.3%, which is higher than in Chiang Mai province, Thailand where the prevalence of cercarial infection was 17.27% (428/2457) in 8 snail species collected (Chontananarth & Wongsawad, 2013). In another research, in total, *Bithynia tentaculata* showed a trematode prevalence of 12.9% and 14%, respectively (Schwelm et al., 2020). Thirteen percent of snail specimens were infected with Digenea in the Kenyan part of Lake Victoria. The highest prevalence was recorded in *Melanoides tuberculata* (64.5%), followed

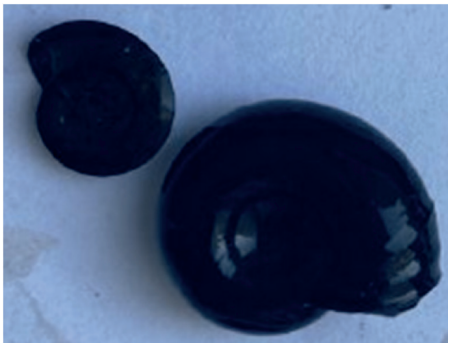

Fig. 2. ***Planorbis corneus***

Fig. 3. ***Lymnea stagnalis***

Fig. 4. *Radix auricularia*

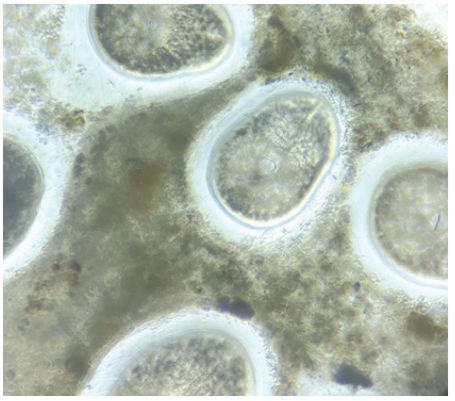

Fig. 5. Encysted metacercaria of several trematode species

by *Pila ovate* (15.4%), *Radix natalensis* (9.5%), *Bulinus ugandae* (9.1%), *Bellamya unicolor* (8.9%), *Biomphalaria pfeifferi* (7.3%), and *Biomphalaria sudanica* (4.4%) (Outa et al., 2020).

To the most frequently recorded species belong *Diplostomum spathaceum* (Rudolphi, 1819) (8% of the records), D. *pseudospathaceum Niewiadomska*, 1984 (6% of records), and *Echinoparyphium recurvatum* (von Linstow, 1873) (6% of the records) (Faltýnková et al., 2016).

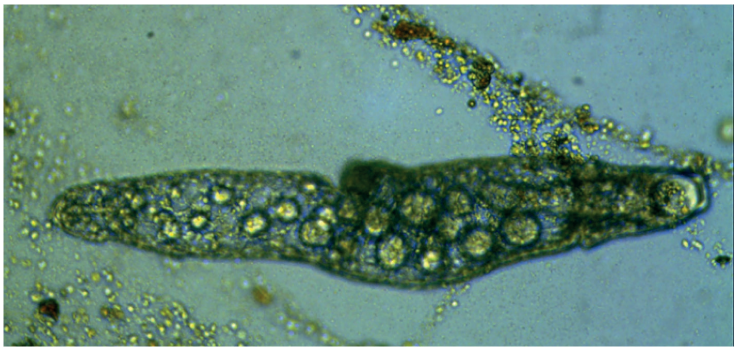

Fig. 6. Redia in hepatopancreas

Consequently, the results of the studies established the presence of larval stages of trematodes agents at different stages of the development, such as redia and metacercaria, which parasitize in the body of freshwater snails of water bodies of the Chornobyl Exclusion Zone.

Conclusions and future prospects

Studies have shown a significant infestation of snails of the species *Radix auricularia* by larval stages (metacercaria) of echinostamatid trematodes. Definitive hosts for these agents could be different species of waterfowl.

References

Iskova, N. I., Sharpilo, V. P., Sharpilo, V. D., & Tkach, V. V. (1995). Catalogue of helminths of vertebrates of Ukraine: Trematodes of terrestrial vertebrates. Kyiv: Naukova Dumka.

Semenko, O., Vishnevskiy, D., & Galat, M. (2020). The role of freshwater musclus of the Chernobyl zone of radioactive pollution in the dissemination of parasitic diseases. Scientific reports of NULES of Ukraine, 0(4(86)). doi: 10.31548/dopovidi2020.04.017

Stadnichenko, A. P. (1990). Lymnaeiformes (Physidae, Bulinidae, Planorbidae). Fauna of Ukraine; Vol. 29. Molluscs, 4.

Stadnichenko, A. P. (2006). Lymnaeidae and Acroloxidae of Ukraine: methods of sampling and studying, biology, ecology and practical importance. Zhytomyr: Ruta.

Kruglov, N. D. (2005). Lymnaeid snails of Europe and Northern Asia. Smolensk: Smolensk State Pedagogical University Press.

Rastyazhenko, N. M., Vodyanitskaya, S. N., & Yurlova, N. I. (2015). The emission of Plagiorchismultiglandulariscer cariae from naturally infected snails Lymnaea stagnalis in chany lake, south of West Siberia. Parazitologia, 49(3), 190-199.

Brandt, R. A. M. (1974). The non-marine aquatic Mollusca of Thailand. German: Waldeman Kramer.

Bray, R. A., Gibson, D. I., & Jones A. (Eds.). (2008). Keys to the Trematoda. Vol. 3. London: CABI Publishing Wallingford and Natural History Museum.

Brian, J. I., & Aldridge, D. C. (2020). An efficient photograph-based quantitative method for assessing castrating trematode parasites in bivalve molluscs. Parasitology, 147(12), 1375-1380. doi: 10.1017/S0031182020001213.

Chai, J. Y., Sohn, W. M., Na, B. K., & Nguyen, V. D. (2011). Echinostoma revolutum: metacercariae in Filopaludina snails from Nam Dinh Province, Vietnam, and adults from experimental hamsters. Korean Journal of Parasitology, 49(4), 449-455. doi: 10.3347/kjp.2011.49.4.449

Chantima, K., & Rika, C. (2020). Snail-borne zoonotic trematodes in edible viviparid snails obtained from wet markets in Northern Thailand. Journal of Helminthology, 1(94), e198. doi: 10.1017/S0022149X20000814

Chantima, K., Chai, J. Y., & Wongsawad, C. (2013). Echinostoma revolutum: freshwater snails as the second intermediate hosts in Chiang Mai, Thailand. Korean Journal of Parasitology, 51(2), 183-189. doi: 10.3347/kjp.2013.51.2.183

Chontananarth, T., & Wongsawad, C. (2013). Epidemiology of cercarial stage of trematodes in freshwater snails from Chiang Mai province, Thailand. Asian Pacific Journal of Tropical Biomedicine, 3(3), 237-43. doi: 10.1016/S2221-1691(13)60058-1

Curtis, L. A. (2002). Ecology of larval trematodes in three marine gastropods. Parasitology, 124 Suppl, 43-56. doi: 10.1017/s0031182002001452

Curtis, L. A. (2009). The gastropod Ilyanassa obsoleta as a resource: utilization by larval trematodes in a low-prevalence system.

Journal of Parasitology, 95(4), 799-807. doi: 10.1645/GE-1545.1

Dellagnola, F. A., Montes, M. M., Martorelli, S. R., & Vega, I. A. (2019). Morphological characterization and molecular phylogeny of zoonotic trematodes in the freshwater snail Asolene platae. Parasitology, 146(7), 839-848. doi: 10.1017/S0031182019000027

Faltýnková, A., & Haas, W. (2006). Larval trematodes in freshwater molluscs from the Elbe to Danube rivers (Southeast Germany): before and today. Parasitology Research, 99(5), 572-582. doi: 10.1007/s00436-006-0197-9

Faltýnková, A., Sures, B., & Kostadinova, A. (2016). Biodiversity of trematodes in their intermediate mollusc and fish hosts in the freshwater ecosystems of Europe. Systematic Parasitology, 93(3), 283-293. doi: 10.1007/s11230-016-9627-y

Fernández M.V., Hamann M.I., de Núñez M.O. (2016) New larval trematodes in Biomphalaria species (Planorbidae) from Northeastern Argentina. Acta parasitologica 61(3):471-92. https://doi.org/10.1515/ap-2016-0064

Poulin, R., Kamiya, T., & Lagrue, C. (2019). Evolution, phylogenetic distribution and functional ecology of division of labour in trematodes. Parasites and vectors, 12(1), 5. doi: 10.1186/s13071-018-3241-6

Fried, B. (1994). Metacercarial excystment of trematodes. Advances in Parasitology, 33, 91-144.

Galaktionov, K. V., & Dobrovolskyi, A. A. (2003). The main types of trematode life cycles. In: Fried B., Graczyk T.K. (eds) The Biology and Evolution of Trematodes. Springer, Dordrecht. doi: 10.1007/978-94-017-3247-5_3

Gilardoni, C., Di Giorgio, G., Bagnato, E., & Cremonte, F. (2019). Survey of trematodes in intertidal snails from Patagonia, Argentina: new larval forms and diversity assessment. Journal of Helminthology, 93(3), 342-351. doi: 10.1017/S0022149X18000329

Horák, P., Bulantová, J., & Mikeš, L. (2019). Schistosomatoidea and Diplostomoidea. Advances in Experimental Medicine and Biology, 1154, 217-254. doi: 10.1007/978-3-030-18616-6_8

Kołodziejczyk, L., Podraza, W., Gonet, B., Dzika, E., & Kosik-Bogacka, D. I. (2016). The Effect of an Extremely Low Frequency Magnetic Field on Larvae Production in the Parasite-Host System: Fasciola hepatica-Galba truncatula: a Preliminary Study. Folia Biologica (Krakow), 64(1), 55-58. doi: 10.3409/fb64_1.55

Kuris, A. M., Hechinger, R. F., Shaw, J. C., Whitney, K. L., Aguirre-Macedo, L., Boch, C. A., ... & Lafferty, K. D. (2008). Ecosystem energetic implications of parasite and free-living biomass in three estuaries. Nature, 454(7203), 515-518. doi: 10.1038/nature06970

Magalhães, L., Freitas, R., & de Montaudouin, X. (2015). Review: Bucephalus minimus, a deleterious trematode parasite of cockles Cerastoderma spp. Parasitology Research, 114(4), 1263-1278. doi: 10.1007/s00436-015-4374-6

Moema, E. B, King, P. H., & Rakgole, J. N. (2019). Phylogenetic studies of larval digenean trematodes from freshwater snails and fish species in the proximity of Tshwane metropolitan, South Africa. Onderstepoort Journal of Veterinary Research, 86(1), e1-e7. doi: 10.4102/ojvr.v86i1.1729

Moraes, J. D., Silva, M. P., Ohlweiler, F. P, & Kawano, T. (2009). Schistosoma mansoni and other larval trematodes in Biomphalaria tenagophila (Planorbidae) from Guarulhos, São Paulo State, Brazil. Revista do Instituto de Medicina Tropical de São Paulo, 51(2), 77-82. doi: 10.1590/s0036-46652009000200004

Morley, N. J., & Lewis, J. W. (2013). Thermodynamics of cercarial development and emergence in trematodes. Parasitology, 140(10), 1211-1224. doi: 10.1017/S0031182012001783

Mouritsen, K. N., & Elkjær, C. K. (2020). Cost

of interspecific competition between trematode colonies. Journal of Helminthology, 2(94), e139. doi: 10.1017/S0022149X20000243

Nguyen, P. T. X., Van Hoang, H., Dinh, H. T. K., Dorny, P., Losson, B., Bui, D. T., & Lempereur, L. (2021). Insights on foodborne zoonotic trematodes in freshwater snails in North and Central Vietnam. Parasitology Research, 120(3), 949-962. doi: 10.1007/s00436-020-07027-1.

Outa, J. O., Sattmann, H., Köhsler, M., Walochnik, J., & Jirsa, F. (2020). Diversity of digenean trematode larvae in snails from Lake Victoria, Kenya: First reports and bioindicative aspects. Acta Tropica, 206, 105437. doi: 10.1016/j.actatropica.2020.105437

Pantoja, C., Faltýnková, A., O'Dwyer, K., Jouet, D., Skírnisson, K., & Kudlai, O. (2021). Diversity of echinostomes (Digenea: Echinostomatidae) in their snail hosts at high latitudes. Parasite, 28, 59. doi: 10.1051/parasite/2021054. PMCID: PMC8336728

Paviotti-Fischer, E., Lopes-Torres, E. J., Santos, M. A. J., Brandolini, S. V. P. B, & Pinheiro, J. (2019). Xiphidiocercariae from naturally infected Lymnaea columella (Mollusca, Gastropoda) in urban area: morphology and ultrastructure of the larvae and histological changes in the mollusc host. Brazilian Journal of Biology, 79(3), 446-451. doi: 10.1590/1519-6984.182501

Poulin, R., Kamiya, T., & Lagrue, C. (2019). Evolution, phylogenetic distribution and functional ecology of division of labour in trematodes. Parasit Vectors, 12(1), 5. doi: 10.1186/s13071-018-3241-6

Schwelm, J., Kudlai, O., Smit, N. J., Selbach, C., & Sures, B. (2020). High parasite diversity in a neglected host: larval trematodes of Bithynia tentaculata in Central Europe. Journal of Helminthology, 94, e120. doi: 10.1017/S0022149X19001093

Selbach, C., Soldánová, M., Feld, C. K., Kostadinova, A., & Sures B. (2020). Hidden parasite diversity in a European freshwater system. Scientific Reports, 10(1), 2694. doi: 10.1038/ s41598-020-59548-5

Sohn, W., Yong, T., Eom, K. S., Sinuon, M., Jeoung, H., & Chai, J. Y. (2017). Artyfechinostomum malayanum: Metacercariae Encysted in Pila sp. Snails Purchased from Phnom Penh, Cambodia. The Korean Journal of Parasitology, 55, 341-345.

Sorensen, R. E., Curtis, J., & Minchella, D. J. (1998). Intraspecific variation in the rDNA its loci of 37-collar-spined echinostomes from North America: implications for sequence-based diagnoses and phylogenetics. Journal of Parasitolology, 84, 992-997.

Toledo, R., Radev, V., Kanev, I., Gardner, S. L., & Fried, B. (2014). History of echinostomes (Trematoda). Acta Parasitolologica, 59(4), 555-567. doi: 10.2478/s11686-014-0302-7

Ünlü, A. H., Bilgiç, H. B., Eren, H., & Karagenç, T. (2017). Prevalence of Larval-Stage Dicrocoeliidae (Digenea) Trematodes in Helix lucorum (Mollusca: Pulmonata) in Van Province. Türkiye Parazitoloji Dergisi, 41(4), 204-207. doi: 10.5152/tpd.2017.5444

Van den Broek, E., & de Jong, N. (1979). Studies on the life cycle of Asymphilodora tincae (Modeer, 1790) (Trematoda, Monorchidae) in a small lake near Amsterdam. Part 1. The morphology of various stages. Journal of Helminthology, 53, 79-89.

Wang, M. L., Chen, H. Y., & Shih, H. H. (2017). Occurrence and distribution of yellow grub trematodes (Clinostomum complanatum) infection in Taiwan. Parasitology Research, 116(6), 1761-1771. doi: 10.1007/s00436-017-5457-3

Wiroonpan, P., Chontananarth, T., & Purivirojkul, W. (2021). Cercarial trematodes in freshwater snails from Bangkok, Thailand: prevalence, morphological and molecular studies and human parasite perspective. Parasitology, 148(3), 366-383. doi: 10.1017/S0031182020002073.

Zbikowska, E., & Nowak, A. (2009). One hundred years of research on the natural infection of freshwater snails by trematode

larvae in Europe. Parasitology Research, 105(2), 301-311. doi: 10.1007/s00436-009-1462-5

Żbikowska, E., & Żbikowski, J. (2015). Digenean larvae – the cause and beneficiaries of the changes in host snails' thermal behavior. Parasitology Research, 114(3), 1063-1070. doi: 10.1007/s00436-014-4276-z

Zbikowski, J., & Zbikowska, E. (2009). Invaders of an invader – trematodes in Potamopyrgus antipodarum in Poland. Journal of Invertebrate Pathology, 101(1), 67-70. doi: 10.1016/j.jip.2009.02.005

Zhytova, E. P., & Kornyushin, V. V. (2017). The role of different mollusk species in maintaining the transmission of polyhostaltrematodes species in Ukrainian Polissya waters: the specificity of trematode parthenogenetic generations to mollusk hosts. Vestnik Zoologii, 51(4), 295-310.

Zhytova, E., Romanchuk, L., Guralska, S., Andreieva, O. Y., & Shvets, M. (2019). Circulation pathways of trematodes of freshwater gastropod mollusks in forest biocenoses of the Ukrainian Polissia. Vestnik Zoologii, 53, 13-22.

Сторожук В. І., Вишневський Д. О., Галат В. Ф., Семенко О. В., Галат М. В. (2021). ЛИЧИНКОВІ СТАДІЇ ТРЕМАТОД ПРІСНОВОДНИХ МОЛЮСКІВ ЧОРНОБИЛЬСЬКОЇ ЗОНИ РАДІОАКТИВНОГО ЗАБРУДНЕННЯ.

Ukrainian Journal of Veterinary Sciences, 12(4): 105–114, https://doi.org/10.31548/ujvs2021.04.008

Анотація. *В 1986 році на Чорнобильській атомній електростанції в зоні відчуження після аварії, екосистеми почали мати низку особливостей, що відрізняють їх від об'єктів природно-заповідного фонду. Інформативним індикатором стану екосистеми, який наразі спорадично застосовується в зоні відчуження, є паразитарні системи. До змін популяції паразита може призвести будь-яка зміна в популяції хазяїна. Ступінь дисбалансу системи «паразит-хазяїн» залежить від сили та характеру впливу зовнішніх факторів. У цей же час, наявність взаємних адаптацій паразитичних організмів і молюсків, дає підстави розглядати комплексно систему «паразит-хазяїн».*

Об'єктом дослідження було відібрано прісноводних черевоногих молюсків різних систематичних груп, які можуть бути проміжними та додатковими хазяями збудників трематодозів.

Для дослідження паразитичних стадій гельмінтів, прісноводних черевоногих молюсків було відібрано з таких водних об'єктів: озеро Красне, річка Ілля, Водойма-охолоджувач Чорнобильської АЕС, обвідний канал водойоми-охолоджувача Чорнобильської АЕС, лівий берег пойма Прип'яті, стариця Кошевка, Грубчанський канал с. Мешево.

За результатами проведених досліджень встановлено наявність личинкових стадій збудників трематодозів на різних стадіях їхнього розвитку (редія, метацеркарій), що паразитують в організмі прісноводних молюсків Lymnaea stagnalis і Radix auricularia.

Ключові слова: *прісноводні молюски, трематоди, личинкові стадії, Чорнобильська зона відчуження*

UDC 619:616–091:579.882:636 https://doi.org/10.31548/ujvs2021.04.009

PATHOHISTOLOGICAL CHANGES IN PIGS WITH MYCOPLASMOSIS

***V. N. B. KOLYCH*[1],**
Candidate of Veterinary Sciences, Associate Professor, Academician V. G. Kasyanenko Department of Anatomy, Histology and Pathomorphology
https://orcid.org/0000-0001-8024-0810
***N. V. HUDZ*[2],**
Candidate of Veterinary Sciences, Senior Researcher
https://orcid.org/0000-0002-2175-1431
E-mail: Natasha-vet@ukr.net
[1]National University of Life and Environmental Sciences of Ukraine, 15 Heroiv Oborony st., Kyiv 03041, Ukraine
[2]Institute of Veterinary Medicine of the National Academy of Agrarian Sciences of Ukraine, 30 Donetska st., Kyiv 03151, Ukraine

Abstract. *A pathological autopsy was performed on 6 corpses of piglets during the first week of their life who died from mycoplasmosis. Examination of the visible mucous membranes revealed hyperemia of the mucous membrane of the nasal cavity and thymus. Simultaneous lesions of the pharyngeal, parotid, cervical and mandibular lymph nodes were noted. They were slightly enlarged, from dark pink to dark red. The heart is irregularly shaped due to the expansion of the right ventricle or the diffuse expansion of all departments. Lungs have doughy consistency, uneven color. In some cases, there are diffuse red areas covering the entire lobe of the lungs, in other cases, there are lesions of small areas. The liver has a smooth surface, soft or pasty consistency, the parenchyma pattern is slightly smoothed in section. The color of the liver is different: dark red areas without clear boundaries turn into creamy-clay. A characteristic feature was flatulence of the stomach and intestines. Catarrhal enteritis was registered in animals, which manifested itself in the form of moderate hyperemia of the intestinal mucosa and serous membranes.*

Microscopically, there is a significant blood supply to the vessels in the lungs. Alveoli are half fall down, in the form of slit-like lumens. In areas of tissue infiltration by inflammatory infiltrate, the alveolar wall is thickened, alveolocytes are in a state of turbid swelling and vacuolar dystrophy, they are impregnated with erythrocytes. Peribronchial pneumonia of lymphocytic character is observed. The liver is in a state of acute venous hyperemia. The central and intraparticle capillaries are sharply dilated and filled with blood in some lobes, and the hepatic beams are compressed accordingly. In the center of other lobes, diffuse infiltration of liver tissue by erythrocytes as a consequence of diapedesis is noted. Hepatocytes are in a state of granular dystrophy. Destructive changes are strongly expressed in the mucous membrane of the small intestine: desquamation of the epithelium, necrosis of epitheliocytes and villi, destruction of crypts. In the brain tissue, there is dilation of the lumens of large and small blood vessels, extracellular and perivascular edema, areas of reactive necrosis.

Keywords: *mycoplasmosis, pathomorphological changes, pigs, lungs, pneumonia*

Introduction

Mycoplasma infection in pigs is widespread in countries with developed pig farming and is one of the reasons for economic losses in meat production. Losses from the disease include treatment costs, decrease in production indicators in piglets for rearing and fattening, lower market cost of carcasses for sale. The introduction of pathogenic mycoplasmas into farms never reporting the disease occurs mainly with infected livestock and semen under violation of quarantine measures and requirements for supplier farms (Rusalesv et al., 2006; Arsenakis et al., 2016).

Analysis of recent researches and publications

Enzootic pneumonia of pigs (mycoplasma pneumonia, respiratory mycoplasmosis, mycoplasmosis of pigs (pneumonia enzootica suum)) is a chronic infectious disease characterized by inflammation of the lungs, serous membranes, and impaired reproductive function of sows.

In 1957, Whittlestone (England), and then Goodwin et al. (1965) showed that the causative agent of porcine enzootic pneumonia, which was previously described as flu, influenza, or viral pneumonia, are microorganisms of the Mycoplasmataceae family. The etiological role of mycoplasmas in porcine enzootic pneumonia was later proved by many researchers.

Most of the mycoplasmas that infect animals are superficial, so-called "membrane parasites", which are firmly attached to the epithelial membranes of the respiratory and urogenital tract. Mycoplasmas have no cell wall. They cannot synthesize peptidoglycan precursors (muramic and diaminopimelic acids) and are bounded only by a thin three-layer membrane. They were allocated to a special division Tenericutes, the Mollicutes class (mollis – soft, tender; cutis – "delicate skin"), the order Mycoplasmatales. The last one includes several families, particularly Mycoplasmataceae, which are pathogenic mycoplasmas, opportunistic (asymptomatic carriers of which are often cell cultures) and Saprophytic Mycoplasma (Ferrarini et al., 2016; Frey et al., 2016; Liu et al., 2016; Xiong et al., 2016).

Piglets can get infected in the womb either by direct contact or by aerosol (vertical transmission) (Calsamiglia & Pijoan, 2000; Vicca et al., 2002).

In modern pig breeding, porcine enzootic pneumonia does not have a pronounced seasonality – the disease occurs any time of the year.

The manifestation of mycoplasma infections is usually associated with a violation of the symbiotic system due to the massive interaction of endo- and exogenous (including environmental) factors.

Mycoplasma infections are a kind of indicator of stress in animal. The severity of the course depends on the general health of pigs, the presence of helminths, as well as on the conditions of animal keeping. In farms where animals are kept in poorly ventilated cold rooms and have an unbalanced diet with an insignificant content of the necessary vitamins and minerals, the incidence of diseases in the livestock can reach 40–85%, moreover, the difference in conditions of keeping can reach about 15%. The disease may not show clinical signs, while the productivity of sick pigs is reduced by about 20% (Samuylenko et al., 2006; Giacomini et al., 2016; Kolych, 2016).

Materials and methods of research

The research was carried out at a private enterprise for pigs raising and fattening in the Poltava region. The material for the study was the pathological material taken during the pathological necropsy of the carcasses of dead piglets (n = 6) at the age of 7 days, in which the causative agent of mycoplasmosis was diagnosed and identified during life by laboratory methods.

The main method used in the study was a histological examination, during which microstructural changes in organs and tissues were recorded and described. After sampling, the pathological material was fixed in a 10% aqueous solution of neutral formalin, followed by embedding in paraffin. The prepared histological sections were stained with hematoxylin and eosin according to standard prescriptions (Goralskyi et al., 2011).

The general histological structure and microstructural changes in histological sections were studied under a light microscope (MC 100LED, Micros Austria).

Results of the research and their discussion

In several cases, the corpses of piglets of the first week of life had a cyanotic coloration of the dewlap, limbs, ears, which we associate with cardiac disorders in animals shortly before death.

Examination of visible mucous membranes revealed hyperemia of the nasal mucosa, thymus, anemic mucous membranes of the trachea, esophagus, and pharynx.

The heart had an irregular shape due to enlargement of the right ventricle or diffuse enlargements of all parts. In some animals, hemorrhages were observed in the pericardium along large vessels, which were filled with blood significantly. In some cases, the epicardium had an unevenly gray-pink color, moderately wet, in others, it was diffusely clay color, anemic. The myocardium was flabby, clay-colored.

Simultaneous damage of the pharyngeal lymph nodes, parotid and cervical, mandibular ones (slightly enlarged, from dark pink to dull red color). The lymph nodes of the chest cavity acquired pronounced or indistinct pronounced tuberosity of the surface, uneven color (pink, cyanotic, dark red areas, the cut surface was significantly wet, scrape was not available).

Insignificant enlargement in the lymph nodes of the middle and posterior parts of the digestive tract (abdominal lymphatic center: gastric, pancreatic-duodenal; cranial mesenteric lymphatic center: jejunal, ileocolic; lymph nodes of the caudal mesenteric lymphatic center). Lymph nodes are pale pink with light red areas, in some animals, there was significant enlargement, intense red color (Fig. 1).

In young boars, changes in the lymph nodes of the iliofemoral and inguinal-femoral lymphatic centers were observed, especially there was a significant enlargement in the superficial inguinal lymph nodes, which were lumpy, dense, had irregular red-brown or red-pink color.

The lungs had doughy consistency, uneven color. In some cases, there were diffuse red areas covering the entire lobules of the lungs, in other cases, small areas were affected. A large amount of blood was released from the vessels on the cut surface and a frothy liquid was registered in the alveoli. In some areas, crepitus foci were recorded. A mucous mass was released from the bronchi.

Fig. 1. Hyperemia and enlargement of the mandibular lymph nodes

The spleen had a regular, elongated-oval shape, pink with a bluish tinge of color. The cranial edge of the organ was often much wider than the caudal one, dark red hemorrhages were traced in parenchyma thickness. In some cases, hemorrhages in the form of black small cells were located along the edge of the organ.

Different levels of flatulence severity of stomach and intestines were characteristic. The animals' stomach was filled moderately, contained milk clots, the mucous membrane was moderately hyperemic. Catarrhal enteritis was registered in animals manifested as moderate hyperemia of the mucous and serous membranes of the intestine, accumulation of the insignificant amount of cloudy gray mucus on the inner lining of the intestine.

Uneven color of the liver occurs in piglets: dark red areas without clear boundaries changed into creamy clay ones.

The liver had a smooth surface, soft or doughy consistency, parenchyma pattern on the cut surface was smoothed insignificantly. In areas of dark red color on the cut surface, a large amount of dark red blood was released when pressed.

The organ contained small single striped or punctate hemorrhages. Small gray-white cells were registered under the liver capsule, which are barely visible against the general background of the organ. the gallbladder was enlarged by 2–3 times in up to 50% of cases, bile was yellow and had liquid consistency.

In the majority of the studied cases of piglet death, uneven color of the kidneys was observed, indistinctly delineated diffuse rounded areas of darker (up to bluish-red) or, conversely, lighter (up to creamy-pink) color were observed. The capsule was transparent and removed easily. The renal cortex was clay-colored, the renal medulla varied from pink to dark red color (due to hyperemia of the renal medulla). The cut surface was

smooth, the parenchyma was significantly wet.

In the reproductive system of females, changes were not expressed at the macroscopic level. The vaginal tunic of the testes of aborted male fetuses was translucent and insignificantly thickened. Vessels in the thickness of the tunic were full-blooded with small punctate hemorrhages. Testes had a bluish tint due to full-blooded vessels.

The brain had milky color, often with a pale pink tinge, blood vessels were filled with blood.

In the lungs, on the histological level, both large and small vessels were full-blooded significantly. In large areas, the alveoli were semicollapsed, in the form of slit-like gaps. In areas of the tissue infiltrated with inflammatory infiltrate, the alveolar wall was thickened, the alveoli were semicollapsed, alveolocytes were in a state of cloudy swelling and vacuolar dystrophy, they were saturated with erythrocytes (Fig. 2).

Peribronchial pneumonia of a lymphocytic nature was noted. The walls of blood vessels were in a state of mucoid swelling, hydropic degeneration of endothelial cells, and perivascular edema was also observed.

Thickening of the interlobular connective tissue fibers was noted. There were registered areas, in which the lumens of the alveoli were enlarged and contain a homogeneous pale pink mass in the field of view.

In small bronchi and alveoli, there were a large number of lymphocytes, single leukocytes, a significant part of which were in a state of decay and necrosis. Among these cells, there were desquamated (destroyed) cells of the epithelium of the bronchi and erythrocytes. Connective tissue and the wall of the bronchi were infiltrated with lymphocytes and monocytes. Alveoli with elongated lumens and thinned walls often with cystic formations can be noted along the periphery of such areas. There

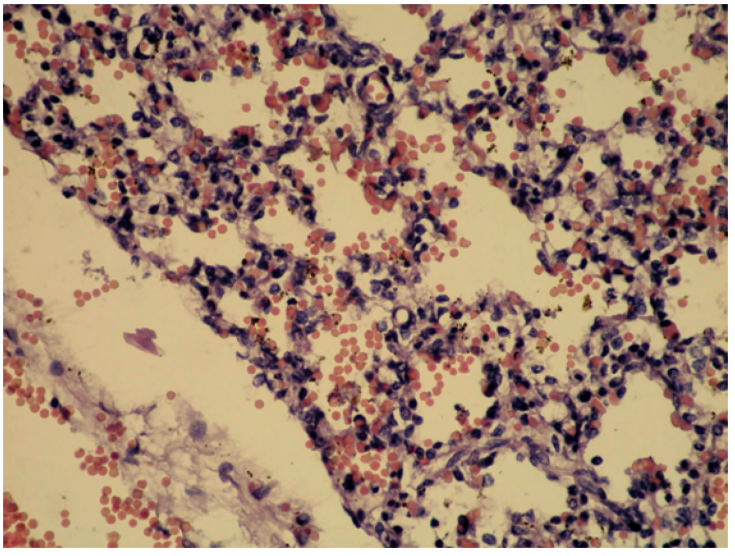

Fig. 2. Thickened walls of alveolocytes and their infiltration with erythrocytes

were single hemorrhages in the alveoli and stroma of the organ.

The heart. Cardiomyocytes were in a state of cloudy swelling, thickened, the contours of the nuclei were not clear, sometimes did not register at all. The cytoplasm was not transparent, pink-colored. The vessels were filled with blood, their walls were thickened and also in a state of mucoid swelling (Fig. 3).

The pancreas. The histoarchitecture of the pancreas was preserved, the blood vessels had moderate blood filling, the lumens contained concentrated eosinophilic secretions, and the pancreocytes were mostly without visible changes. In some areas (with clear edema) parenchyma was with signs of necrosis. Destruction of the glands occurred, and shapeless mass was observed in the field of view, in which fragments of cells can be noticed.

In the spleen, there was a thickening of the capsule, trabeculae, and the walls of the blood vessels of the white and red pulp, also insignificant fiber dissociation was observed as well as increased volume of the cells' nuclei of connective tissue, but blood vessels were average blood-filled. Severe edema of the reticular tissue was registered. Lymph nodules were paler than normal, lack of leukocytes, single small foci of necrosis were visible in the field of view. In some areas, the structure of the trabecula fibers was not clear, there was thickening and homogenization of the intima of the blood vessels and narrowing of their lumen. In some areas of the organ, in areas with edema, foci of unreactive necrosis, which did not have clear contours, were recorded.

In the thymus of piglets, vessels were blood-filled, pronounced perivascular edema of the tissue was observed. In the cortical zone of the thymus lobule, conglomerates of destroyed lymphocytes were formed, acquiring basophilic properties; scattered single erythrocytes were also observed between thymocytes. In the medulla of the thymus lobules, lymphocytes in most animals were scattered, the nuclei of individual lymphocytes were in a state of karyorrhexis,

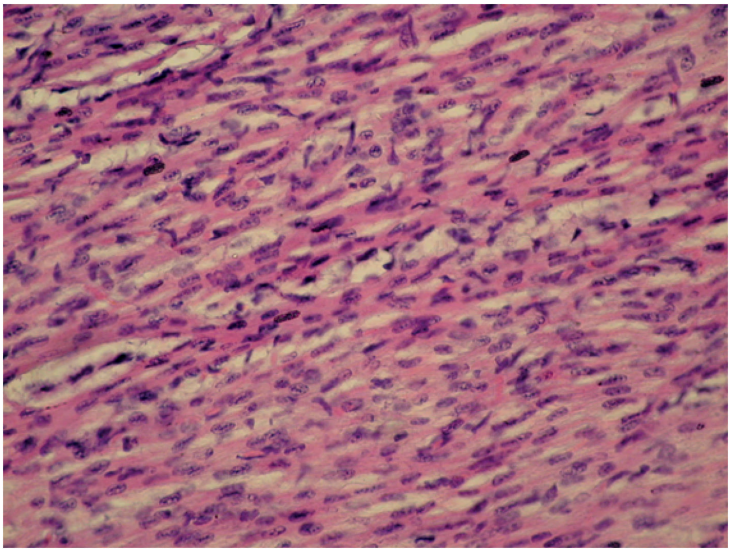

Fig. 3. Histological slide of the myocardium of a 3-days-old piglet with signs of protein myocardosis. Staining with hematoxylin and eosin, ×200

and some of the nuclei had an irregular shape. There were a large number of eosinophils between thymocytes.

In addition, pink-red colored cells were observed in significant areas, while the contours of such cells were barely traced and nuclei were not expressed.

Lymph nodes (mesenteric) contained focal hemorrhages, hyperemia of blood vessels, mucoid and fibrinoid swelling and single areas of necrosis of their walls were revealed. The lymph nodes of the abdominal cavity contained small areas of necrosis and stromal proliferation.

In the lymph nodes (chest cavity), there were hyperemia, serous edema of the sinuses and parenchyma, increase of lymph nodules' size, but the lymphocytes in them were sparsely located, also accumulation of plasmacytes, macrophages, and lymphocytes in the cortex and medulla were observed.

The liver was in a state of acute venous hyperemia. At a low magnification of the microscope, in some lobules, pronouncedly enlarged and blood-filled central and intralobular capillaries were found, and the hepatic plates were respectively compressed. In the center of other lobules, there was a diffuse infiltration of liver tissue with erythrocytes, as a result of diapedesis. In such places, protein and fatty degeneration were observed in hepatocytes. There were often areas with hepatocytes in a state of decomposition (phanerosis). At the same time, the cells had a reticular structure, larger than normal nuclei were located in the center but in many cases, they were destroyed (fatty decomposition).

In some areas, there were foci where the cytoplasm of hepatocytes contained large vacuoles, the nucleus was displaced to the periphery – ring-shaped cells (fatty infiltration). Fatty infiltration occurred much less frequently than decomposition.

There were often areas of tissue in a state of paranecrosis in the field of view: foci in which histological structure of the organ was barely noticed, also fragments of nuclei, swelling of individual nuclei, contours of individual cells could be detected. Small blood vessels were filled with blood, erythrocytes were registered between the plates.

At the periphery of the lobule, the structure of the cells remains normal. The plates structure of hepatocytes was damaged, which had the form of conglomerates without clear boundaries that merged. Up to 40% of parenchyma cells did not contain nuclei. In all other cases, the nuclei did not have clear contours. They had increased volume, up to 10% of them were in a state of lysis. Hepatocytes were in a state of granular dystrophy, in their cytoplasm a large number of grains of protein nature were registered. The interlobular connected tissue is poorly noticed. In some cases, significant swelling of the intralobular connective tissue was observed. Fatty extracellular degeneration was also registered (fatty vacuoles were located in the interlobular connective tissue). There were single hepatocytes with signs of fatty infiltration. Fat in such cells in the form of one large drop pushed the nucleus and cytoplasm to the periphery, so the liver cells looked like typical fat cells (ring-shaped cells). Such cells were increased in their volume (Fig. 4).

In some areas, hepatic lobules had different sizes, interlobular connective tissue was infiltrated with lymphoid, plasma cells, and fibroblasts. Around the central veins of the hepatic lobules plate structure of the parenchyma was not registered, single hepatocytes with signs of dystrophy and necrosis were observed, the vessels contain a small number of erythrocytes.

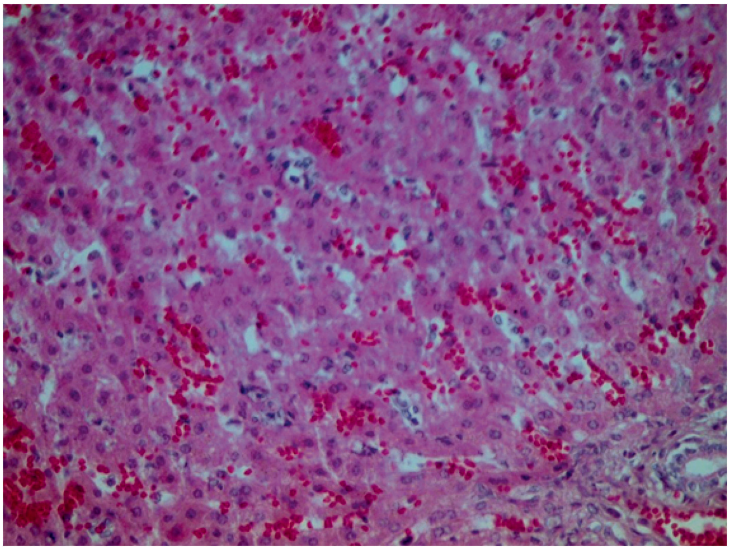

Fig. 4. The liver of a 2-days-old piglet: blood-filled sinusoids and granular degeneration of hepatocytes. Staining with hematoxylin and eosin; ×200

The wall of the stomach and small intestine. Destructive changes were strongly expressed in the mucosa (desquamation of the epithelium, necrosis of epithelial cells and villi) that resulted in the partial absence of epithelial cover, the crypts were half-destroyed.

On the surface of the mucous membrane, a pale pink mass (mucus containing proteins) with an admixture of desquamated epithelial cells, a small number of polymorphonuclear leukocytes, and single erythrocytes. In large areas, the destruction of the villi up to crypts was observed. The submucosa was thickened, the blood vessels were filled with blood, moderate infiltration of the connective tissue by cells of the inflammatory infiltrate was registered – mainly lymphocytes and macrophages, which were most pronounced in the tissue around the blood vessels, where small (diapedesis) hemorrhages were also visible.

In the kidneys, there was a lesion of the parenchyma (straight and convoluted tubules), blood-filled of the renal medulla vessels. Epithelium of the convoluted tubules in some areas was in a state of hydropic dystrophy, the cells were enlarged, rounded, protrude into the lumen of the tubules, often desquamated, the nucleus and cytoplasm were dissolved, only the cell membranes were visible. The structure of epithelial cells was absent in some areas. In cell cytoplasm, fine acidophilic granularity was noticed. Some cells had foamy cytoplasm, some others were separated from the basal membrane and each other. Desquamated cells were registered in the lumen of the tubules.

In addition, a large number of areas were recorded with epithelial cells of the tubules (mainly convoluted ones) increased in the volume containing a different number of small pink grains. Boundaries of tubules' epithelial cells were not clearly visible; lumens of the vessels were narrowed with different diameters due to the cells increased volume. In some tu-

bules, lumens were well noticed, in others – they looked like gaps, or were not visible at all. The cytoplasm was cloudy, dull, the nuclei were barely visible. In the most affected cells nuclei were in a state of karyolysis or not registered at all. In the general background, areas with complete blockage of the tubule's lumens by the protein were well noticed.

In some areas around the vessels, glomeruli, and between the tubules, there was an accumulation of a significant amount of proliferating tissue (lymphoid, epithelioid cells, and histiocytes). Between the tubules there were cells that looked like a coarse-grained deep mass of dark red color, in which fragments of epithelial cells were registered with nuclei forming pale blue homogeneous spheres.

In the cortical layer, blood-filled vessels of the capillary network of the glomeruli were observed. Glomeruli were increased in volume and occupied the entire lumen of the Bowman's capsule. There were up to 40% of such glomeruli. Twenty % of the Bowman's capsule in the glomeruli contained serous exudate. There were also single glomeruli with the destroyed walls. In these cases, there was bleeding into the lumen of the capsule.

The blood-filled vessels of the medulla were clearly visible. In most cases, up to 60–70%, the lumens of the straight tubules were not registered due to increased volume of epithelial cells, which were in a state of hydropic dystrophy. Their cytoplasm was vacuolated; in some cases, the cell nuclei were in a state of lysis. One large vacuole occupied almost the entire cell, and the nucleus and the remnants of the cytoplasm were pushed out to the periphery and compressed. The cells looked like a balloon. Up to 40% of the tubules had dilated spherical lumen.

The testicles contained punctate diffuse hemorrhages. The parenchyma looked like a single-layer spermatogenic epithelium (Fig. 5).

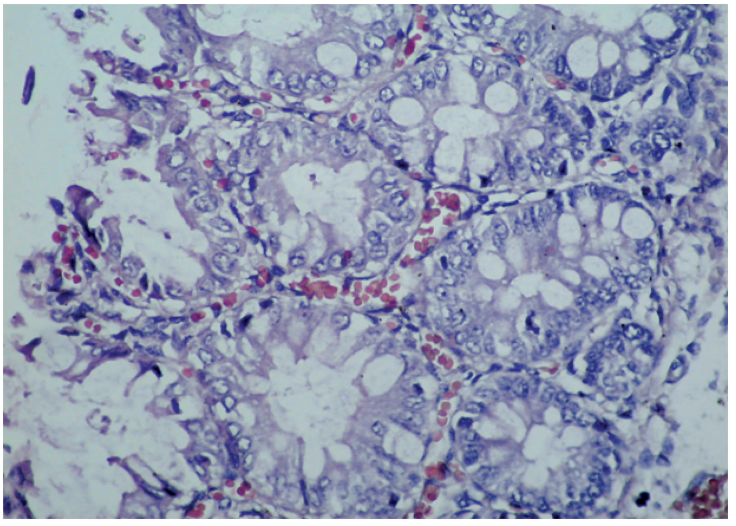

Fig. 5. Histological section of testes of a 5 days-old piglet: blood-filled vessels, hydropic dystrophy and epithelial necrosis. Staining with hematoxylin and eosin; ×400

Distention of the lumens of large and small blood vessels was registered in brain tissue, a "sludge" phenomenon in individual vessels. Around the blood vessels of neurons, there were clearing zones (extracellular and perivascular edema), areas of paranecrosis, and unreactive necrosis (Fig. 6).

In the spinal cord, individual neurons were increased in volume, cytoplasm opacity and its intense pink color, nucleus enlarged in size that did not have clear contours. Individual neurons were in a state of decay (both the cell and the nucleus had an irregular shape, the nucleus was shrunken, colored intensely blue-violet, and in other cases, it was enlarged, with no clear boundaries, smoky colored). The blood vessels contained a large number of erythrocytes as a homogeneous mass.

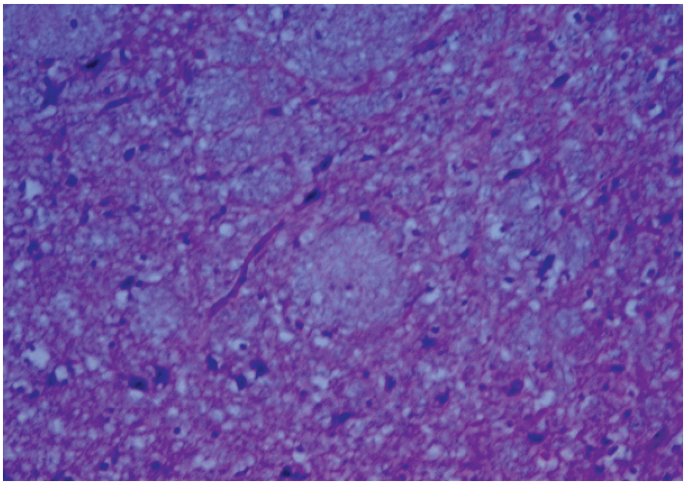

Fig. 6. Brain tissue of a piglet of the first week of life: blood-filled capillaries and extracellular edema. Staining with hematoxylin and eosin; ×100

Conclusions and future prospects

Mycoplasmosis in piglets under 7 days of age is characterized by hyperemia of the upper respiratory tract and exudative bronchopneumonia. Damage of the digestive tract manifested as catarrhal and serous-catarrhal gastroenteritis.

A histological study found that in the piglets with mycoplasmosis, there was a violation of the general protein metabolism, which manifested by granular degeneration of the liver, heart muscle, and kidneys.

There was unreactive necrosis of the parenchyma of the liver, kidneys, pancreas, and brain, necrosis of the intestinal villi up to the crypt cells.

In the organs of immunopoiesis (thymus, spleen), edema, areas of unreactive necrosis, and mucoid swelling of stromal elements were registered.

The study of the mycoplasma pneumonia issue in pigs indicates the need for further continuous monitoring in pig farms in Ukraine. Correct and timely diagnostics is important in the control of the disease; therefore, it is imperative to learn modern and develop new methods for studying mycoplasmosis.

References

Arsenakis, I., Panzavolta, L., Michiels, A., Sacristán, R. D. P., Boyen, F., Haesebrouck, F., & Maes, D. (2016). Efficacy of Mycoplasma hyopneumoniae vaccination before and at weaning against experimental challenge infection in pigs. BMC veterinary research, 12(1), 1-7. doi: 10.1186/s12917-016-0685-9.

Samuylenko, A. Y., Solovyeva, B. V. Nepoklonova, Y. A., & Voronina, Y. S. (2006). Infeccionnaya patologiya zhivotnih [Infectious paphology of animals]. Moscow: Akademkniga.

Garcia-Morante, B., Segalés, J., López-Soria, S., De Rozas, A. P., Maiti, H., Coll, T., & Sibila, M. (2016). Induction of mycoplasmal pneumonia in experimentally infected pigs by means of different inoculation routes. Veterinary Research, 47(1), 1-10. doi: 10.1186/s13567-016-0340-2.

Giacomini, E., Ferrari, N., Pitozzi, A., Remistani, M., Giardiello, D., Maes, D., & Alborali, G. L. (2016). Dynamics of Mycoplasma hyopneumoniae seroconversion and infection in pigs in the three main production systems. Veterinary research communications, 40(2), 81-88. doi: 10.1007/s11259-016-9657-6. Epub 2016 May 4.

Goralskyi, L. P., Khomych, V. T., & Kononskyi, O. I. (2011). Osnovy histologichnoyi tehniky i morfofunkcionalni metody doslidjen u normi ta pry patologiyi [Foundations of histological engineering and morphofunctional methods of research in norm and pathology]. Zhytomyr: Polissia.

Goodwin, R. F., Pomeroy, A. P., & Whittlestone, P. (1965). Production of enzootic pneumonia in pigs with a mycoplasma. Veterinary Record, 77, 1247-1249.

Grechuhin, A. N. (2002). Diagnostica micoplasmoznoy pnevmonii sviney [Diagnostic of mycoplasmas swine pneumonia]. Veterynarnaia Practica, 1, 10-15.

Kolych, N. B. (2016). Features of pathological changes in the associative flow of mycoplasmosis. Scientific Messenger of LNU of Veterinary Medicine and Biotechnologies. Series: Veterinary Sciences, 18(3(70), 146-149. doi: 10.15421/nvlvet7034

Liu, M., Du, G., Zhang, Y., Wu, Y., Wang, H., Li, B., ... & Shao, G. (2016). Development of a blocking ELISA for detection of Mycoplasma hyopneumoniae infection based on a monoclonal antibody against protein P65. Journal of Veterinary Medical Science, 15-0438.

Marchioro, S. B, Simionatto, S., & Dellagostin O. (2016). Development of Mycoplasma hyopneumoniae Recombinant Vaccines. Methods in Molecular Biology, 1404, 39-50. doi: 10.1007/978-1-4939-3389-1_2.

Pantoja, L. G., Pettit, K., Dos Santos, L. F., Tubbs, R., & Pieters, M. (2016). Mycoplasma hyopneumoniae genetic variability within a swine operation. Journal of Veterinary Diagnostic Investigation, 28(2), 175-179. doi: 10.1177/1040638716630767

Rusalesv, V. S., Gnevashev, V. M., & Pruntovaya, O. V. (2006). Problemy profilaktiki respiratornyh boleznej svinej bakterial'noj etiologii. Veterinariya, 7, 18-20.

Ferrarini, M. G., Siqueira, F. M., Mucha, S. G., Palama, T. L., Jobard, É., Elena-Herrmann, B., ... & Sagot, M. F. (2016). Insights on the virulence of swine respiratory tract mycoplasmas through genome-scale metabolic modeling. BMC genomics, 17(1), 1-20. doi: 10.1186/s12864-016-2644-z.

Frey, J., Haldmann, A., Kobisch, M., & Nicolet, J. (1994). Immune response against the lactate degidrogenase of Mycoplasma hyopneumonia in enzootic pneumonia swine. Microbial Pathogenesis, 17, 313-322.

Xiong, Q., Wang, J., Ji, Y., Ni, B., Zhang, B., Ma, Q., ... & Shao, G. (2016). The functions of the variable lipoprotein family of Mycoplasma hyorhinis in adherence to host cells. Veterinary microbiology, 186, 82-89. doi: 10.1016/j.vetmic.2016.

Колич Н. Б. , Гудзь Н. В. (2021). ПАТОГІСТОЛОГІЧНІ ЗМІНИ У СВИНЕЙ ПРИ МІКОПЛАЗМОЗІ. *Ukrainian Journal of Veterinary Sciences, 12(4): 115–126, https://doi.org/10.31548/ujvs2021.04.009*

Анотація. *Проведено патологоанатомічний розтин 6 трупів поросят першого тижня життя, які загинули від мікоплазмозу. Під час дослідження видимих слизових оболонок встановлено гіперемію слизової оболонки носової порожнини й тимуса. Відмічали одночасне ураження заглоткових, привушних, шийних і нижньощелепних лімфатичних вузлів. Вони були незначно збільшені, від темно-рожевого до темно-червоного кольору. Серце неправильної форми внаслідок розширення правого шлуночка або дифузного розширення всіх відділів. Легені тістуватої консистенції, нерівномірного забарвлення. В одних випадках спостерігаються дифузні червоні ділянки, що охоплюють цілі долі легень, в інших випадках відбувається ураження невеликих ділянок. Печінка має гладку поверхню, м'якої чи тістуватої консистенції, на розрізі малюнок паренхіми дещо згладжений. Забарвлення печінки різне: темно-червоні ділянки, без чітких меж переходять у кремово-глинисті. Характерною ознакою був метеоризм шлунку та кишечнику. У тварин зареєстровано катаральний ентерит, який проявлявся у вигляді помірно вираженої гіперемії слизової та серозної оболонок кишечника.*

На мікроскопічному рівні в легенях спостерігається значне кровонаповнення судин. Альвеоли напівспалі, у вигляді щілеподібних просвітів. У ділянках інфільтрації тканини запальним інфільтратом стінка альвеол потовщена, альвеоцити були в стані мутного набухання та вакуольної дистрофії, вони просочені еритроцитами. Спостерігається перибронхіальна пневмонія лімфоцитарного характеру. Печінка була в стані гострої венозної гіперемії. В одних часточках знаходять різко розширені й заповнені кров'ю центральні і внутрішньочасточкові капіляри, а печінкові балки відповідно стиснуті. В інших часточках у центрі відмічається дифузна інфільтрація тканини печінки еритроцитами, як наслідок діапедезу. Гепатоцити були в стані зернистої дистрофії. У слизовій оболонці тонкого кишечника сильно виражені деструктивні зміни: десквамація епітелію, некроз епітеліоцитів та ворсинок, руйнування крипт. У тканині головного мозку спостерігається розширення просвітів великих і дрібних кровоносних судин, екстрацелюлярний та периваскулярний набряк, ділянки ареактивного некрозу.

Ключові слова: *мікоплазмоз, патоморфологічні зміни, свині, легені, пневмонія*

UDC 602.9 : 591.81 :[636.92.09 : 612.12 : 616.74-001.4] https://doi.org/10.31548/ujvs2021.04.010

SERUM CREATINE PHOSPHOKINASE ACTIVITY IN RABBITS DURING REGENERATION OF EXPERIMENTALLY DAMAGED MUSCLE TISSUE AND AFTER ITS STIMULATION BY TRANSPLANTED MSC

N. V. STADNYK,
Graduate Student, Department of Surgery and Pathophysiology named after Academician I. O. Povazhenko
https://orcid.org/ 0000-0002-8732-490X
E-mail: stadnyk7288@gmail.com
R. R. BOKOTKO,
Candidate of Veterinary Sciences, Department of Surgery and Pathophysiology named after Academician I. O. Povazhenko
https://orcid.org/0000-0002-6217-5266
E-mail: bokotko28@gmail.com
T. L. SAVCHUK,
Candidate of Veterinary Sciences, Department of Surgery and Pathophysiology named after Academician I. O. Povazhenko
https://orcid.org/0000-0002-8732-490X
M. A. KULIDA,
Candidate of Veterinary Sciences, Associate Professor, Department of Surgery and Pathophysiology named after Academician I. O. Povazhenko
https://orcid.org/0000-0001-8937-1972
E-mail: mkulida@ukr.net
A. Y. MAZURKEVYCH,
Doctor of Veterinary Sciences, Professor, Department of Surgery and Pathophysiology named after Academician I. O. Povazhenko
https://orcid.org/0000-0003-3573-6600
E-mail: a.Mazurkevych@nubip.edu.ua
National University of Life and Environmental Sciences of Ukraine, 15 Heroiv Oborony st., Kyiv 03041, Ukraine

Abstract. *According to statistics, in modern veterinary practice, the percentage of muscle injuries among sport and working animals ranges from 40–70% of sports injuries. Quite often there are cases with muscle injuries of skeletal muscles, namely extremities. This scientific work describes the research methodology, stages of research step-by-step, and studies the relationship of dynamics of the activity of a single biochemical blood*

indicator. The essence of the method was to model the injury of muscle tissue performed by the skin and fascia dissection and cutting off in the area of the midplane of the pelvic head of the biceps femoris muscle, measuring 1.5×1.5 cm to a depth of 1.5 cm of muscle tissue in 105 laboratory animals, divided into 4 groups with the use of various treatment methods. We analyze the results of one of the most effective biochemical methods for diagnosing damage of muscle fibers in the skeletal system and compare the activity of the creatine phosphokinase iso-enzyme depending on the stage of the study. Other research methods such as clinical, biochemical, ultrasonographic, and histological were recorded on 4, 7, 10, 14, 21, and 28 days. We analyzed the latest literature sources and concluded that on the 4th and 7th days, the level of creatine phosphokinase in the groups with intravenous and intramuscular administration of allogeneic mesenchymal stem cells is higher than the reference values but significantly lower compared to the control groups and the traditional method of treatment. But we observe a significant decrease in serum creatine phosphokinase levels 2 times in rabbits on the 10th day in the intravenous administration group compared with the control group of animals and in 1.6 times compared with traditional treatment. The group of animals with intramuscular administration has reference values on the 14th day, compared with the control in 1.3 times lower, traditional treatment in 1.2 times. And on the 21st day, we get reference values for a group of animals with traditional treatment. The level of creatine phosphokinase activity decreases in the control group of animals on the 28th day of the research, which indicates a complete muscle rupture. The results of studies showed that the highest activity of the creatine phosphokinase enzyme during the study was shown by groups of animals with control and traditional treatment, which indicated significant structural, functional, and destructive disorders of the muscle fibers of skeletal tissues with severe trauma. Thus, it is noted that the activity of the enzyme in conditions of damage of skeletal muscle tends to increase in accordance with the severity of the injury.

Keywords: *allogenic mesenchymal stem cells, muscle tissue regeneration, laboratory animals, activity, isoform*

Introduction

In recent years, such sports as equestrian sports have become very popular among animals. Among dog sports: agility, weight pulling, dog sled racing, dog frisbee, dog races among Greyhound breeds of dogs, and cynological training (IGP international service dog testing system, mondioring), and other training of service dogs. The relevance of this topic lies in the fact that in modern veterinary practice, muscle injuries are quite common among sports animals, namely ruptures, damage of the skeletal muscle tissue of the extremities. Therefore, the study, analysis, and effectiveness of treatment of animals with damaged muscle tissue using cellular regenerative therapy methods are very relevant, since it can significantly speed up the recovery time of animals after injury compared to traditional methods of injury treatment.

Analysis of recent researches and publications

Motion activity of animals is a coordinated contraction of skeletal muscles, which is accompanied by a change in the position of the body in space.

It is commonly known that the motion activity of a living organism is provided by the organs of the motor system. The central nervous system is responsible for body movement coordination, and the movements themselves are performed by muscles with the help of skeletal bones, their connections (joints, as well as the immobile and arthrodial connection of bones) (Mazurkevych et al., 2013; Mazurkevych et al., 2015). Muscles account for about 40–45% of the animal's body weight (Fabri et al., 2014).

Cell therapy using mesenchymal stromal cells (MSCs) is a promising approach to skeletal muscle regeneration after injuries and diseases. MSCs, which are initially present in muscle tissue or come to it from the bone marrow in response to damage, secrete various biologically active regulatory compounds that stimulate the survival, reproduction, and differentiation of cells, enhance the formation of new blood vessels (capillaries), have anti-inflammatory and antifibrotic effects (Mazurkevych et al., 2015). The ability of MSCs to produce various factors that affect all stages of the reparative process allows them to be used to accelerate regeneration, which has been repeatedly shown in various experimental models of muscle damage (Mazurkevych et al., 2009). The effect of increasing the effectiveness of transplanted MSCs can be enhanced by improving the method of cells delivering to the tissue and improving their survival; in addition, the secretory profile of cells can be changed in the appropriate direction by the method of influence of various physical or chemical stimuli or genetic modification. A new direction of regenerative medicine is the use of extracellular vesicles produced by MSCs and the regulatory molecules contained in them, primarily micro-RNAs. Activation of the regenerative potential of MSCs can be used as a tissue engineering tool in vivo that stimulates tissue repair using internal reserves (Mazurkevych et al., 2010).

Biochemical changes that occur in skeletal muscles during work are usually determined by the content of muscle metabolic products in the blood, urine, exhaled air, or directly in the muscles. For example, the maximum oxygen consumption is often used as an indicator of the intensity of aerobic processes. The intensity of glycolysis is determined by measuring the content of lactic acid. The creatine phosphokinase reaction is determined by the content of creatine and creatinine in blood; the inclusion of fats in energy exchange is identified by the content of free fatty acids and ketone bodies in blood. Conclusion about the ability of the body to resist the adverse effects of acidic products of anaerobic metabolism is made according to the indicators of acid-alkaline balance. Long-term work leads to an increase in the content of proteins, ammonia, and urea in blood, which indicates significant changes in amino acid exchange and protein metabolism (Skidanov et al., 2016).

Laboratory markers of structurally functional disorders of muscle tissue are a small number of biochemical parameters, which in a certain way reflect the processes of energy exchange and muscle damages during pathological processes (Mazurkevych et al., 2008).

Creatine kinase (CK) molecule is a dimer consisting of two types of subunits: M (muscle) and B (brain). From these subunits are formed 3 isoenzymes: BB, MB, and MM. The BB isoenzyme is mainly found in the brain, MM – in skeletal muscle, and MB – in the heart muscle. Normal CK activity should not

exceed 140-372 U/L in rabbits. The amount of the MM isoform may increase with injuries and damages of skeletal muscles (Payushina et al., 2011).

Creatine phosphokinase (CPK) is an enzyme that catalyzes the creatine phosphorylation reaction, which provides an energy substrate for muscle contraction. CPK is found in the cytoplasm and mitochondria of myocardial cells, skeletal muscles, and brain tissues, where it catalyzes the reaction:

$$\text{Creatine} + \text{ATP} \leftarrow \text{CPK} \rightarrow \text{ADP} + \text{creatinephosphate}.$$

CPK is a heterogeneous protein that consists of two types of subunits – B (brain) and M (muscle). Therefore, CPK is found in four forms: mitochondrial and three fractions of cytosolic isoenzymes (MM is found in skeletal muscles and myocardium, BB – mainly in the brain and smooth muscles, MB – in the heart muscle). Enzymes are distinct in their physicochemical and immunological properties. The level of total CPK in healthy people is represented almost entirely by CPK-MM (Boncharuk et al., 2009; Payushina et al., 2011).

Materials and methods of research

The study was conducted in the conditions of the Research and Educational Laboratory Center of Cell Technologies in Veterinary Medicine of the Faculty of Veterinary Medicine of the National University of Life and Environmental Sciences of Ukraine. Keeping animals and conducting research was carried out at the hospital on the basis of the Department of Surgery and Pathophysiology Named after Academician I. O. Povazhenko. Laboratory methods of research were carried out in the conditions of the educational and research and development clinical center Vetmedservis and the veterinary laboratory Bald.

In experiments, we used rabbits of the English Spot breed, 105 males, 3 months of age, with a weight of 2.5–3.0 kg. All selected animals had the same standard conditions of keeping and breeding, care and feeding. Rabbits are carefully selected for research and their overall health is checked. All animals were healthy according to performance in vivo. The conditions for keeping experimental animals and using them in experiments comply with the requirements and provisions of the current domestic regulatory documents and Directive No. 2010/63/EU On Protection of Animals Used for Scientific Purposes.

Prior to the study, all animals were vaccinated with the first dose at 6 weeks of age and again after 4 weeks with a combined preventive vaccine Pestorin Mormix preheating to +25 ºC, which is effective against viral hemorrhagic disease and rabbit myxomatosis. Experimental animals were kept in the appropriate conditions of the hospital of the Department of Surgery and Pathophysiology Named after Academician I. O. Povazhenko of the National University of Life and Environmental Sciences of Ukraine, all animals had identical conditions of keeping, care, and feeding. The animals were kept individually in a separate cage with the animal's number on it. The animal feeding diet was comprehensive. It consisted of sweet-smelling hay, enriched granulated feed Purina, and clean tap water from automatic drinking bowls. Everything was freely available for animals. Sterile sawdust from non-coniferous species was used for bedding. Cleaning of rabbit hutches and ventilation of the room took place

2 times per day. The room temperature ranged from +21–23 ºC, the indoor air humidity is about 70–80%. Experimental rabbits had normal conditions of changing darkness and light (12-hour cycle).

Animal experiments were conducted in compliance with the requirements of the Law of Ukraine On the Protection of Animals from Brutal Treatment and General Ethical Principles of Animal Experiments approved by the National Congress on Bioethics (Kiyv, Ukraine) on the care of laboratory animals in accordance with the Directive of EU on Protection of Vertebrate Animals used for Experimental and other Scientific Purposes (Strasbourg, 1987). The research was confirmed, verified, and approved by the local commission on Bioethics of the National University of Life and Environmental Sciences of Ukraine in accordance with Protocol No. 110/3-pr – 2018 from November 2, 2018.

Allogeneic MSCs culture was performed according to the methodological recommendations developed by the staff members of the Department of Surgery and Pathophysiology Named after Academician I. O. Povazhenko of the National University of Life and Environmental Sciences of Ukraine on Obtaining of mononuclear cells' fraction of rabbit bone marrow with high proliferative activity (Mazurkevych et al., 2017). MSCs were obtained from the red bone marrow of donor animals, taken according to the designed method of intravital obtaining of red bone marrow in small animals. It includes the selection of bone marrow in the area of the proximal and distal epiphysis of the corresponding bones of the shoulder and femur, sedation of the animal and tissues anesthesia in the area of surgical access, skin shaving, and its treatment with 5% iodine solution in the area of the proximal and distal epiphysis of the corresponding bones (Mazurkevych et al., 2016). After preparation and cleaning of the operating field, a bone marrow aspiration is performed using a medical needle for spinal anesthesia and a diagnostic puncture with Pencil-point needle bevel with a mandrel (Mazurkevych et al., 2013).

Procedures of cell isolation and manipulation of cellular material were performed in Class II Biosafety Cabinet of the Research and Educational Laboratory (ESCO). Cell culture was carried out in a CO_2 incubator (HERA CELL, Germany), which provided absolute humidity, a temperature of +37 °C, and a content of 5% of CO_2 in the air. Cell counting was performed in a Goriaev chamber using a PrimoVert microscope (Germany) with a magnification of 200 times. The total number of cells was calculated using the formula (Jennifer et al., 2011).

A cryogenic storage dewar with liquid nitrogen (SDS-20, Ukraine) was used to freeze the cells. Defrosting of the cells was carried out at a temperature of +37 °C in a water bath (EL 20, Poland). Culture media, other solutions, components, preparations were stored at a temperature of 4 °C and -18 °C in a household refrigerator Nord (Ukraine). Centrifugation of cell-rich fluids was performed by centrifuge (UNICO, USA). A TC-80M thermostat (Ukraine) was used to heat the solutions. Dehumidification and sterilization of laboratory utensils were carried out in a hot-air sterilizer HS–62A (Poland) and in an air sterilizer GPO-50 (Ukraine).

The animal was kept on a starvation diet for 12 hours before the operation. The operation of experimental muscle tissue injury was performed under general anesthesia. After fixing the animal

on the operating table, the operation field was freed from hair fibers by shaving with an electric machine and treated with a solution (Kutasept F).

Before introducing the animal to general anesthesia, an anticholinergic agent was intramuscularly introduced. It blocks mainly peripheral cholinoreactive systems, as well as atropine sulfate at a dose of 0.05 mg/L kg of animal body weight for prevention of bronchospasm and laryngospasm, decreasing gland secretion, reflex reactions, and side effects caused by excitation of vagus nerve. In due course of time, the drug Zoletil 100 was administered intramuscularly at a dose of 8 mg/L kg of animal body weight.

At the site of surgical access, infiltration anesthesia was previously performed with a 0.5% novocaine solution (a dose of 3 mL/animal) in the planned part of the simulated defect. Modeling of muscle tissue injury was performed by skin and fascia dissection process and cutting off the midplane of the pelvic head of the biceps femoris muscle in the measure of 1.5×1.5 cm to a depth of 1.5 cm of muscle tissue, which is shown in Fig. 1.

After cutting off 1.5 cm in width and 1.5 cm to the deep of muscle tissue (from the pelvic head of the biceps femoris), the wound was measured using a stationery ruler and a surgical scalpel with a replaceable blade. During the operation, each of the animals was placed on the operating table covered with a wool blanket to prevent excessive heat loss. All surgical procedures were performed in accordance with the requirements of aseptic and antiseptics (Mazurkevych et al., 2015).

Animals with experimental muscle tissue injuries were divided into 4 main groups. Rabbits of the 1st group were injected into the site of the experimental defect using an insulin syringe with pre-prepared doses (in the amount of 3 million/animal) of allogeneic MSCs, which were obtained according to methodological recommendations developed by the staff of the Department of Surgery and Pathophysiology Named after

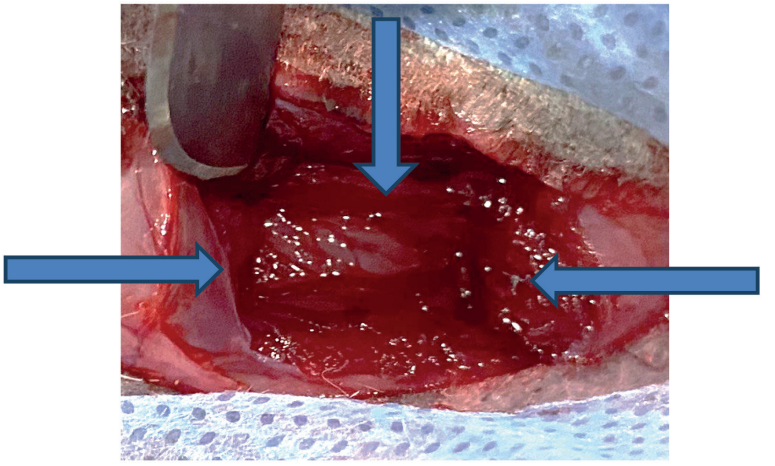

Fig. 1. Arrows show a simulated wound defect on the photo (size of 1.5×1.5 cm to a depth of 1.5 cm)

Academician I. O. Povazhenko of the National University of Life and Environmental Sciences of Ukraine on Obtaining of mononuclear cells` fraction of rabbit bone marrow with high proliferative activity (Mazurkevych et al., 2009). Cultivation took place from biological material (red bone marrow of donor animals), taken according to the designed method of intravital production of red bone marrow in small animals. It includes a selection of bone marrow in the area of the proximal and distal epiphysis of the corresponding bones of the shoulder and femur, sedation of the animal and tissues anesthesia in the area of surgical access, skin shaving and its treatment with 5% iodine solution, in the area of the proximal and distal epiphysis of the corresponding bones (Mazurkevych et al., 2016; Pristupa et al., 2018). After preparation and cleaning of the operating field, a bone marrow aspiration is performed using a medical needle for spinal anesthesia and a diagnostic puncture with Pencil-point needle bevel with a mandrel (Mazurkevych et al., 2017; Payushina et al., 2019).

Procedures of cell isolation and manipulation of cellular material were performed in Class II Biosafety Cabinet of the Research and Educational Laboratory (ESCO). Cell culture was carried out in a CO_2 incubator (HERA CELL, Germany), which provided absolute humidity, a temperature of +37 °C, and a content of 5% of CO_2 in the air. Cell counting was performed in a Goriaev chamber using a PrimoVert microscope (Germany), magnification ×400 and ×50 (Antosyuk et al., 2011; Skidanov et al., 2016).

A cryogenic storage dewar with liquid nitrogen (SDS-20, Ukraine) was used to freeze the cells. Defrosting of the cells was carried out at a temperature of +37 °C in a water bath (EL 20, Poland). Culture media, other solutions, components, preparations were stored at a temperature of 4 °C and -18 °C in a household refrigerator Nord (Ukraine). Centrifugation of cell-rich fluids was performed by centrifuge (UNICO, the USA). A TC-80M thermostat (Ukraine) was used to heat the solutions. Dehumidification and sterilization of laboratory utensils were carried out in a hot-air sterilizer HS–62A (Poland) and in an air sterilizer GPO-50 (Ukraine).

After that, the fascia and skin were stitched with synthetic polyfilament absorbable ligatures and sutures Vicryl (Belgium).

Animals of the 2nd experimental group were injected with the same amount of allogeneic MSCs into the bloodstream by puncturing the jugular vein at the edge of the upper and middle third of the neck. After that, the fascia and skin were stitched with synthetic polyfilament absorbable ligatures and sutures Vicryl (Belgium).

Animals of the 3rd experimental group were prescribed traditional trauma treatment, namely:

1. Surgical method: interrupted stitching on the site of muscle tissue rupture; fascia and skin were sewn with synthetic polyfilament absorbable ligatures and sutures Vicryl (Belgium), muscle tissue was sewn with absorbable material (wicker Chirasorb braided).

2. Pharmacological method: in the place where the wound was sewn up, we smeared 0.5 ml of surgical glue Dermabond. There were intramuscularly administered 0.2 mL/kg of animal body weight once a day for 5 days. And Tylosin 5% at a dose of 6 ml/L animal once a day for 5 days.

Animals of the 4th experimental group (control group) were given an

intravenous 0.9% sodium chloride solution. In addition, there was the 5th experimental group – intact animals.

In the postoperative period, the animals were provided with complete rest, proper conditions for keeping, feeding and watering in accordance with the requirements.

Animal from each experimental group was removed with the use of euthanasia (after deep anesthesia) at a certain stage. In such a way, we took muscle tissue samples for morphological and histological studies. In the postoperative period, the animals were provided with complete rest, proper conditions for keeping, feeding and watering in accordance with the requirements. A clinical examination of animals was conducted during the entire study period.

Samples of biological material for laboratory tests were taken at the initial condition (before the start) and on the 4th, 7th, 10th, 14th, 21st, and 28th days of the experiment (Table 1). The animal was fixed, the skin was stretched in the area of the jugular vein passage at the edge of the upper and middle third of the neck, and the animal's head was taken to the other side for obtaining blood samples for laboratory tests. The puncture was performed by needling the skin (inserting the needle into the blood flow at an angle of 45 ° and the vein wall. The selected fresh blood was placed in a coagulant tube (Fig. 2).

Biochemical studies were conducted in the veterinary laboratory Bald by the kinetic method using a biochemical analyzer RT-9600, using commercial kits of the company Filisit-Diagnostics (Ukraine) according to the instructions.

Statistical processing of the obtained digital data was carried out using a package of statistical programs Microsoft Excel. The arithmetic mean was calculated using the Student's t-test. The difference between the values was considered a statistically reliable result, in accordance to which coefficient (P) was no more 0.05 that is common in biological research.

Fig. 2. Blood sampling from the jugular vein

1. The number of animals in experimental design

Animal groups	Initial condition	4th day	7th day	10th day	14th day	21st day	28th day
Administration of MSCs in the muscles	3	3	3	3	3	3	3
Administration of MSCs into blood	3	3	3	3	3	3	3
Traditional treatment	3	3	3	3	3	3	3
Control group	3	3	3	3	3	3	3
Intact animals	3	3	3	3	3	3	3
Total animals used:			105				

Results of the research and their discussion

The findings of CPK activity in rabbit blood associated with the activity of regeneration of experimentally injured muscle tissue in different periods of the experiment are shown in Table 2.

The results of the analysis of the obtained data indicate that changes in the activity of the creatine phosphokinase type (MM) isoenzyme occurred during the studies. As can be seen from Table 1 and Fig. 3, on the 4th day after transplantation of allogeneic MSCs, the level of creatine phosphokinase in blood of animals of all groups was the highest for the entire experimental period. CPK activity in blood serum of animals of the 1st and 2nd experimental groups significantly exceeds the reference val-

2. Creatine phosphokinase activity in blood of rabbits after application of allogeneic MSCs for stimulating myogenesis in experimentally damaged muscle tissue, U/L (M ± m, n = 3)

Animal groups	Initial condition	After applying MSCs					
		4th day	7th day	10th day	14th day	21st day	28th day
Administration of MSCs in the muscles	237.8 ± 52.4	676.8 ± 8.6 ***	402.6 ± 3,7**	370.6 ± 3**	322.5 ± 18.3**	271.4 ± 52.7**	308 ± 21.9*
Administration of MSCs into blood		804.3 ± 54.4**	525.7 ± 32.5**	400.9 ± 8.1**	368.5 ± 4.5**	338.7 ± 34 **	335.5 ± 26.4
Traditional treatment		926.3 ± 39.6*	802.6 ± 11	596.2 ± 69.5	460.7 ± 61.5	442.6 ± 31.7	325.1 ± 49
Control group		1082.6 ± 40.2	877 ± 63.3	761.8 ± 36.5	618.4 ± 47.7	563.9 ± 15.2	393.6 ± 6.5
Intact animals	226.6 ± 21.2	287.5 ± 15.4**	296.9 ± 27.2**	283.3 ± 19.5**	257.7 ± 41.2**	240.9 ± 33.5**	245.9 ± 43*
Total animals used:			105				

Note: * P < 0.05; ** P < 0.01; *** P < 0.001.

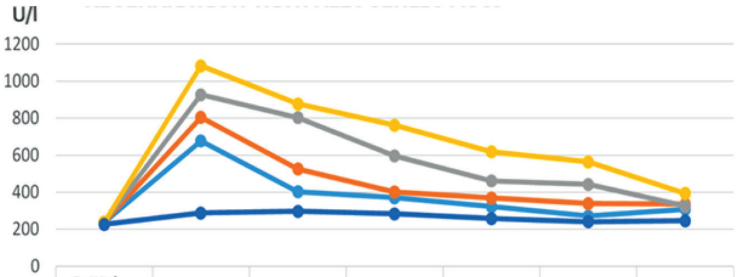

	Initial condition	4th day	7th day	10th day	14th day	21th day	28th day
MSCs into muscle	237,8	676,8	402,6	370,6	322,5	271,4	308
MSCs into blood	237,8	804,3	525,7	400,9	368,5	338,7	335,5
Traditional treatment	237,8	926,3	802,6	596,2	460,7	442,6	325,1
Control group	237,8	1082,6	877	761,8	618,4	563,9	393,6
Intact animals	226,6	287,5	296,9	283,3	257,7	240,9	245,9

Fig. 3. Creatine phosphokinase activity in blood of rabbits after application of allogeneic MSCs for stimulating myogenesis in experimentally damaged muscle tissue

ues but is significantly lower compared with this indicator in animals of the 3rd groups (traditional treatment) and the 4th (control group). Later, on the 7th, 10th, 14th, 21st, and 28th days of the experiment, there is a gradual decrease in the enzyme activity with slight fluctuations in the groups, but with unchanged dynamics between the groups.

It is known that an increase in the activity of this enzyme in blood indicates the destruction of myocytes. The dynamics of its activity allow to determine the degree of muscle injury and the intensity of recovery of damaged muscle tissue (Francchi et al., 2021). In the first 4 days of the experiment, the highest activity of CPK obviously indicates significant destruction of damaged muscle tissue as a result of the active phase of the inflammatory process, stage of its alteration, and vascular reaction.

The lowest level of CPK activity in blood of animals was observed during the entire observation period in the 1st experimental group, which gives grounds to conclude that allogeneic MSCs transplanted directly into the inflammatory zone are reliably highly effective.

The second place in terms of effectiveness is the animals of the 2nd group that were administered MSCs intravenously.

The traditional method of treating experimentally damaged muscle reliably ranks third place. It's significant to pay attention to the dynamics of indicators in the intermediate observation period between the 4th and 28th days. In particular, CPK activity in the blood decreased against the initial condition in animals of the 1st and 2nd experimental groups, while in animals of the 3rd experimental group (traditional treatment), this indicator only approached but did not reach this level only on the 14th day. It indicates a significantly lower activity of regenerative processes in experimentally injured muscle tissue.

Creatine phosphokinase activity of the control group decreases on the 28th

day of the study. It indicates severe consequences of an injury of this nature without medical care for the body.

Conclusions and future prospects

Application of allogeneic mesenchymal stromal cells for stimulation regenerative processes in experimentally damaged muscle tissue by the method of administration it directly into the area of damage significantly increases the regeneration activity of damaged tissue and reduces the healing time more effectively than the method of administration it into the blood, as well as in comparison with the method of traditional treatment.

Method for modeling of experimental damage in muscle tissue by damage of muscle tissue in the pelvic head of the biceps femoris of rabbits is a possibility to study the comparative effectiveness of the stimulating effect of transplanted allogeneic mesenchymal stem cells.

References

Antosyuk, G. S. (2017). Hygienic requirements for keeping laboratory animals.

Boncharuk, E. G., Goncharuk, E. G., Kundiev, Y. I., & Bardov, V. G. (2009). A Guide to Laboratory Animals and Alternative Models in Biomedical Research. Kyiv: Higher School.

Datsenko, I. I. (Ed.). (2001). Laboratory animals. Breeding, maintenance, use in the experiment. Laboratory animals. Lviv: World. Retrieved from http://labanimal.ru/laboratoryanimals.

Fabri, Z. Y., & Chernov, V. D. (2014). Biochemical bases of physical culture and sports [Textbook for students of higher educational institutions of physical culture and sports]. Uzhhorod. Retrieved from https://www.uzhnu.edu.ua/uk/infocentre/get/25223

Frinchi, M., Morici, G., Mudó, G., Bonsignore, M. R., & Di Liberto, V. (2021). Beneficial role of exercise in the modulation of mdx muscle plastic remodeling and oxidative stress. Antioxidants, 10(4), 558.

Mazurkevych, A., Malyuk, M., Bezenezhnik, N., Starodub, L., Kharkevich, Yu., Yakubchak, A., & Gryzinska, M. (2017). Immunophenotypic characteristics and karyotype analysis of mesenchymal stem cells derived from bone marrow of rabbits during in vitro cultivation. Polish Journal of Veterinary Sciences, 20(4), 687-695. doi: 10.1515 / pjvs-0086

Mazurkevych, A. Y., Karpovskyi, V. I., & Malyuk, M. O. (2015). Obtaining, cultivating, cryopreservation and use of stem cells. Kyiv: National University of Life and Environmental Sciences of Ukraine.

Mazurkevych, A. Y., Malyuk, M. O., Danilov, V. B., Bokotko, R. R., Kovpak, V. V., Kharkevich, Yu. O., & Zhurba, V. I. (2010). A method of stimulating proliferative processes in the wound skin of rats by transplantation into the wound area of mesenchymal stem cells. Kyiv: National University of Life and Environmental Sciences of Ukraine.

Mazurkevych, A. Y., Malyuk, M. O., Kovpak, V. V., & Bokotko, R. R. (2009). Method of obtaining fraction of bone marrow mononuclear cells with high proliferative activity. Kyiv: National University of Life and Environmental Sciences of Ukraine.

Mazurkevych, A. Y., Malyuk, M. O., Kovpak, V. V., & Bokotko, R. R. (2009). Method of obtaining fraction of bone marrow mononuclear cells of dogs with high proliferative activity. Patent 50905 Ukraine. Kyiv: State Patent Office of Ukraine.

Mazurkevych, A. Y., Malyuk, M. O., & Kovpak, V. V. (2006). Prospects for the use of stem cells in veterinary medicine. Lviv: Scientific Bulletin of the Lviv National Academy of Veterinary Medicine S. Z. Gzhytsky, 128-134.

Mazurkevych, A. Y., Malyuk, M. O., Kovpak, V. V., & Bokotko, R. R. (2009). Method of obtaining fractions of bone marrow mononuclear cells with high proliferative activity. Patent 46600 Ukraine. Kyiv: State Patent Office of Ukraine.

Mazurkevych A. Y., Malyuk, M. O., Kovpak, V. V., Bokotko, R. R., Danilov, V. B., & Kharkevich, Yu. O. (2009). Method of creating biological graft based on osteogenically induced mesenchymal stem cells of dogs in vitro. Kyiv: National University of Life and Environmental Sciences of Ukraine.

Mazurkevych, A. Y., Malyuk, M. O., Kovpak, V. V., Sushko, M. I., & Bokotko, R. R. (2008). Influence of different trypsinization methods on proliferative activity of embryonic cells. Kyiv: Scientific Bulletin of the National Agrarian University.

Mazurkevych, A. Y., Malyuk, M. O., Tkachenko, S. M., Kovpak, V. V., & Bokotko, R. R. (2015). Method of lifelong production of stromal stem cells of bone marrow of animals. Patent Ukraine. Kyiv: State Patent Office of Ukraine.

Mazurkevych, A. Y., Savchuk, T. L., Bokotko, R. R., Malyuk, M. O., Kharkevich, Y. O., Kovpak, V. V., ...& Danilov, V. B. (2021). Stimulation by stem cells of regenerative processes in experimentally damaged bone tissue of rabbits. Monograph. Kyiv: NULES of Ukraine.

Mazurkevych, A. Y., Malyuk, M. O., Kovpak, V. V., & Kharkevich, Yu. O. (2017). Stem cells in veterinary medicine. Monograph. Volume 2. Kyiv: Comprint Securities LLC.

Mazurkevych, A. Y., Malyuk, M. O., Kovpak, V. V., Kharkevich, Y. O., & Zhurba, V. I. (2013). Stem cells in veterinary medicine, volume one. Monograph. Kyiv: Comprint Securities LLC.

Nakonechna, O. A., & Bachynsky, R. O. (2020). Biochemistry of enzymes. Aspects of medical enzymology: teaching method. manual for preparation for practice. classes in biological chemistry [for students of medical and dental faculties]. Kharkiv.

Payushina, O. V., Domaratka, E. I., & Sheveleva, O. N. (2019). Involvement of mesenchymal stem cells in muscle tissue regeneration. Basics of laboratory.

Pristupa, T., Klyutsuk, M., Danchuk, O. (2018). Methods of studying motor activity in animals of Ukraine Podolsk State Agrarian University.

Shadrach, J. L., & Wagers, A. J. (2011). Stem cells for skeletal muscle repair. Philosophical Transactions of the Royal Society B: Biological Sciences, 366(1575), 2297-2306. doi: 10.1098/rstb.2011.0027

Skidanov, A. G, Leontieva, F. S., Morozenko, D. V., Piontkovsky, V. K., & Radchenko, V. O. (2016). Biochemical markers for assessing muscle condition in degenerative diseases of the spine. Orthopedics, Traumatology and Prosthetics, 4.

Стадник Н. В., Бокотько Р. Р. , Савчук Т. Л. , Куліда М. А., Мазуркевич А. Й. (2021). АКТИВНІСТЬ КРЕАТИНФОСФОКІНАЗИ В СИРОВАТЦІ КРОВІ КРОЛІВ ЗА РЕГЕНЕРАЦІЇ ЕКСПЕРЕМЕНТАЛЬНО УШКОДЖЕНОЇ М'ЯЗОВОЇ ТКАНИНИ ТА ПІСЛЯ ЇЇ СТИМУЛЯЦІЇ ТРАНСПЛАНТОВАНИМИ МСК.

Ukrainian Journal of Veterinary Sciences, 12(4): 127–139,
https://doi.org/10.31548/ujvs2021.04.010

Анотація. *За статистикою в сучасній ветеринарній практиці відсоток м'язових травм серед спортивних та робочих тварини складає від 40–70% спортивних травм. Досить часто трапляються випадки із м'язовими травмами скелетних м'язів, а саме кінцівок. У цій науковій праці описано методику досліджень, етапи досліджень та вивчено взаємозв'язок динаміки активності певного біохімічного показника крові. Суть методу по-*

лягала в моделюванні травми м'язової тканини проведеного методом розтинання шкіри та фасції і відсікання в ділянці серединної площини тазової голівки двоголового м'яза стегна, розміром 1,5×1,5 см на глибину 1,5 см м'язової тканини у 105 лабораторних тварин, поділених на 4 групи за застосування різних методів лікування. Проаналізовано результати одного із найефективніших біохімічних методів діагностики ушкодження скелетних м'язових волокон та порівняно активність ферменту ізоферменту креатинфосфокінази (ММ) залежно від етапу дослідження. Інші методи досліджень такі як, клінічні, біохімічні, ультрасонографічні та гістологічні реєструвалися на 4, 7, 10, 14, 21, 28 добу. Нами проаналізовано останні літературні джерела та зроблено висновки, що на 4 та 7 доби рівень креатинфосфокінази в групах із внутрішньовенним і внутрішньом'язовим введенням алогенних мезенехімальних стовбурових клітин вище референтних значень, але значно нижче, ніж у групах контролю та з традиційним методом лікування. А от значну динаміку зниження рівня креатинфосфокінази в сироватці крові у кролів ми спостерігаємо на 10 добу в групі із внутрішньовенним введенням порівнюючи із контрольною групою тварин у 2 рази та в 1,6 раза порівнюючи із традиційним лікуванням. Група тварин із внутрішньом'язовим введенням має референтні значення на 14 добу, порівнюючи із контролем нижче в 1,3 раза, традиційним лікуванням – в 1,2 раза.

Та на 21 добу отримуємо референтні значення в групи тварин із традиційним лікуванням. Рівень активності креатинфосфокінази знижується в контрольної групи тварин на 28 добу дослідження, що свідчить про повний м'язовий розрив. Результати досліджень показали, що найбільш високу активність ферменту креатинфосфокінази впродовж дослідження показали групи тварин контрольна та із традиційним лікуванням, що свідчило про значні структурно-функціональні й деструктивні порушення м'язових волокон скелетної м'язової тканини із тяжкою травмою. Отже відзначено, що активність ферменту за умов ушкодження скелетної м'язової тканини має тенденцію збільшуватися відповідно до ступеня тяжкості травми.

Ключові слова: *алогенні мезенхімальні стовбурові клітини, регенерація м'язової тканини, лабораторні тварини, активність, ізоформа*